Hydraulic Performance of Staggered-Barrel Culverts for Stream Crossings

Theodore G. Cleveland, Kyle B. Strom,
Wade J. Barnes, Jeremy V. Dixon

Texas Department of Transportation

Disclaimer

The United States Government and the State of Texas do not endorse products or manufacturers. Trade or manufacturers' names appear herein solely because they are considered essential to the object of this report.

Technical Report Documentation Page

1. Report No. FHWA/TX-13/0-6549-1	2. Government Accession No.	3. Recipient's Catalog No.
4. Title and Subtitle Hydraulic Performance of Staggered-Barrel Culverts for Stream Crossings		5. Report Date May 2013
		6. Performing Organization Code
7. Author(s) Theodore G. Cleveland, Kyle B. Strom, Wade J. Barnes, Jeremy V. Dixon.		8. Performing Organization Report No. 0-6549-1
9. Performing Organization Name and Address Texas Tech University, Water Resources Center 10th and Akron, Room 203 Lubbock, TX 79409-1022		10. Work Unit No. (TRAIS)
		11. Contract or Grant No. 0-6549
12. Sponsoring Agency Name and Address Texas Department of Transportation Research and Technology Implementation Office P.O. Box 5080 Austin, TX 78763-5080		13. Type of Report and Period Covered Technical Report 1 Sep 2009 – 31 Aug 2012
		14. Sponsoring Agency Code

15. Supplementary Notes
Project performed in cooperation with the Texas Department of Transportation and the Federal Highway Administration.

16. Abstract
Literature interpretation, laboratory experimentation, and data analysis was used to infer guidelines to assist in assessing multiple barrel staggered-systems that mimic natural stream behavior to facilitate solids migration, yet still provide the sufficient clear-water hydraulic capacity to meet their transportation infrastructure drainage needs.

A database developed from literature data pertaining to solids transport was developed along with a screening tool for estimating solids transport. The laboratory study examined staggered barrel and conventional culverts both in-line with the stream axis and skew to that axis to develop tools to predict culvert performance.

Experiments showed culvert open area was correlated with solids transport while culvert shape was not. Staggered systems showed some advantage in skew-settings performing slightly better than anticipated based on in-line studies. Stage-conveyance plots showed that our largest open area systems to have a curve closest to the approach section stage-conveyence until submergence; a finding supportive of matching the approach section conveyance and the culvert system conveyance to maintain solids continuity through the system.

Examples illustrating the screening tool on selected experiments are presented, as are suggestions for future study.

17. Key Words **STAGGERED BARREL CULVERTS, CULVERT HYDRAULICS, PHYSICAL MODEL, SOLIDS TRANSPORT**	18. Distribution Statement No restrictions. This document is available to the public through the National Technical Information Service, Springfield, Virginia 22161, www.ntis.gov		
19. Security Classif. (of this report) Unclassified	20. Security Classif. (of this page) Unclassified	21. No. of Pages 135	22. Price

Form DOT F 1700.7 (8-72)   **Reproduction of completed page authorized**

Hydraulic Performance of Staggered-Barrel Culverts for Stream Crossings

by

Theodore G. Cleveland, Associate Professor,
TechMRT, Texas Tech University

Kyle B. Strom, Associate Professor,
Civil and Environmental Engineering, University of Houston

Wade J. Barnes, Graduate Researcher
Civil and Environmental Engineering,Texas Tech University

Jeremy V. Dixon, Graduate Research Assistant,
Civil and Environmental Engineering,Texas Tech University

Research Report 0-6549-1 (Final Report)
Research Project 0-6549

Research Project Title: Hydraulic Performance of Staggered-Barrel Culverts for Stream
Crossings

Disclaimer

The contents of this report reflect the views of the author(s), who is (are) responsible for the facts and the accuracy of the data presented herein. The contents do not necessarily reflect the official view or policies of the Federal Highway Administration (FHWA) or the Texas Department of Transportation (TxDOT). This report does not constitute a standard, specification, or regulation. This report is not intended for construction, bidding, or permit purposes. The United States Government and the State of Texas do not endorse products or manufacturers. Trade or manufacturers names appear herein solely because they are considered essential to the object of this report. The researcher in charge of this project was Dr. Kenneth A. Rainwater at Texas Tech University.

There was no invention or discovery conceived or first actually reduced to practice in the course of or under this contract (to date), including any art, method, process, machine, manufacture, design, or composition of matter, or any new useful improvement thereof, or any variety of plant, which is or may be patentable under the patent laws of the United States of America or any foreign country.

Acknowledgments

**0-6549 Hydraulic Performance of Staggered-Barrel Culverts
for Stream Crossings: Final Report**

Contents

List of Figures

List of Tables

1   Introduction

This research project developed knowledge to address solids accommodation in Texas stream crossings, and to suggest design considerations for building systems that mimic stream behavior to facilitate solids migration, and provide sufficient clear-water hydraulic capacity to meet their transportation infrastructure drainage needs.

1.1   Research Context

The interaction of sediment transport, particularly bed load, and drainage structures at highway stream crossings is a relatively ignored component of engineering design. Use of hydraulic structures to accommodate aquatic species is progressing and this knowledge, at least conceptually, is relevant to the transport of stream-carried solids through Tx-DOT hydraulic structures. The transport of smaller solids that are carried suspended (or dissolved) within the water column are reasonably well addressed by current clear-water formulas[1].

However, when bed material transport rates are relatively high, and comprised of solids that are too large to travel in suspension, then current drainage structures might not function as intended. Under such conditions, solids may become trapped in and around the structure and lead to untimely service failures. This project attempted to understand how to accommodate such episodic loads of solids material using different culvert geometries.

The major reason for deposition and erosion surrounding culverts is a lack of sediment continuity from one side of the culvert to the other. The lack of continuity arises from designing the culvert system for flows which are larger than the channel forming "effective discharge" of the stream. The effective discharge typically has a return period of one to two years and produces the most geomorphic work in a stream. The overall cross sectional flow area and slope of the culvert system should match that of the bankfull stream geometry and slope during a 1 to 2 year return period flow to maintain sediment continuity. Culvert systems are typically designed to handle flows with return periods that are larger than 1 to 2 years, and therefore single and multi-barrel culverts acquire a cross-sectional flow area that is larger than that of the natural bankfull stream geometry.

The increased cross-sectional area can lead to flow deceleration and deposition of sediment at lowflow conditions, destabilization of stream banks, and erosion of sediment downstream of the crossing. Figure 1 is a photograph on the downstream side of a culvert system in a mobile bed drainage channel. The right two barrels on the upstream side were obstructed

---

[1]Clear-water is a concept used by the authors of this report to distinguish between liquid flows that do not contain substantial, depositable solids content as opposed to liquid flows that transport substantial, depositable amounts of solids. As a working hypotheses, slurries of civil engineering significance start at solids fractions of 10 percent by weight. Sanitary flows typically contain solids of 5 percent by weight, so in the present work sanitary flows would be classified as clear-water.

by debris (they are on the outside of a bend in the stream) as was the left most barrel, which was essentially in the middle of an eddy. The only active barrel was the second from the left as well as flow over the roadway. The four barrels span a distance far wider than the upstream bankfull width, and as such create an incompatible stage-area (conveyance) relationship which lead to three of the barrels being essentially useless.

Figure 1: 4-Barrel Culvert System at Caprock Canyons State Park (G.R. Herrmann)

Project 0–4695 (*Design guidance for low-water crossings in areas of extreme bed mobility, Edwards Plateau, Texas*) (Thompson et al., 2009) examined the interaction between sediment transport (particularly bed load) and low-water crossings in the Edwards Plateau region of Texas and developed guidance for creating designs to reduce crossing damage or loss of performance. Simple generic laboratory testing of a number of potential solutions demonstrated anecdotal evidence that water and solids could best be accommodated through culvert like structures using a flow contraction that actually accelerates (rather than decelerate) the incoming flow.

During the course of that project (0–4695), a problem occurred on Texas RM 335 in Real County, where a low-water crossing was destroyed and a replacement was required. The hydraulic engineer responsible for design of the replacement structure used results and experience developed in association with Project 0–4695 to develop a hydraulic design. The design approach was to use three circular culverts of two different diameters in a staggered invert configuration[2]. Site details and the design solution were documented in two reports authored by George R. (Rudy) Herrmann, P.E. who, at the time was in the San Angelo District — he has since retired from the department. The fundamental technical approach behind the RM 335 effort was to calculate the stage-conveyance (*growth curves* of the hydraulic properties) of various culvert barrel shapes and sizes, then assemble a combination of barrels at varying elevations to mimic the stage-conveyance (*growth curves* of the hydraulic properties) of the channel immediately up and downstream of the structure to maintain sediment continuity, and thus the ability to transport water and sediment. The concept is called the "stream simulation" approach.

---

[2]That is, the invert elevation of the largest culvert was substantially lower in elevation than the inverts of the two smaller culverts.

1.2 Staggered Barrel Performance Hypothesis

The idea behind staggered-barrel culverts is to design a system which mimics the natural stream hydraulics and improves sediment and flow continuity over a range of flow conditions (Johnson and Brown, 2000; Wargo and Weisman, 2006). Figure 2 is a sketch comparing a single (larger) culvert barrel to the staggered barrel system. The left panel (A) is a single barrel system, while the right panel depicts the staggered system. The system is built around a larger centralized culvert designed to handle flows lower than the bankfull discharge. The capacity of this larger culvert is then augmented with smaller culverts whose inverts are elevated relative to the main barrel. During low flow periods, all flow and sediment pass through the main barrel. The reduction in flow area in this main barrel relative to a larger single barrel or vertically aligned multi-barrel system means that flow depths and bed stresses are higher at these low flow conditions. At higher stage, the smaller culverts become accessible and the hydraulic capacity of the system is increased. These invert-raised barrels can be thought of as the flood plains of the culvert system.
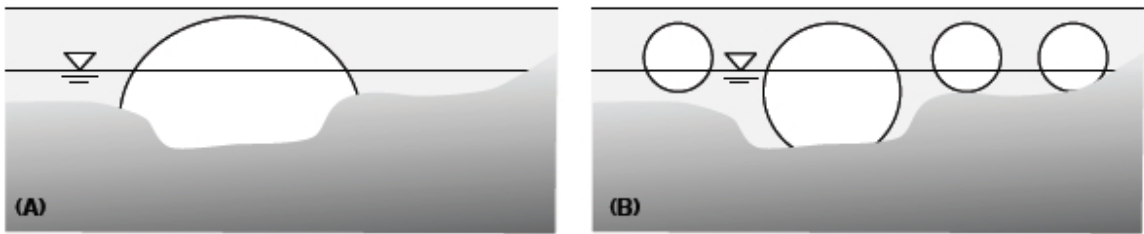
Figure 2: Sketch of stream conditions and staggered barrel systems.

1.3 Project Objectives

The project objectives were to develop design guidelines for culvert systems that will maintain sediment transport of natural streams at stream crossings. These objectives were addressed in several broad but related tasks as listed below;

1. Literature Review, Synthesis, and Data Capture

2. Creation of Screening Tools

3. Quantitative Physical Modeling

4. Data Analysis and Interpretation

2 Literature Review

The goal of project 0-6549 is to develop knowledge to address the issue of solids accommodation in Texas Department of Transportation stream crossings[3], and to develop design guidelines to assist in building multiple barrel systems that mimic the necessary stream behavior to facilitate solids migration, yet still provide the sufficient clear-water hydraulic capacity to meet their transportation infrastructure drainage needs. This literature review focuses on the movement of solids (sediment, bedload, etc.) in and near culverts. This literature review constitutes the technical memorandum for Task 1 of the project.

2.1 Overview

Little information exists from systematic studies of sediment transport in single or multi-barreled culverts. Most recent work on culvert flow and sediment transport has focused on scour process and mitigation at culvert outlets (e.g., Abt et al., 1984, 1985; Abida and Townsend, 1991; Liriano et al., 2002), and on determining the maximum allowable velocity to allow fish to pass from one side of the culvert to the other (e.g., Warren and Pardew, 1998; Dodd et al., 2004; Peake, 2004; House et al., 2005). Recent studies have been conducted examining flow, sediment transport, and bed morphologies in bottomless or buried-invert culverts, also known as countersunk culverts, (Maxwell et al., 2001; Crookston and Tullis, 2006; Crookston, 2008). These bottomless or buried systems are intended to improve fish migration through the culvert by maintaining stream bed and sediment load continuity from one side of the culvert to the other.

Flow in culvert systems ranges from open-channel to pressurized pipe flow depending on stream stage. The literature review is organized into sub-sections as follows: 1) a review of basic sediment transport mechanics in open-channel flows, with a focus on bed load mechanics, quantification, and a summary of available bed load data; 2) an overview of relevant information from past studies on transport of solids in pipeline systems; 3) a review of specific studies examining sediment transport in single barrel, multi-barrel, and bottomless culverts; and 4) a synthesis of the knowledge compiled.

2.2 Sediment Transport in Open-Channel Flows

This review of sediment transport in open-channel flows is presented to provide context for sediment transport mechanics in culverts and is by no means an exhaustive review of the subject. The reader is referred to García (2008a) for a more thorough and expansive presentation of the state of knowledge pertaining to sediment transport in open channels.

---

[3]In this context the authors mean culverts, and low water crossings. Bridges are outside the scope of this project.

Figure 3: Categorization of fluvial sediment [reproduced after Church (2006)].
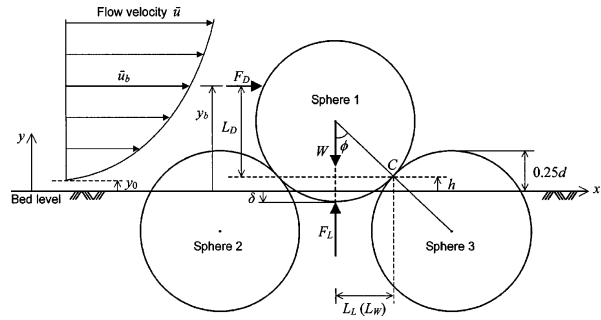
Figure 4: Schematic of forces acting on an idealized grain within the bed [after Wu and Chou (2003)]

2.2.1   Mechanics and Methods of Quantification

Sediment transported by open-channel flows such as those in rivers falls into two broad categories: 1) Bed-Material Load, i.e. material found in, and originating from, the river bed and lower banks; and 2) Wash Load, which is composed of fine material that travels through the river system without depositing (Fig. 3). Bed material load is further demarcated by the mode in which the sediment moves. Sediment moving fully suspended in the water column is termed "suspended load" and sediment moving in contact with the bed is referred to as "bed load." The state between these two, saltation, defines a condition where particles take long hops in the water column between times of contact with the bed. In the consideration of culvert clogging, bed material load is of primary interest over the wash load. In addition, because clogging occurs during moderately high flow events, and often in gravel bed streams, it is likely that sediment moving as bed load will be the clogging agent leading to reduced culvert capacity. In this section, we review the basic forces involved in defining particle motion of non-cohesive bed material (silt, sands, and gravels), review methods for quantifying bed load, and discuss methods for differentiating between bed load and suspended load.

The primary forces acting in the movement of bed material in non-cohesive sediment are the drag force exerted by the flow on individual particles and the resisting forces generated by particle weight and the grain-to-grain contact of a particle with its surrounding neighboring particles (Fig. 4). Lifting forces are also present but are of secondary importance to the drag. Grains move once the overturning moment, caused primarily by the drag force, $F_D \propto u_b^2 d^2$ where u_b is the mean flow velocity approaching the grain and d is the grain diameter, exceeds the resisting moment; the force resisting motion of an individual grain is proportional to the submerged weight of the particle, $W_{sub} = (\rho_s - \rho)gd^3$ where ρ is the fluid density, ρ_s is the sediment density, and g is the acceleration of gravity. Rather than estimating the drag on each individual particle in the bed, the average drag force exerted by the flow on the bed is quantified with the bed shear stress, τ_B; the bed shear stress represents the average force in the downstream direction applied to the bed by the flow

per unit area. Note that the drag force on an individual grain, F_D, is $F_D \propto \tau_B d^2$.
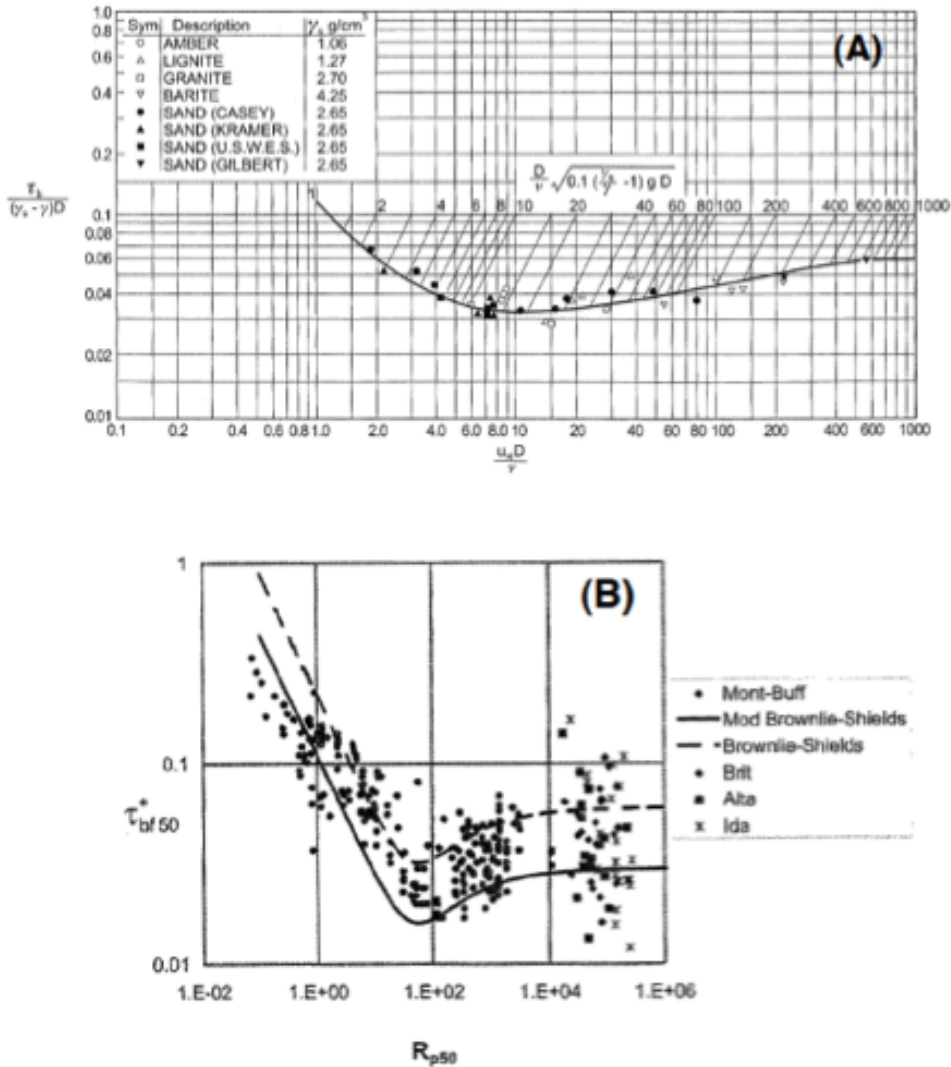
Figure 5: (A) Shield diagram, (B) plot of Brownlie (1981) equation (Eq. 3) along with the modified Brownlie equation (Eq. 4) and the τ_{cr}^* data of Buffington and Montgomery (1997). [from García (2008a)]

Because of the forces involved, an important ratio in the mechanics of sediment transport is the ratio of the drag and resisting forces. For horizontal and low-slope beds, the proportionality ratio of these two forces is expressed as:

$$\tau^* = \frac{\tau_B}{(\rho_s - \rho)gd} \tag{1}$$

τ^* is referred to as the dimensionless bed shear stress. For steady, uniform channel flow τ_B can be expressed as $\tau_B = \rho g R_h S$, where R_h is the hydraulic radius, and S is channel

slope. Using this definition, a critical dimensionless shear stress above which the bed is in motion and below which the bed is stable can be conceptually defined as:

$$\tau_{cr}^* = \frac{\tau_{B,cr}}{(\rho_s - \rho)gd} \tag{2}$$

where $\tau_{B,cr}$ is the critical bed shear stress and τ_{cr}^* is the critical dimensionless shear stress or the "Shields Parameter" (Shields, 1936; Chang, 1988; Julien, 1998; García, 2008a). Because the drag force acting on a particle is a function of the flow state surrounding the particle (laminar, transitional or turbulent), τ_{cr}^* is also a function of flow state, i.e. $\tau_{cr}^* = \tau_{cr}^*(Re_{p*})$ where Re_{p*} is a particle Reynolds number defined by $Re_{p*} = u_*d/\nu$ and u_* is the shear velocity $u_* = \sqrt{\tau_B/\rho}$. The functionality of $\tau_{cr}^* = \tau_{cr}^*(Re_{p*})$ is depicted in the form of the Shields diagram (Fig. 5a), but can also be evaluated using the explicit equation for $\tau_{cr}^* = \tau_{cr}^*(Re_{p*})$ developed by Brownlie (1981):

$$\tau_{cr}^* = 0.22 Re_{p*}^{-0.6} + 0.06 \exp(-17.77 Re_{p*}^{-0.6}) \tag{3}$$

As Re_{p*} gets large and the flow transitions to a hydraulically rough condition, which occurs around $Re_{p*} = 500$, τ_{cr}^* goes to a constant value. For Eq. (3) this constant value is $\tau_{cr}^* = 0.06$; this is consistent with the original work of Shields and the value of $\tau_{cr}^* = 0.06$ typically associated with Fig. 5a. Measured values of the τ_{cr}^* condition in the hydraulically rough zone, $Re_{p*} > 500$, vary widely in both the field and laboratory (e.g., Buffington and Montgomery, 1997; Monteith and Pender, 2005; Lamb et al., 2008). This is due in part to the variability in grain shape and gradation, grain protrusion (Fenton and Abbott, 1977), and the structural organization of grains within the surface layer (Monteith and Pender, 2005; Strom et al., 2004). On average, τ_{cr}^* values in the hydraulically rough zone tend to be less than 0.06. This is especially true for gravel bed rivers. After a re-analysis of available data, Neill (1968) suggested that a more reasonable average, constant value of τ_{cr}^* would be 0.03. Taking this suggestion, a simple modification of the Brownlie equation (Eq. 3) is:

$$\tau_{cr}^* = \frac{1}{2}[0.22 Re_{p*}^{-0.6} + 0.06 \exp(-17.77 Re_{p*}^{-0.6})] \tag{4}$$

Eqs. (3) and (4) can be thought of as the upper and lower bounds of likely τ_{cr}^* values for natural sediment, resulting in hydraulically rough values ranging from $\tau_{cr}^* = 0.03$–0.06 (Buffington and Montgomery, 1997; García, 2008b).

The concept that the bed is stationary for bed shear stresses less than the critical condition, and in motion for stresses greater than the critical condition, is useful. However, it is important to note that this sharp break between no-motion and motion defined by τ_{cr}^* is a conceptual tool rather than a very detailed model of reality. Because flows are turbulent, the forces experienced by individual particles fluctuate above and below the mean value defined by $F_D \propto u_b^2 d^2$. This means that even if the resisting force is equivalent for all particles in a bed made of uniform sized spheres, there may be conditions where some particles are in motion and others are not (McEwan and Heald, 2001; Papanicolaou et al., 2002). This is then complicated by variable particle arrangement, shape, and size (Dietrich et al., 1989; Parker and Sutherland, 1990; Hofland et al., 2005; Hofland and Battjes, 2006;

Oldmeadow and Church, 2006). This is further complicated by the subjectivity involved in defining τ_{cr}^* experimentally. Because of these factors, it may be better to think of τ_{cr}^* as a reference critical shear stress that may mark the transition from a condition of very sporadic dislodgment of grains which are quickly redeposited, to a condition of low but sustained transport rate.

Quantification of the bed load transport rate has been expressed in many different forms (Yang, 1996; García, 2008a), but the most prevalent form is to express the transport rate as a function of the excess bed shear stress, or the difference between the applied bed shear stress and that needed to produce motion. A typical relation expressing this type of formulation in dimensionless form is:

$$q_b^* = \alpha(\tau^* - \tau_{cr}^*)^\beta \tag{5}$$

where α and β are constant coefficients and q_b^* is the dimensionless bed load transport rate:

$$q_b^* = \frac{q_{bv}}{\sqrt{Rgd_m^3}} = \frac{q_{bw}}{g\rho_s}\frac{1}{\sqrt{Rgd_m^3}} = \frac{q_{bm}}{\rho_s}\frac{1}{\sqrt{Rgd_m^3}} \tag{6}$$

q_{bv}, q_{bw}, and q_{bm} are the unit-width transport rates of bed load by volume (L^3/t $\cdot$ L), weight (F/t $\cdot$ L), and mass (M/t $\cdot$ L) respectively, and R is the submerged specific gravity of the sediment $R = (\rho_s - \rho)/\rho$. An example of a specific bed load equation of the form of Eq. (5) is the well-known Meyer-Peter and Müller (1948) equation (MPM) for plane beds:

$$q_b^* = 8(\tau^* - \tau_{cr}^*)^{3/2} \tag{7}$$

For the MPM equation, the critical condition is $\tau_{cr}^* = 0.047$. Similar to this is the suggested modified form of the MPM equation developed by Wong and Parker (2006),

$$q_b^* = 3.97(\tau^* - \tau_{cr}^*)^{3/2} \tag{8}$$

For this modified form, $\tau_{cr}^* = 0.0495$. The Wong and Parker (2006) modification was motivated by the observation that the MPM equation has a tendency to over estimate transport rates in the lower-regime plane bed morphologies by up to 2–2.5 times. Wong and Parker (2006) suggested that the overestimation was due to an improper formulation of the grain shear where a theoretically unneeded correction for the presence of bedforms was used. Reformulating the shear and removing the correction for bedforms, Wong and Parker (2006) suggested that Eq. (8) actually provided a better fit of the original data.

The relationships presented here (Eqs. 5, 7, and 8) are only a few examples of published expressions for quantification of bed load transport rates. Many other equations have been proposed using the excess shear stress approach as well as other formulations such as a direct power-law functionality between q_b^* and τ^* (Einstein, 1950; Paintal, 1971). For example the Paintal (1971) formulation for low transport rates $(0.007 < \tau^* < 0.06)$ is:

$$q_b^* = 6.56 \times 10^{18}\tau^{*16} \tag{9}$$

Another well used method for gravel bed streams is the excess unit discharge equation of (Schoklitsch, 1949):

$$q_{bm} = 2500 S^{3/2}(q - q_c) \tag{10}$$

where q is in units of m^3/s-m, q_{bm} has units of kg/s-m, and q_c is the critical unit-width discharge defined for non-uniform sediment as, $q_c = 0.21 S^{-1.12}\sqrt{g d_{16}^3}$ with d_{16} is in units of meters (Bathurst et al., 1987).

To this point in the review, the expressions presented have only considered transport of a uniform sized sediment or have based the transport rates of a sediment mixture on the d_{50} of the bed material. When dealing with gravel, or gravel and sand mixtures, using a single grain size to represent the whole bed may not be most appropriate. In these cases, it is more appropriate to calculate the transport rate capacity for each individual size fraction and then calculate a total transport rate based on the percentage of grains in each size class (Yang, 1996). For example the total transport rate from Eq. (8) would be $q_b^* = \sum_{i=1}^n q_{bi}^* = \sum_{i=1}^n p_i q_{bci}^*$ where q_{bci}^* is the bed load transport capacity for size class i computed using Eq. (8) with d defined by d_i, q_{bi}^* is the transport rate per size fraction i, and p_i is the percentage of grains in size fraction i. Other relations have also been developed to account for the modifications to the incipient motion condition caused by variable grain sizes through hiding functions (Egiazaroff, 1965; Parker et al., 1982; Parker and Klingeman, 1982), and bed load transport equations have been developed which specifically account for sediment grain-size mixtures in gravel bed rivers using both substrate and surface layer grain size data (e.g., Ashida and Michiu, 1972; Parker et al., 1982; Parker, 1990; Wilcock and Crowe, 2003). The reader is referred to García (2008b) for details on these and other bed load transport rate equations.

Recently, Recking (2010) compiled an extensive database of transport rates from laboratory and field data, and developed an equation which appears to outperform previously developed equations over a broad range of grain sizes, sorting, and scales. To do this Recking (2010) considered that bed load motion can be decomposed into three phases. Phase 1 pertains to a sparse transport condition where the armor layer is left in tact; Phase 2 describes conditions of armor breakup; and in Phase 3, all grains are in motion. For lower transport rates, the Recking (2010) model is based on the principle that transport rate is a function of the applied bed shear stress and the critical bed shear stress required to produce motion (e.g. as in Eq. 5). For high transport rates, the model only takes the transport rate to be a function of the applied shear stress (e.g. as in Eq. 9)

The transition from bed load to suspended load occurs when flows and turbulent stress become high enough so that the upward drag caused by vertical turbulent fluctuations in the flow are strong enough to continually overcome the downward acting submerged weight of the particle. The value of the Rouse number,

$$Z_R = \frac{w_s}{\kappa u_*} \tag{11}$$

provides a convenient estimation of whether bed load or suspended load will dominate for a particular flow and sediment size. In Eq. (11) w_s is the settling velocity of a particle

of size d and κ is the von Karman constant. w_s can be easily calculated from the explicit relation of Ferguson and Church (2004) and κ is typically taken to be 0.4. Physically, the Rouse number represents the ratio of sediment settling due to gravity and the sediment diffusion upwards due to turbulent motion. As Z_R goes down, the system becomes more prone to suspension. Estimates of Z_R value ranges for the different modes are as follows (Julien, 1998): $6.25 < Z_R$ any transport will likely occur as bed load; $1 < Z_R < 6.25$ mixed bed load and suspended load; and $Z_R < 1$ full suspension. The Rouse number also provides and index for how uniformly distributed suspended sediment concentration is over the vertical. The lower the Z_R value, the more uniformly distributed. Higher Z_R values for suspended or mix suspended and bed load transport are indicative of profiles with higher concentrations near the bed.

Estimating whether or not the material passing through a culvert is traveling in suspension or as bed load may be important in design considerations of the culvert systems, and the Rouse number provides one way to estimate which transport mode will dominate.

2.3   Available Data

A specific objective of the literature review was to compile all available bed load, and general sediment transport, data into a single database that can be used to help guide the research. The research team has collected and compiled a database consisting of both field and laboratory data over a range of sediment sizes from published work over the time period of 1914–2008. Much of the earlier experimental sediment transport data from 1914–1973 was tabulated in Peterson and Howells (1973). This dataset included flow discharge, Q, channel width, w, depth, h, slope, S, the grain size for which 50% of the material is finer than by weight, d_{50}, gradation, $\sigma = 0.5(d_{50}/d_{16} + d_{84}/d_{50})$, sediment charge, C — which is a fractional volumetric sediment concentration in parts per hundred thousand of water, and water temperature.

More recently, Recking (2010) compiled a large volume of bed load specific data which includes much of the more recent work on transport with gravel and cobble sized material that has been conducted since the 1970's. The Recking (2010) compiled data consist of three main databases (Set 1, 2, and 3). Set 1 includes bed load transport data for fairly uniform sediment in laboratory flume studies. This set contains data from the studies listed in table 2 of Recking et al. (2008b) and data from table 1 of Recking et al. (2008a); some of the data in Set 2 are also listed in Peterson and Howells (1973). Data Set 2 from Recking (2010) includes the Idaho river field data from King et al. (2004), and Set 3 is a compilation of data from 21 different studies on over 19 different gravel bed rivers; the river names and study references are summarized in table 2 of Recking (2010). Each of these three sets contain slightly different parameters. Consistent parameters in all three sets include: discharge, channel width, slope, grain size, grain sorting, and either a measured bed load transport mass rate per unit width of channel, q_{bm}, or as a sediment concentration in units of mass per volume of water.

Table 1: Summary of addition bed load data added to database

Author	q (m^3/s-m)	w (m)	S (m/m)	d_{50} (mm)	Sorting	q (kg/s-m)
Wilcock et al. (2001)	0.03–0.13	0.6	0.001–0.020	1.0–13.4	0.53–2.41[1]	0.000–0.780
Lee et al. (2004)	0.05–0.14	0.6	0.002	2.1	1.38[2]	0.005–0.048
Wong et al. (2007)	0.07–0.20	0.5	0.008–0.015	7.2	1.20[2]	0.052–0.300

[1]defined as standard deviation in ϕ units.
[2]defined as the geometric standard deviation

Additional data on bed load transport not reported in the Peterson and Howells (1973) or Recking (2010) data sets was further compiled from the literature. This includes the laboratory data from Wilcock et al. (2001), Lee et al. (2004), and Wong et al. (2007). Table 1 list a summary of these studies.

All four databases of Peterson and Howells (1973) and Recking (2010) were merged with the data listed in Table 1 to create a single electronic database with common units; all duplicate entries between the Peterson and Howells (1973) and Recking (2010) data were removed. In all, the newly compiled data set consisted of 12,687 unique records of: Q volumetric water discharge in (m^3/s), q volumetric water discharge per unit width of channel (m^3/s-m), U bulk cross-sectionally averaged velocity (m/s), W channel width at cross section (m), H channel flow depth at cross section (m), R_h hydraulic radius of flow at cross section (m), S channel slope (m/m), d_{16} grain size of bed for which 16% of the material is finer than by weight (m), d_{50} grain size of bed for which 50% of the material is finer than by weight (m), d_{84} grain size of bed for which 84% of the material is finer than by weight (m), d_{90} grain size of bed for which 90% of the material is finer than by weight (m), a Sorting index which — defined differently among the different studies but typically taken as $\sigma_g = \sqrt{d_{84}/d_{16}}$, ρ_s sediment density (kg/m^3), ρ water density (kg/m^3), q_{bm} mass flow rate of sediment per unit width of channel (kg/s-m), and C_{ppht} sediment charge in parts per hundred thousand — a form of mass or volume fraction concentration.

2.4 Sediment Transport in Pipeline Systems

A significant body of work pertaining to the transport of solids in pipelines was conducted by numerous researchers from the early 1900's up through the 1970's. Applications for this work were largely focused on industry processes such as dredging, slurry transport, and the material conveyance of particulates such as coal, ores, pulp, and raw chemicals (Vanoni, 1975; Chien and Wan, 1999). Much of this work, as it pertains to sediment movement, has been summarized in Graf (1971), Vanoni (1975), and Chien and Wan (1999). While the material is slightly removed from the context of short culvert sections, a brief introduction to the main relevant findings is presented to aid in gaining a further appreciation for the processes and methods of analysis that might be involved in transport of sediment through culverts under high stage.

Transport of sediment in pipeline systems has been classified into five different categories, or regimes (Vanoni, 1975; Chien and Wan, 1999). These regimes are: I) homogeneous flows where all particles are nearly uniformly distributed through the conduit section; II) heterogeneous flow conditions where all particles are in suspension but the vertical concentration is not uniform; III) flows with active bed load transport and possible development of bedforms within the pipe; IV) flows where an immobile bed exists and acts as a solid wall; and V) conditions of complete blockage by immobile deposited sediment. Fig. 6a graphically depicts these regimes as a general function of flow velocity and particle size.

In pipeline systems, important items to consider are the head loss and the sediment concentration that can be transported at a given hydraulic gradient. In general, head loss increases with increasing sediment concentration, and the region dividing heterogeneous flow (regime II) and flows with moving beds (regime III) is closely related to the region of minimum head loss for a given concentration (Fig. 6b) (Vanoni, 1975). Because of this, the optimum condition for transporting the largest amount of sediment per unit of energy expended is in the heterogeneous flow regime just at the limiting deposition velocity (Vanoni, 1975).
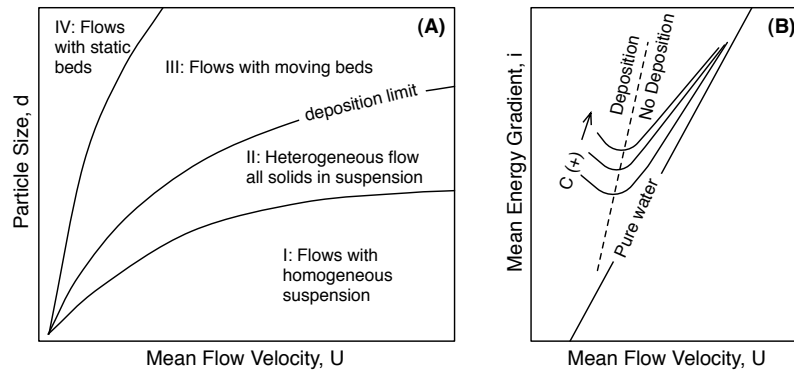
Figure 6: (A) pipeline flow regimes, and (B) general head loss and sediment concentration curves for a given pipe size. [both figures reproduced after Vanoni (1975)]

Pipeline flows with bed load transport are likely somewhat similar to the critical conditions leading to clogging in culvert systems. Head loss in pipeline systems with bed load (regime III) is greater than when all material travels in suspension at the critical deposition velocity. From regime III experiments with gravel and other solids, the semi-empirical analysis of Newitt et al. (1955) suggested that the head loss in pipeline flow with bed load transport could be calculated as:

$$\frac{i_m - i}{C_v i} = 66R\frac{gD}{V^2} \tag{12}$$

where i and i_m are the gradients of the piezometric head line for a pure fluid and mixture respectively, C_v is the sediment discharge concentration by volume, R is the submerged specific gravity of the sediment, D is the pipeline diameter, and V is the cross-sectionally averaged velocity. This is in contrast to the head loss in a clear fluid which can be expressed

as:

$$\frac{i_m - i}{C_v i} = R \tag{13}$$

These relations are based on the assumption that resistance can be linearly decomposed into a clear water and sediment component, such that the summation of the two results in the total resistance of the mixture, i.e. $i_m = i + i_s$ or $i_s = i_m - i$.

The equation of Newitt et al. (1955) suggest that the hydraulic gradient of the mixture, i_m, is a function of sediment concentration, pipe size, and average flow velocity. However, summarizing data pertaining to the transport of sand in pipelines, Laursen (1956) found i_m to be most strongly a function of concentration and practically independent of pipe size, sediment size, and flow velocity (Fig. 7a). A third expression for head loss in pipeline systems with deposition of sand came from the analysis of Gilbert (1960):
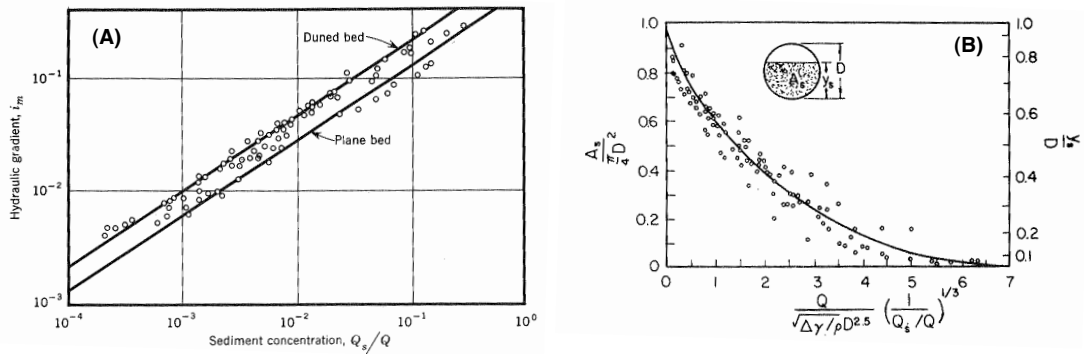
Figure 7: (A) Effects of sediment concentration on the hydraulic gradient, i_m, and (B) blockage due to deposition, A_s is blocked area. [Both figures were developed by Laursen (1956) and are taken from Vanoni (1975)].

$$\frac{i_m - i}{C_v i} = 150 \left[\frac{V}{g4R_h R} \sqrt{C_D} \right]^{-3/2} \tag{14}$$

where C_D is the drag coefficient for the sediment particles. Other equations exist to predict head loss in pipeline systems when deposition and bed load transport occur; however, no single equation is regarded the most accurate for all cases (Chien and Wan, 1999). Eq. (12) was proposed by Babcock (1970) to represent the upper limit for head loss and correspond to a condition where particles are sliding along the bottom of the pipe.

The work of Laursen (1956) also resulted in Fig. (7b), which is useful in estimating the percentage of pipeline blockage due to sedimentation. If a critical blockage ratio is defined, then Fig. (7b) can be used to aid in designing a system for which the maximum blockage ratio is not exceeded. For example, if we choose a maximum blockage ratio or

$A_s/(0.25\pi D^2) = 0.75$, a pipe can be design to insure that:

$$\frac{Q}{\sqrt{Rgd^5}} \left(\frac{1}{Q_s/Q}\right)^{1/3} > 1 \tag{15}$$

If deposition does occur within a pipeline, the flow becomes one with a movable boundary. Chien and Wan (1999) notes that such flows are not essentially different than flows in rivers, and that most of the research pertaining to bed load transport and sediment laden flows in open-channels are directly applicable to pipeline systems (Chien and Wan, 1999, p.837). Bed load transport rates can therefore be expressed in the form of an excess bed shear stress model (Eq. 5) or other forms which are also applied to open channels.

For total sediment transport load estimation, i.e. bed load plus suspended load, Graf and Acaroglu (1968) examined the functionality of a dimensionless transport parameter, ϕ', with a dimensionless shear intensity parameter, ψ', and determined that the power law relation of:

$$\phi' = 10.39\psi'^{-2.52} \tag{16}$$

best fit a large range of data containing experimental results from both closed conduit and open-channel flows (fig. 8); in Eq. (16), ϕ' and ψ' are defined as:

$$\phi' = \frac{C_v V R_h}{\sqrt{Rgd_s^3}}, \quad \text{and,} \quad \psi' = \frac{Rd_s}{i_m R_h} \tag{17}$$
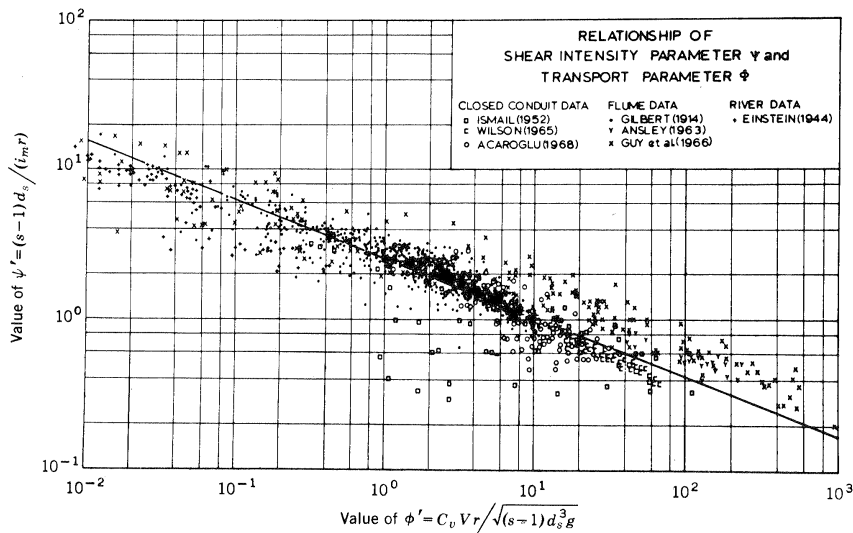
Figure 8: The ZSGrafAcaroglu1968 plot of ψ' vs ϕ' with experimental data. [from Vanoni (1975)]

A few other closing notes can be made regarding the transport of solids in pipeline systems. First, Zenz and Othmer (1960) observed that a circular pipe cross-section allowed for the

lowest critical velocity between deposition and no deposition when all other conditions were equal. This implies that a circular pipe is the optimum shape for transporting solids. Secondly, because particles are largely kept in suspension by upward directed flow momentum due to secondary currents or turbulent diffusion, pipe geometries which enhance these flow features will result in an increased carrying capacity of sediment. For example, Chiu and Seman (1971) noted that even small amounts of spiraling secondary currents aided in keeping particles in suspension in both circular and square pipes; this principle is reinforced by the work of Howard (1939, 1941) which showed that pipe spiraling helped to keep sands and gravels in suspensions at lower flow rates.

2.5   Flow and Sediment Transport in Staggered-Barrel Culverts

2.5.1   General Principles and Specific Studies

Vertically offset multi-barrel culvert systems, also known as multicell and staggered barrel systems, are beneficial for reducing the disturbance that a road crossing and single-barrel culvert can create to the continuity of a stream. The natural cross-sectional geometry of a stream is a dynamic equilibrium condition that results from the coupled flow and local bed material. The discharge which is most responsible for this shape is the discharge that produces the most geomorphic work and is typically associated with the flow condition that, over a period of time, moves the most bed load. This flow condition is known as the "effective discharge" of a stream (Wolman and Miller, 1960; Biedenharn et al., 2000), and is typically associated with the bankfull flow condition and events that have return periods of 1 to 2 years (Whiting et al., 1999; Emmett and Wolman, 2001). Therefore, to obtain stream continuity under the road, the overall cross sectional flow area and slope of the culvert system should match that of the bankfull stream geometry and slope during a 1 to 2 year return period flow. However, culvert systems are typically designed to handle flows with return periods that are much larger than this (5–100 yr return periods), and therefore single-barrel culverts require a cross-sectional flow area that is larger than that of the natural bankfull stream geometry (Fig. 9a). This increased cross-sectional area can lead to flow deceleration and deposition of sediment at low-flow conditions, destabilization of stream banks, and erosion of sediment downstream of the crossing (Johnson and Brown, 2000).

The idea behind staggered barrel culverts is to design a system which mimics the natural stream and improves sediment and flow continuity over a range of flow conditions (Johnson and Brown, 2000; Wargo and Weisman, 2006). The system is built around a larger centralized culvert designed to handle the bankfull or effective discharge. The capacity of this larger culvert is then augmented with smaller culverts whose inverts are elevated relative to the main barrel (Fig. 9b). During low flow periods, all flow and sediment pass through the main barrel. The reduction in flow area in this main barrel relative to a larger single barrel culvert means that flow depths and bed stresses are higher at these low flow conditions. It is likely that this would lead to better sediment continuity and also allow
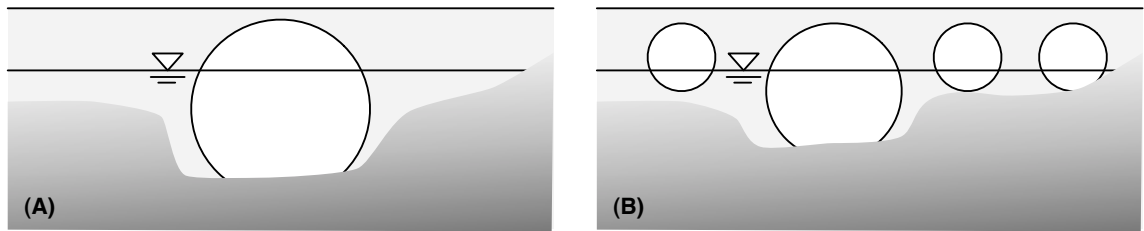
Figure 9: Road crossing with (A) standard single-barrel design; channel has been widened and deepened. (B) staggered barrel approach. Natural stream geometry has been left in-tact.

for better fish passage. At higher stage, the smaller culverts become accessible and the hydraulic capacity of the system is increased. These invert-raised barrels can be thought of as the "flood plains" of the culvert system.

Very few studies have been conducted to examine the hydraulics or sediment transport characteristics of staggered barrel systems. The two studies known to the authors which specifically experiment with staggered barrel, or multicell, systems (i.e., Wargo and Weisman, 2006; Haderlie and Tullis, 2008) are summarized next. These summaries are followed by the presentation of pertinent information from other studies on self-cleaning of multi-barrel box culvert systems and sediment transport in single barrel and bottomless culverts.

Wargo and Weisman (2006) performed experiments on single and staggered barrel culvert systems with movable sediment in the laboratory specifically looking at flow depths within the culvert and outlet scour. The study downscaled a prototype single-cell culvert which was designed for a 25 year flow on the Benson Hollow Tributary, a gravel bed stream in Wyoming County, PA. The prototype had built up a region of deposition on the upstream side of the culvert and had developed a scour pool on the downstream end. The experiments of Wargo and Weisman (2006) considered a scaled low-flow, bankfull, and 25-year flow event. Figure 10 depicts a cross section of the experimental setup. For all three flow conditions, flow depths in the multicell culvert were higher than those in the single cell and scour depths were less. The average reduction in the volume of scour with the multicell system was 52% compared to the single cell culvert with an average reduction in perch height of 55%. Overall, the study demonstrated the increased flow and sediment continuity of the multicell system relative to the single cell. The increased flow depths through the culvert would be beneficial for fish passage as stated by the authors (Wargo and Weisman, 2006), but the increased flow depths can also be interpreted as an increase in the bed shear stress, $\tau_B = \rho g R_h S$, and therefore an increase in the bed load transport rate relative to the single cell for equivalent discharge.

Haderlie and Tullis (2008) performed laboratory experiments on single and multi-barrel culvert systems with rigid boundaries to examine the differences in hydraulics between the two systems. A main objective of the study was to evaluate the ability of single barrel
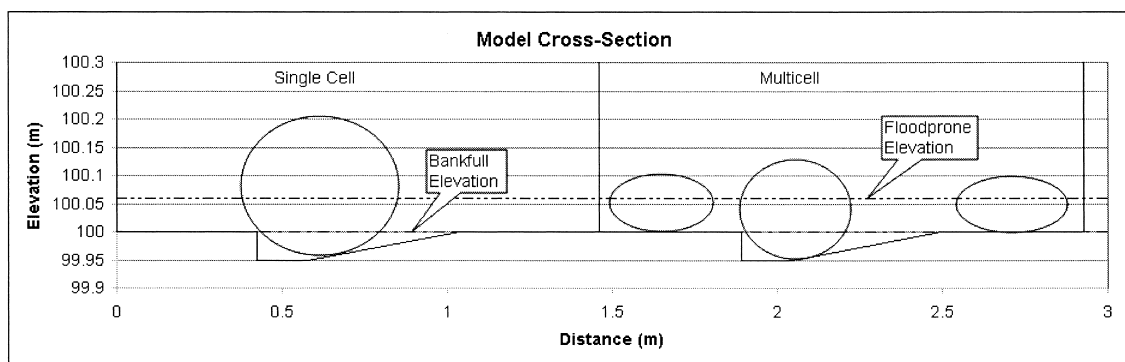
Figure 10: Cross section of the experimental setup of Wargo and Weisman (2006). [from Wargo and Weisman (2006)]

culvert head-discharge relations to predict multi-barrel head-discharge relations using superposition with circular culverts under inlet control conditions. The study also sought to examine the individual flow rates and velocities in multi-barrels systems and the impact of inlet vortices on flow rate capacity. Haderlie and Tullis (2008) compared one, two, and three barrel arrangements while varying inlet conditions and culvert spacing in the horizontal and vertical. Approach flow conditions included uniform and skewed arrangements in approach geometries of rectangular and trapezoidal channels as well as a reservoir condition. All experiments were run under inlet control conditions. Results of the experiments showed that superposition of single barrel head-discharge relations reasonably predicted ($\pm 3\%$) the multi-barrel head-discharge relations for non-skewed approach flows in all but the vertically staggered arrangement in a trapezoidal channel. Skew in the approach flow led to an over prediction of the flow rate in the multi-barrel system by the superposition method using the single-barrel relation. For the trapezoidal channel inlet condition with three barrels and a lowered center-barrel invert, it was found that superposition could be used only when the ratio of the upstream headwater depth to culvert diameter was less than 1.4 ($H_w/D < 1.4$). For conditions of $1.4 < H_w/D < 2.3$ with this arrangement, Haderlie and Tullis (2008) found that the center lowered-invert barrel became more efficient (by 7%) compared to the single barrel case; the flow through the two outside barrels remained consistent with the single-barrel relation. This increased flow capacity in the middle barrel was also noticed in the non-staggered arrangements and was attributed in part to flow contraction and intermittent surface vortices near the barrel inlets (Haderlie and Tullis, 2008). Based on the various magnitudes of the percentage difference between the head-discharge relations, Haderlie and Tullis (2008) suggested that superposition of single-barrel head-discharge relations are suitably accurate for hydraulic design purposes.

Other studies examining transport of sediment in culverts have done so with vertically aligned multi-barrel box culverts (Muste et al., 2010), single-barrel bottomless culverts (Kerenyi et al., 2003; Crookston and Tullis, 2006; Kerenyi et al., 2007; Crookston, 2008), and single-barrel circular culverts (Goodridge, 2009).

Ho and Muste (2009); Muste et al. (2010) examined flow velocity and sediment transport in multi-barrel box culverts for the purpose of developing self-cleaning design guidelines. The study used laboratory experiments and numerical simulations. To achieve the self-cleaning properties and restore the natural stream functionality, the study focused on methods of increasing the centerline velocity of the approach flow. This was accomplished using fillets on either side of the inlet which caused flow contraction and acceleration. Ho and Muste (2009) note that the fillets can be implemented at the time of construction or at anytime during the lifetime of the culvert system. The study also observed that sedimentation patterns and problems are compounded by the complex flow structure in various regions of the culverts, particularly near the inlet. For example, Muste et al. (2010) notes that the assumption of uniform flow conditions in the transitional expansion between the natural channel and road crossing was violated due to the presence of strongly non-uniform flow in this region. Muste et al. (2010) further suggests that flood-wave propagation and asynchronous correlation between the flow hydrograph and sedigraph may factor in to deposition patterns.
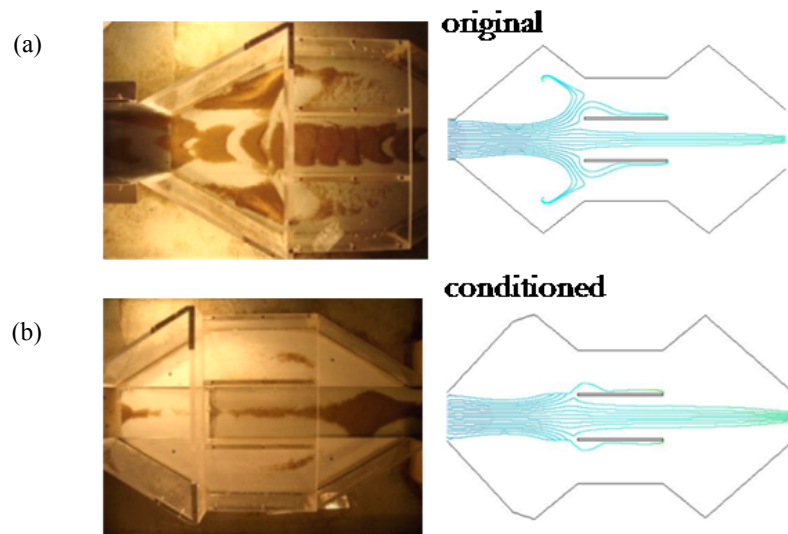
Figure 11: Comparison of a three-box culvert design studied by Ho and Muste (2009), (a) without the self-cleaning system, and (b) with the suggested self-cleaning system [from Ho and Muste (2009)].

Similar to the staggered barrel system, bottomless culvert design (Fig. 12) is motivated by a desire to increase stream continuity from one side of the road to the other for the purpose of retaining the geomorphic function of the stream and minimizing deterrents for fish passage (Maxwell et al., 2001). With bottomless culverts, the goal is to maintain a consistent grain size and morphologic state in the bed under the roadway. The most recent work in this area was conducted by Crookston and Tullis (2006) and Crookston (2008). These studies looked at the stability of different sized sediment in circular buried-invert culverts and bottomless arch culverts and the response of the bed to variable H_w/D and

inlet conditions. Experiments were carried out in a laboratory flume, and general scour patterns were examined for both open channel and partially pressurized flows. The study tested pea gravel, 19 mm angular gravel, 50 mm rounded cobbles, and 50 mm angular rock as substrate material for the system. Results from the study showed that the Shields criteria for particle motion (Eq. 3) performed reasonably well in defining the incipient motion condition within the culvert, and that scour in the culvert vicinity was deepest near the exit of the culvert. Scour was also observed near the entrance within the culvert. Kerenyi et al. (2003) and Kerenyi et al. (2007) also examined flow and sediment movement in bottomless culverts with a focus on scour. In their in-depth study, they concluded that primary scour depth for bottomless culverts could be calculated using abutment scour concepts and the flow distribution at the culvert entrance if an adjustment factor was used. Details on their methodology can be found in Kerenyi et al. (2007).

Figure 12: Example of a buried-invert culvert [from Crookston (2008)].

The single barrel study of Goodridge (2009) is a recent study that examined the impact of deposited and movable sediment beds on culvert hydraulics and sediment transport predictions. The study used sand and gravel and measured sediment transport rates through a 30.2 cm inner diameter culvert under open channel and pressurized pipe flow. Figure 13 shows an overview of the experimental setup used. Three different bed elevations, or bed blockage ratios, were considered each using different grain size distributions ($d_{50} = 6.5$ and 1.33 mm) under both open-channel and pressurized flow conditions. The study spent considerable effort in measuring the incipient motion condition under various bed states and much of the data is presented in tabular form in Goodridge (2009). Goodridge (2009) compared measured bed load transport rates with predicted values from eight bed load equations developed for open-channel flows and found that large discrepancies existed between the measured and predicted values. By re-calibrating these equations and accounting for a deposited sediment layer within the culvert, Goodridge (2009) developed a methodology for more accurately calculating sediment yield in experimental culverts. The eight equations used in the study were the: Meyer-Peter and Müller, Engelund and Hansen, Shields, Toffaleti, Schoklitsch, DuBoys, Yang, and Rottner methods. Based on model performance, Goodridge (2009) recommended some models over others. For transport of sediment with $d_{50} = 6.5$ mm, the DuBoys method was recommended. For coarse sands

with $d_{50} = 1.33$ mm, the author recommended the Toffaleti method. The study contains detailed information pertaining to the experimental methods, sediment classification, and analysis procedures. Because of this, the dissertation is a valuable resource for the present study on staggered barrel culverts.

Figure 13: The experimental setup of Goodridge (2009) [figures 14 and 15 from Goodridge (2009)].

2.6 Available Data

The only study to use a movable boundary with a staggered barrel arrangement was the study of Wargo and Weisman (2006). Unfortunately this study only reports perch heights and scour depths downstream of the main culvert and does not include any transport rate data. Data pertaining to sediment yield from the Goodridge (2009) study of flow and transport in single barrel systems has been compiled from several tables in appendix E and K and put in digital form with consistent units. The dataset contains a total of 64 entries of sediment transport rates using two different sediment sizes ($d_{50} = 6.5$ and 1.33 mm) under pressurized and open-channel flow conditions. Included in the dataset are values for: flow state (pressurized or open channel), bed elevation y (m), culvert diameter D_c (m), discharge Q (m^3/s), average cross-sectional velocity V (m/s), the hydraulic radius R_h (m), the energy slope S_e (m/m), d_{50} (m), sorting $\sigma_g = \sqrt{d_{84}/d_{16}}$ (m/m), ρ_s sediment density (kg/m^3), ρ water density (kg/m^3), the bed load mass flow rate Q_{bm} (kg/s), and the sediment charge in parts per hundred thousand C_{ppht}.

2.7 Implications

This literature review provides a summary of the relevant information pertaining to sediment transport in staggered barrel culvert systems looking at transport in open channels, pipeline systems, and culverts. The mechanics of sediment transport in open-channel flow are essentially the same as those in culvert systems. The differences between the two centers primarily on, 1) how the drag force exerted on the bed, or τ_B, is calculated in the culvert under open-channel and pressurized conditions; and 2) on the effects of localized non-uniform flow conditions around the culvert entrance and exit which may produce scour.

The study of Haderlie and Tullis (2008) suggest that using single-barrel head-discharge relations with the principle of superposition is reasonably accurate for most multi-barrel systems when the approach flow is non-skewed. However, the study also highlights that the multi-barrel condition that most deviates from the superposition principle is the case where a central barrel has an invert elevation below the two flanking barrels, however as a practical matter superposition was assumed in the present experimental study reported in subsequent chapters.

The experimental work of Ho and Muste (2009), Muste et al. (2010), and Goodridge (2009) provide a substantial body of work pertaining to methodologies for experimenting with and measuring flow and sediment transport processes in and around single and multi-barrel culvert systems.

In the course of this review, the research team has compiled and developed one of the largest known sediment transport database with an emphasis on bed load transport. The database contains data from laboratory flumes, natural rivers, and laboratory culvert systems. This database itself is an important contribution (a substantial intent of Task 1). This database was used to aid in interpretation of the measured transport rates in the staggered barrel systems and development of screening tools to assist in evaluating culvert solids conveyance capacity.

3   Screening Tool

One major objective of the research project was the development of a screening or assessment tool to potentially assist in the identification of existing stream crossings for which staggered barrel culverts might be appropriate. The development of a screening tool was seen as and remains a formidable challenge in the context of completing an easy-to-use tool suitable for design by TxDOT engineers. However, the promise of such a tool makes it useful to also support experimental and literature interpretation. This chapter describes the screening tool creation process as well as the tool itself.

3.1   Creation of a Screening Tool

The research team selected a heavily empirical or database-search approach founded on literature-derived database constructed as part of Task 1 of the research project. The database-search approach was pursued instead of a regional regression-based analysis, because of the size and variety of the database. Further, it remains an open problem as to how to link the flume-based experimental results in the database directly to field conditions in Texas; for this reason conventional parametric regression likely would result in nuances of application for TxDOT engineers.

3.2   General Approach

After the database was constructed (Task 1), a database-search or "similarity" algorithm was developed to be used in a fashion similar to the following example computation. Peterson (1975) presented a series of design charts that related certain hydraulic properties that the researchers deemed assessable to practicing TxDOT engineers, either by direct measurement or reasonable desktop approximation. These charts can be used to make estimates of mobile solids flux in a stream from predictor variables such as channel slope, clear-water discharge, and solids dimension. These charts provided a generic guide to the screening tool, but the researchers departed from Peterson (1975) in two substantial ways.

First, the charts in Peterson (1975) are regression models of the underlying database considered by Peterson. The researchers chose to directly access the database using a nearest-neighbor algorithm approach, which eliminates a need to interpolate the regression results (the example that follows will illustrate the challenge in using the charts). Secondly, whereas the charts represent an equilibrium condition by virtue of the multi-dimensional "averaging" in the regression analysis and therefore allow some insight into how a system might respond to engineered change, the researchers decided that direct similarity-lookup in database through the use of normalized distances would convey similar insight. Furthermore, the Peterson charts were necessarily segregated into groups by solids characteristics dimension and were all values plotted on a single chart, it would be unreadable and hence

unusable to the researchers and TxDOT engineers. A database searching tool eliminates this readability issue, admittedly at the expense of visual guidance and the benefit of the human-mind's ability to discern patterns and relations.

3.3   The Universal Flow Diagram Charts — The Path to the Database Search Tool

Figure 14 is a universal flow diagram from Peterson (1975). The chart represents the relations between clear water discharge per unit width of channel, q, the depth of flow, h, a characteristic solids diameter, D_{50}, a solids concentration in parts per hundred thousand, C, and energy slope, S.
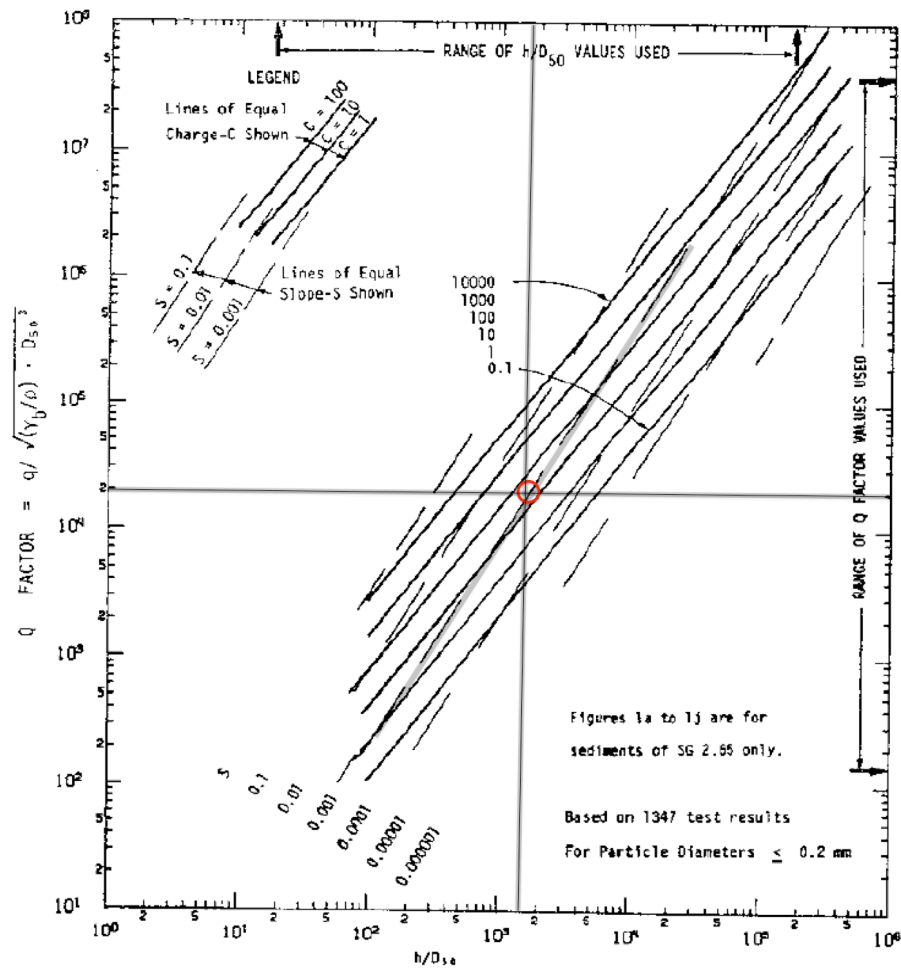

Figure 14: Example of Mobile Bed Design Chart Peterson (1975)

The figure is complex and a numerical example is critical. Suppose a particular channel has

a discharge of about 20 m³/s with a width and depth of about 8 and 0.90 feet, respectively. In SI units (the charts require SI entry), these predictor variables are: $Q = 0.566$ m³/s, $W = 2.439$ m, and $h = 0.274$ m. Further suppose the channel material has a $D_{50} = 0.2$ mm, that specific gravity is 2.65 (quartz), and that energy slope is $S = 0.001$ (0.1 percent). The question to ask and answer is "What is the anticipated solids flux in the system?"

To use the chart, the analyst performs the following computations:

1. Compute the discharge per unit width of the channel[4].
   $q = \frac{0.566}{2.439} = 0.232$ m³/s/m.

2. Compute the "size factor" from
   Size Factor $= (\frac{\rho_s}{\rho_w} - 1)g(1000D_{50})^3 = (\frac{2.65}{1.00} - 1.0)(9.8 \text{ m/s}^2)(1000(0.2))^3 = 1.29 \times 10^{-10}$ m⁶/s²/m².

3. Compute the "Q-factor", which is the vertical axis of the chart from the ratio of discharge per unit width and the square root of the size factor,
   Q-factor $= \frac{q}{\sqrt{\text{Size Factor}}} = \frac{0.232}{\sqrt{1.29 \times 10^{-10}}} = 20,431$
   This value is shown on Figure 14 as the horizontal line that intersects the vertical axis at $\approx 20,000$.

4. Compute the depth to diameter ratio[5]
   $\frac{h}{1000D_{50}} = \frac{0.274}{1000(0.2)} = 1371$
   This value is shown on Figure 14 as the vertical line that intersects the horizontal axis at about 1,300.

5. The intersection of these two lines returns estimates of the energy slope and the solids charge. The location of these estimates is indicated by the circle on Figure 14. In this case the slope is close to the observed slope of 0.001, and the charge is somewhere between 10 and 100 ppht. For the sake of simplicity, a value of 50 is assumed.

6. Once the charge is estimated the estimation of solids mass flow is simply the product of the clear water discharge, clear water mass density, and the charge, as
   $\dot{M}_s = \frac{C_s}{100,000}\rho_w q = \frac{50}{100,000}(1000\text{kg/m}^3)(0.232\text{m}^3/\text{s/m}) = 0.11\text{kg/s/m}$
   This value when multiplied by the channel width estimates the solids mass flux in the system. In this case about 0.3 kg/s, or 0.6 lbs/s.

These computations are as far as the universal flow diagrams originally were intended for application by Peterson (1975). However, the researchers suggest an additional consideration for the purposes of evaluating a culvert system's solids capacity: "What added volume of culvert capacity might be needed to accommodate the solids, by a displacement assumption?" Using the density of the solids and their mass flux as an estimate of the water that would be displaced in the culvert provides a simple estimate of the added capacity the culvert must accommodate. In the example presented, the added capacity for a

---

[4]The hydraulic radius concept is implied in the literature so that every channel is converted into an equivalent rectangular channel.
[5]Peterson (1975) has a factor of 1000 in the denominator — presumably a units scaling factor.

hydraulic structure designed for a clear water discharge of 20 m^3/s would anticipate using this theory is about 0.004 m^3/s. This is obviously a trivial amount. However, if the charge were substantially larger the added capacity needed would change and might materially influence the design decisions of the TxDOT engineer.

These charts and the accompanying computations are reasonably straightforward, but the charts themselves are difficult to read, different charts are used for different size ranges, and re-creating new charts from the expanded database is simply not feasible within the constraints of the research project. Furthermore, the research team wanted to be able to enter the database with missing and possibly arbitrary variables.

3.4   The Screening Tool — A Flexible Search Engine

A database-search approach was designed that would search the literature-derived database with a set of predictor or input values expected to be available to an analyst. The initial values selected were channel slope in vicinity of a stream crossing, a mean particle diameter, and anticipated water discharge or mean velocity. The idea and justification behind the screen tool is to non-parametrically locate within the database a set of 5 nearest (most similar) values using an L2 norm (Euclidean distance) as the measure of "closest" or "most similar" in high-dimensional space. The screening tool then returns the nearest observed value and a distance-weighted interpolated value of the un-queried value of charge (solids concentration), as well as other entries associated with the 5 nearest records in the database.

Unlike the charts, the analyst enters the database in the native unit-space of the input variables (albeit in SI units) and the algorithm searches for nearest matches. In other words, dimensionality, which is so important in Peterson (1975), is not required for the screening tool. Upon completion of the search, the 5 nearest matches are returned and used in a subsequent computation to estimate by either distance-weighted mean or arithmetic mean, the value of charge (or mass flux) associated with the search values. The tool greatly speeds up the process of estimating charge for a stream based on the large database developed in Task 1.

The screening tool was developed using the MatLab (Math Works, Inc., 2008) environment. The GUI tool was developed in the same environment, but a compiled version was developed for deployment to users without installed MatLab instances. The programming was accomplished by USGS researchers with guidance from TTU.

3.5   Concept of Distance

The concept of distance is vital to the search engine. In the screening tool the search values (S, Q, D_{50}, ...) are compared to their commensurate values in the database and a distance is computed from the search values to values in the database. The nearest values

in n-dimensional distance are selected and used for the estimation of charge for the search values. The search engine has several different kinds of distances that the engineer may select.

3.5.1   Minkowski Distance

The distance between the search values and a database record is computed using the equation

$$\text{Distance} = (|(x_{1\ data}-x_{1\ search})|^p + |(x_{2\ data}-x_{2\ search})|^p + \ldots + |(x_{n\ data}-x_{n\ search})|^p)^{\frac{1}{p}} \tag{18}$$

Equation 18 when $p > 0$ and integer produces a quantity known as the Minkowski distance. The Euclidean distance between the two vectors $\mathbf{x}_{data}$ and $\mathbf{x}_{search}$, which is the hypothenuse-type distance that engineers are readily familiar with, is the special case of Equation 18 when $p = 2$.

In many situations, the Euclidean distance is insufficient for capturing the actual distances in a given high-dimensional space, if traverse of that space along a hypothenuse is infeasible. For example, taxi drivers in Manhattan should measure distance not in terms of the length of the straight line to their destination, but in terms of the Manhattan (taxi distance) distance, which takes into account that streets are either orthogonal or parallel to each other. Additionally, when some elements are unknown (as may be the case in our searches) or the noise in the elements is substantial, the Euclidean distance is not the most appropriate (Eriksson and van den Hengel, 2010) measure of distance.

The taxi distance is also called the L1 norm and is the special case of Equation 18 when $p = 1$. This distance measures the shortest path along Cartesian axes (like city streets).

The search tool includes the generalized Minkowski distance and the Euclidean and taxi distances as separate choices. Two other experimental distances are included but are not discussed in this report.

3.6   Data Value Standardization

The variables in the literature-derived database are not expressed in the same magnitude, range, and scale. For example, discharge values are several orders of magnitude larger in the database than mean grain diameter, hence the two are not directly comparable when computing a distance for the search algorithm.

In such a case, one way to facilitate direct interpretation for comparing composite indices of the original data having different magnitudes and unit systems is to use normalization. Normalization serves the purpose of bringing the indicators into the same unit scale or unit base and makes distance computations appropriate.

3.6.1   Z-score Standardization

Z-score standardization is a commonly used method that converts all indicators to a common scale with an average of zero and standard deviation of one. This transformation is the same as computing a standard-normal score for each data value. The average of zero avoids the introduction of aggregation distortions stemming from differences in indicators means. The scaling factor is the standard deviation of the indicator across, for instance, the velocities, slopes or charges being ranked. Thus, an indicator with extreme values will have intrinsically a greater effect on the composite indicator.

The raw score on each data entry is converted to a Z-score, then distances are calculated using the Z-scores for each variable rather than the raw value. Upon completion of the distance calculations and selection of the nearest neighbors, the results are untransformed back into the raw values for subsequent presentation.

3.6.2   Unit-Interval $[0, 1]$ Standardization

An alternate approach built into the screening algorithm is an option to use a mapping of each variable in the database to a $[0, 1]$ scale and linearly weight within the scale. This standardization has the same goal as Z-score, which is to prevent one variable because of its relative magnitude, from overwhelming the distance computations. The unit-interval $[0, 1]$ standardization technique differs from the Z-score in that the variability is governed by the minimum and maximum value for each variable, and hence extrapolation is not tenuous. Fortunately, for the present application, extrapolation is not anticipated to be meaningful, so the limitation is negligible.

3.6.3   Unstandardized

The unstandardized approach was left as an option, but is not recommended. Using this approach, discharge and/or velocity completely dominate the search algorithm, almost to the exclusion of the other variables. The option is useful for method testing and database error detection, but otherwise not recommended.

3.7   Graphical User Interface (GUI) of the Screening Tool

Two user interfaces were simultaneously developed, a conventional command-line-interface that allows the analyst to search the database using any combination of search values and a graphical interface that searches using only slope, D_{50}, discharge, and velocity. Only the graphical user interface (GUI) is described here.

Figure 15 is a screen capture of the screening tool. The GUI version is divided into 5 distinct panels. The upper panel that traverses the entire top portion of the tool is in-
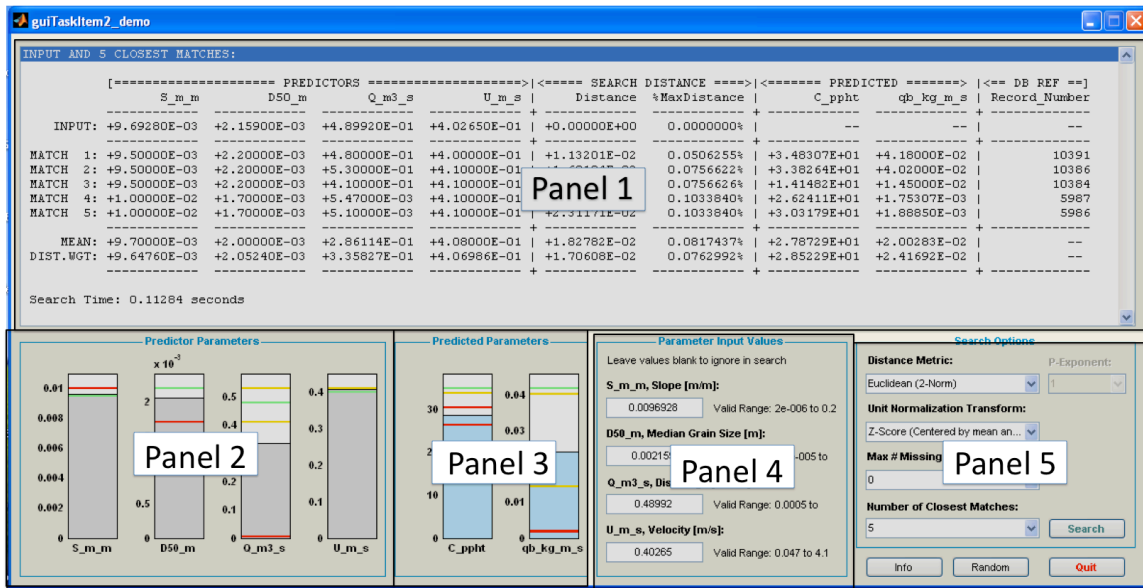
Figure 15: Screening Tool (Graphical User Interface) Database Search Engine.

put/output echo region. The search values appear along the top, and the nearest match values, arithmetic mean, and distance weighted means appear along the bottom of the upper panel. The right panel shows the database record identification. The record identification might be of interest in order to examine the depth and width or other values that are not directly reported by the GUI.

The lower four panels from left to right are the match values represented as color coded bar charts and the arithmetic mean of the variables, the predicted values of charge and mass flux, also represented as bar charts. The input panel is the area to the right of the bar charts where the engineer would enter data, and the right panel is where the engineer selects the distance model, standardization model, missing data model, and runs the search.

The tool also contains instructions for its use, by selecting the Info button in Panel 5, the instructions are presented in a dialog box as depicted in Figure 16.

To illustrate the tool as compared to the charts we can repeat the same problem as earlier. Recall that the prior example used a discharge of 0.566 m³/s, $D_{50} = 0.2$ mm, $S = 0.001$. Other values used the the universal flow diagrams are not used in the GUI (but can be searched using the command-line-interface). If these values are provided to the search algorithm, the search algorithm returns the results shown in Figure 17.

The resulting arithmetic mean value of charge based on the 5-nearest database records is $\dot{M}_s = \frac{50.15}{100,000}(1000 \text{ kg/m}^3)(0.566 \text{ m}^3/\text{s}) = 0.284$ kg/s.

The resulting distance weighted mean value of charge based on the 5-nearest database records is
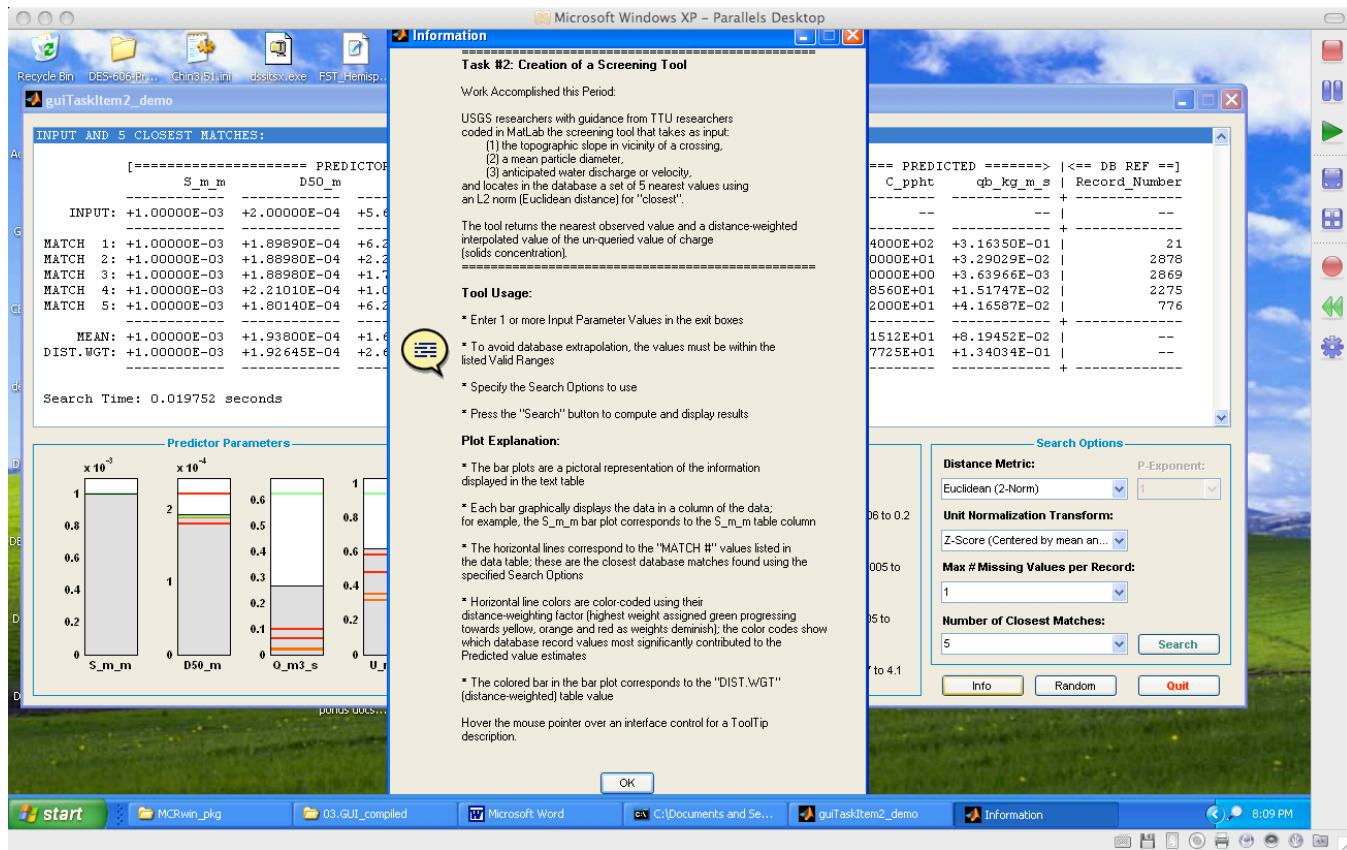
Figure 16: Screening Tool (in background) with Built-In Instructions displayed.

$\dot{M}_s = \frac{66.77}{100,000}(1000 \text{ kg/m}^3)(0.566 \text{ m}^3/\text{s}) = 0.374 \text{ kg/s}.$

Both these $\dot{M}_s$ estimates are about the same as using the universal flow diagrams[6].

3.7.1 Testing of the Screening Tool

The screening tool was tested against actual database entries to ensure the algorithms return exact matches when such matches exist. **This testing was successful.**

The tool was further tested with missing entry items, which was the main reason for the tool development, against actual database entries to ensure the tool returns close and/or exact matches where they exist. **This testing was successful.**

Lastly, as a further test of the tool, three queries from examples in Peterson (1975) are

---

[6]The search engine returns mean and distance weighted means by column. The analyst must be aware that the estimated mass flux reported in the tool is an estimate that correlates with the mean values on the return records and not the search discharge.
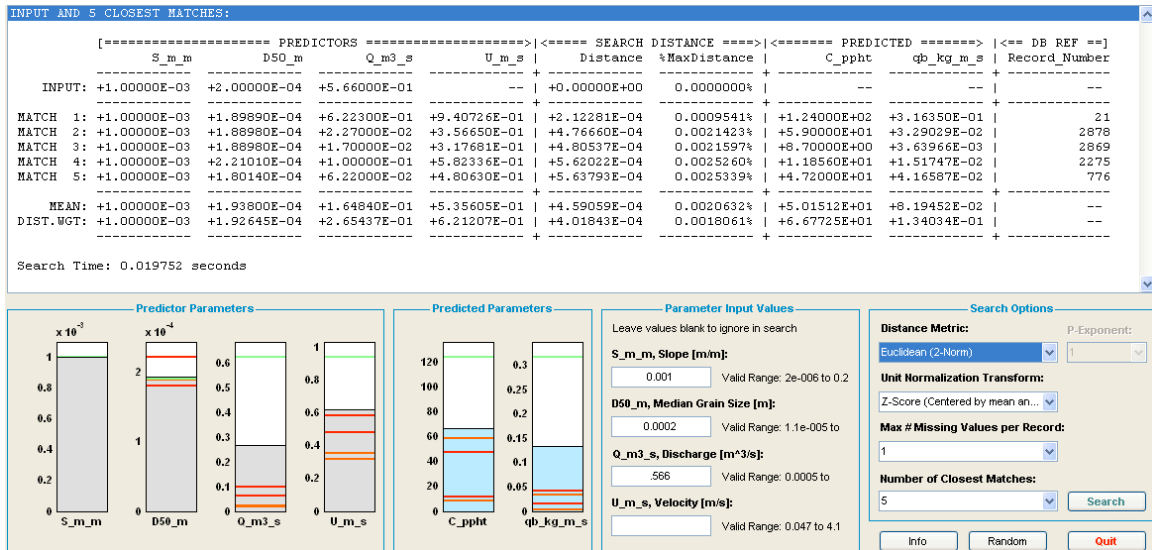
Figure 17: Screening Tool using search values similar to the universal flow diagram example.

listed in Table 2. These queries did not use the full set of information required to enter the universal flow diagrams, but instead the entries were based on either the discharge or velocity as noted in the Table. The agreement in this limited testing was better than anticipated, but not entirely unanticipated. The universal flow diagrams are based on a database that contains these particular values (or close values), and the present database also contains these values. What is remarkable and quite encouraging is that the order of magnitude of the results is about correct. The tool thus is deemed suitable for interpreting the physical model experiments and field data as such information or data records become available.

Table 2: Comparison of Peterson (1975, table 3, p. 554) and Screening Tool Estimates

$Q(\mathrm{m^3/s})$	$V(\mathrm{m/s})$	Slope	C(Peterson)	C(estimated)
0.14	0.30	0.000335	0.1	0.1*
9.1	0.61	0.000165	1	0.33-0.47**
580	1.21	0.000084	10	7.9-10.6

* Velocity based entry, one non-zero return
** Discharge based entry, two non-zero returns

3.8   Summary

The Task 2 objective was the development of a screening or assessment tool to identify existing stream crossings for which staggered barrel culverts might be appropriate. A tool was developed that used the original universal flow diagram approach to motivate how the tool might function. The tool used a flexible search engine approach rather than regression

equations, in part to accommodate different needs in this research.

The screening tool was tested against several reported results in the literature as well as against known database entries to test its ability to return exact matches where such exist.

3.9   Possible Uses

The general approach is to use the screening tool and known hydraulic metrics upstream/downstream of the hydraulic structure to estimate the charge or mass flux that is anticipated approach the structure, and leave the structure as if the structure had no impact on the solids transport. Then apply the concept of solids volume discharge as an added discharge the structure must accommodate and add this volume to the clear-water volume (discharge).

The data analysis of the experimental program intends to compare these two volumes/fluxes to the physical model results to interpret the conditions under which retarded solids flux is anticipated. Such situations (retarded solids flux) are those of interest for future field investigation.

In addition to this intended use, three other uses are envisioned at the conclusion of the data analysis portion of the research. These are described in the following list:

1. Use the tool to anticipate stream changes as a result of placing a hydraulic structure. For instance the tool could identify the anticipated downstream changes (in terms of slope) for a system that is anticipated to block solids discharge, but still pass clear water (a weir or culvert whose invert is well above local stream grade). By assuming a change in the solids flux from pre-structure conditions, the tool can be used to estimate anticipated equilibrium slope, flow depth, and D_{50}. These estimated values could then be field verified.

2. A similar use is the case where a channel is engineered to some specification, then an obstruction (such as a bridge abutment) is introduced. The tool can estimate the required change in slope, and flow depth to continue to accommodate the solids[7].

3. An unusual use is to estimate the increase in depth of flow at the outside bend of a channel in a mobile bed channel. The tool would be used in an iterative approach where the discharge per unit width is compared to the straight channel portion.

3.10   Installing the Tool

The search tool and database are located on the project server at `http://cleveland2.ce.ttu.edu/research/txdot_0-6549/TechnicalMemoranda/TM_2/ScreeningTool/`. Within

---

[7]Similar to a scour computation but the tool is not intended for scour computations — that topic is beyond the scope of the current research project and team.

the directory are several README files that explain how to install the tool.

4   Physical Model

Quantitative physical modeling using small models was conducted to examine relative capability to convey solids through different types of culvert arrays to quantify as far as practical the volume of solids conveyed while accommodating hydraulic requirements.

The guiding experimental questions were:

1. Does a staggered-barrel system accommodate solids as well as a conventional circular or rectangular system with an equivalent hydraulic capacity?

2. Does a staggered-barrel system accommodate solids as well as a conventional multiple-barrel circular or rectangular culvert system with an equivalent hydraulic capacity?

3. Is there a range of configurations where the multiple barrel systems behave as single barrel systems in superposition, thereby permitting the use of existing analytical and design tools?

4. Is there a relationship of solids diameter to culvert diameter that is pathological (the bridging hypothesis)? This question will help answer the question of what multiple of solids diameter should a culvert diameter be to pass solids without bridging within the culvert.

A series of scale-model experiments was envisioned to address the research questions posed in the introduction. Table 3 lists the experiments conducted by the research team. Each experiment was conducted for two different sizes of material (sand was abandoned because it washed out of the model before measurements could be made).

Table 3: Experimental Series — Each series at 0.3%, 0.6%, and 1% channel slope.

Series	Culvert Type	Orientation	Remarks
1	Single Circular	in-line with stream axis	reference case 1
2	Single Rectangular	in-line with the stream axis	reference case 2
3	Single Elliptical	in-line with the stream axis	**Not Performed**
4	Multiple Circular	in-line with stream axis	reference case 1
5	Multiple Rectangular	in-line with stream axis	similar to PAKS
6	Staggered barrel culvert	in-line with stream axis	similar to RM 335
7	Single Circular	skew with stream axis	15° skew angles.
8	Single Rectangular	skew with the stream axis	15° skew angles.
9	Single Elliptical	skew with the stream axis	**Not Performed**
10	Multiple Circular	skew with stream axis	15° skew angles.
11	Multiple Rectangular	skew with stream axis	15° skew angles.
12	Staggered barrel culvert	skew with stream axis	15° skew angles.

4.1   Experimental Apparatus

The Texas Tech University East Loop Research Facility houses the 48-foot long, 8-foot wide, and 4-foot tall flume used for the experiments in this research. Water is pumped from a 13,000 gallon water-storage reservoir into 4,000 gallon head tank, with a rated chute that flows into the flume. Inside the flume is a ramp that directs the flowing water downstream to reduce pool formation and associated energy dissipation before the water contacts the mobile solids. Figure 18 shows a view of the experimental apparatus as viewed looking upstream from the downstream end.
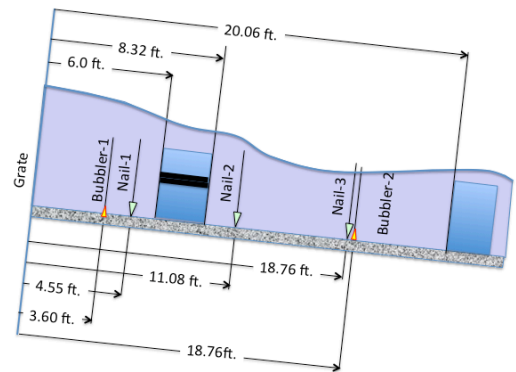
Figure 18: Left Panel: Photograph of flume, looking unstream. Culvert models are visible upstream of the farthest instrument bridge. Right Panel: Elevation view sketch of culvert models. Distances show relative position of experimental instruments. The grate on the left edge of the sketch is coincident with the far end of the experimental section in the photograph.

The model in the flume is a trapezoidal channel that is constructed of wood with outdoor carpet glued to the sides to mimic natural channel roughness. In the channel are two culverts for which the upstream culvert is the experimental model and the downstream culvert acts as a backwater control and rock trap. The experimental model was fabricated with interchangeable barrels to facilitate changes in experimental setup. After the flow encounters the two culverts, it continues into a rock bin, where the rocks that pass the downstream culvert are ultimately trapped and prevented from entering the water-storage reservoir.

The channel model was made of painted wood covered in carpet to increase the wall friction to produce a velocity distribution that mimicked distributions anticipated in full-scale systems. The solids in the channel were leveled at 0.2 feet from the model floor upstream of the culvert where there was a 0.1 foot layer of rocks held in place by an aluminum grate. This layer of rocks was to simulate the full scale condition of a permeable bed beneath the mobile layer. At full scale, this layer could be many feet deep — such a depth was not feasible in the laboratory so to reduce any impact of solids resting on smooth painted wood this layer was added to the model.

The solids in the channel downstream of the experimental model were leveled at 0.3 feet from the model floor with special attention made not to have a sediment layer above the invert of the outlet-sections of the culvert barrels at the beginning of each experimental run.

For the experiments reported herein, eight different culvert configurations (systems) were tested. A naming convention for the culvert configurations was established and is listed in Table 4. Figures 19 through 26 are drawings of the models tested in this research (image perspective is looking upstream). The culvert system was 29 inches wide from culvert entrance to exit, and the roadway was 84 inches long and spanned from bank to bank.

For the experiments reported herein, eight different culvert configurations (systems) were tested. A naming convention for the culvert configurations was established and is listed in Table 4. Figures 19 through 26 are drawings of the models tested in this research (image perspective is looking upstream). The culvert system was 29 inches wide from culvert entrance to exit, and the roadway was 84 inches long and spanned from bank to bank.

Table 4: Alphanumeric codes for the culvert arrays and associated drawings

Culvert Code	Description	Drawing
SB-I	Staggered barrels with inverts equal	Figure 19
SB-C	Staggered barrels with crowns equal	Figure 20
M-6-C	Multiple 6-inch circular barrels	Figure 21
S-6-C	Single 6-inch circular barrel	Figure 22
M-4-C	Multiple 4-inch circular barrels	Figure 23
S-4-C	Single 4-inch circular barrel	Figure 24
M-R	Multiple rectangular barrels	Figure 25
S-R	Single rectangular barrel	Figure 26
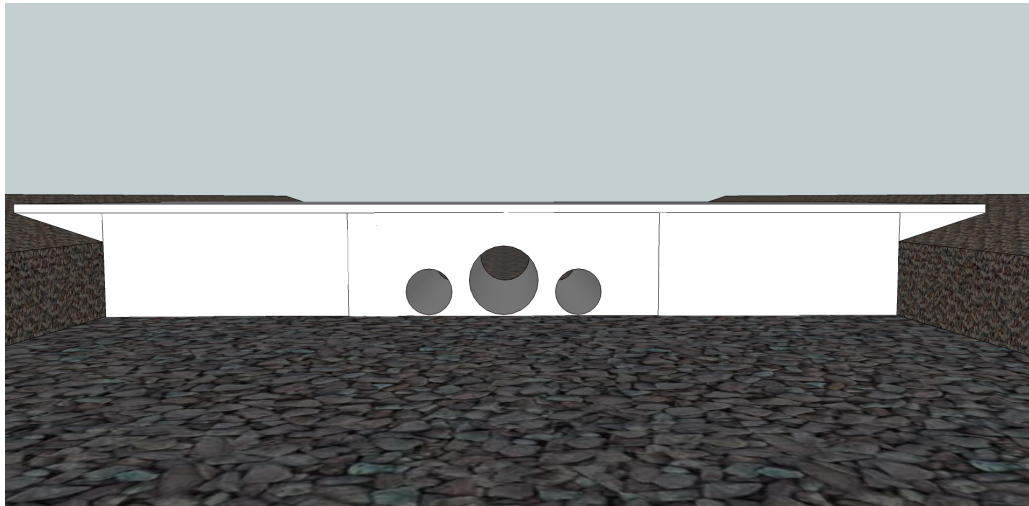
Figure 19: Diagram of Experimental Model SB-I (The outside barrels are 4 inch diameter
and the middle barrel is 6 inch diameter)
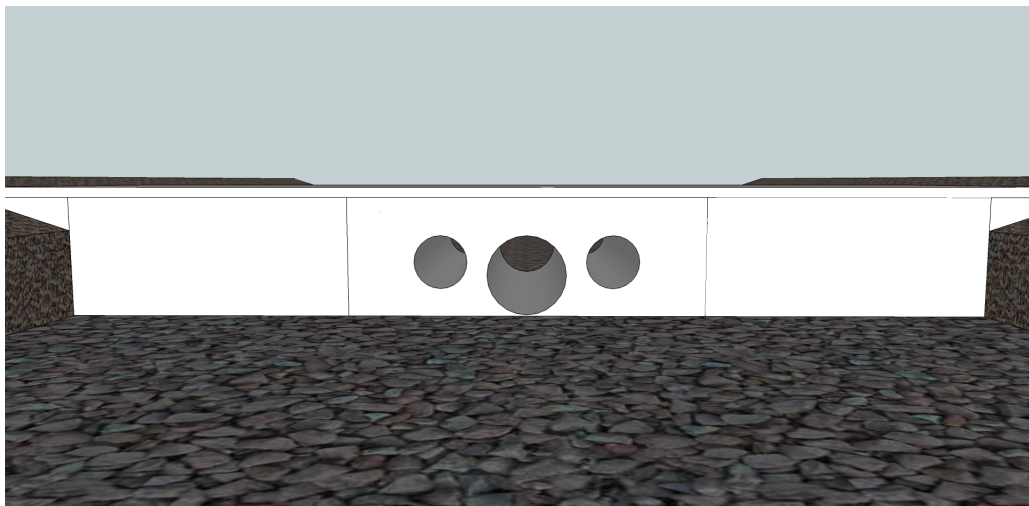
Figure 20: Diagram of Experimental Model SB-C (The outside barrels are 4 inch diameter
and the middle barrel is 6 inch diameter)
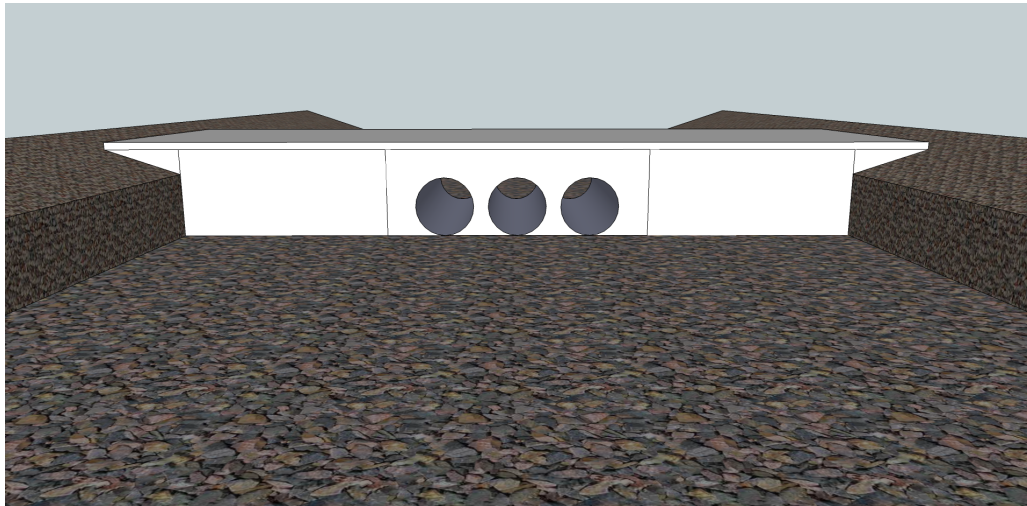
Figure 21: Diagram of Experimental Model M-6-C (The identical barrels are 6 inch diameter)

Figure 22: Diagram of Experimental Model S-6-C (The barrel is 6 inch diameter)
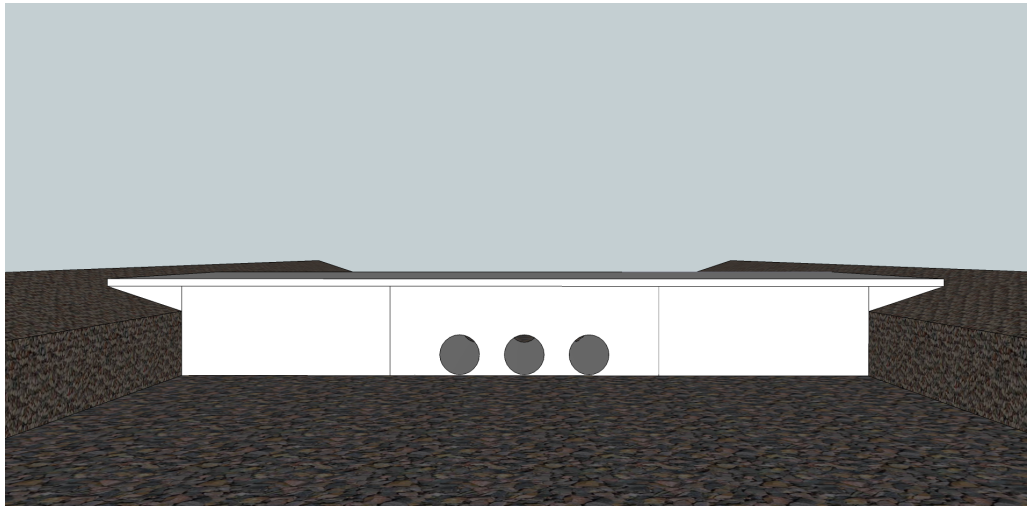
Figure 23: Diagram of Experimental Model M-4-C (The identical barrels are 4 inch diameter)

Figure 24: Diagram of Experimental Model S-4-C (The barrel is 4 inch diameter)
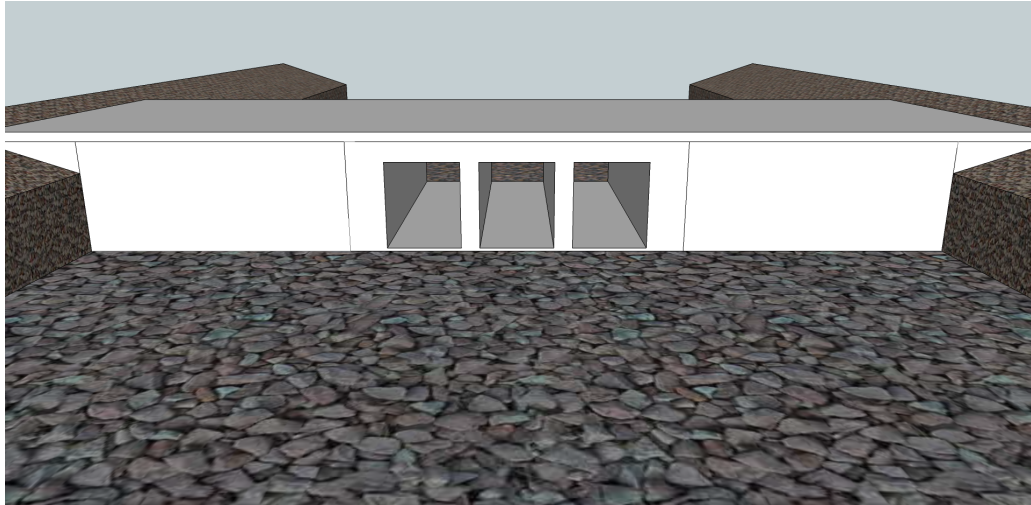
Figure 25: Diagram of Experimental Model M-R (The identical barrels are 6×7 inches)

Figure 26: Diagram of Experimental Model S-R (The barrel is 6×7 inches)

4.2   Measurements

The various measurements in the experiments include total discharge into the flume, flow depths at selected locations within the flume, 2D- and 3D-point velocities at selected locations within the flume, topographic survey of the model streambed downstream of the model before and after each experiment, and a mobilized solids volume direct measurement after each experiment. Each measurement technique is briefly described in the remainder of this section.

4.2.1   Discharge into the flume

The head-tank was rated using various direct and temporary weir computations to form a stage-discharge relation. The stage-discharge relation (rating curve) was used to quantify the flow coming from the head-tank into the flume. The rating curve for the head tank chute is shown in Figure 27.
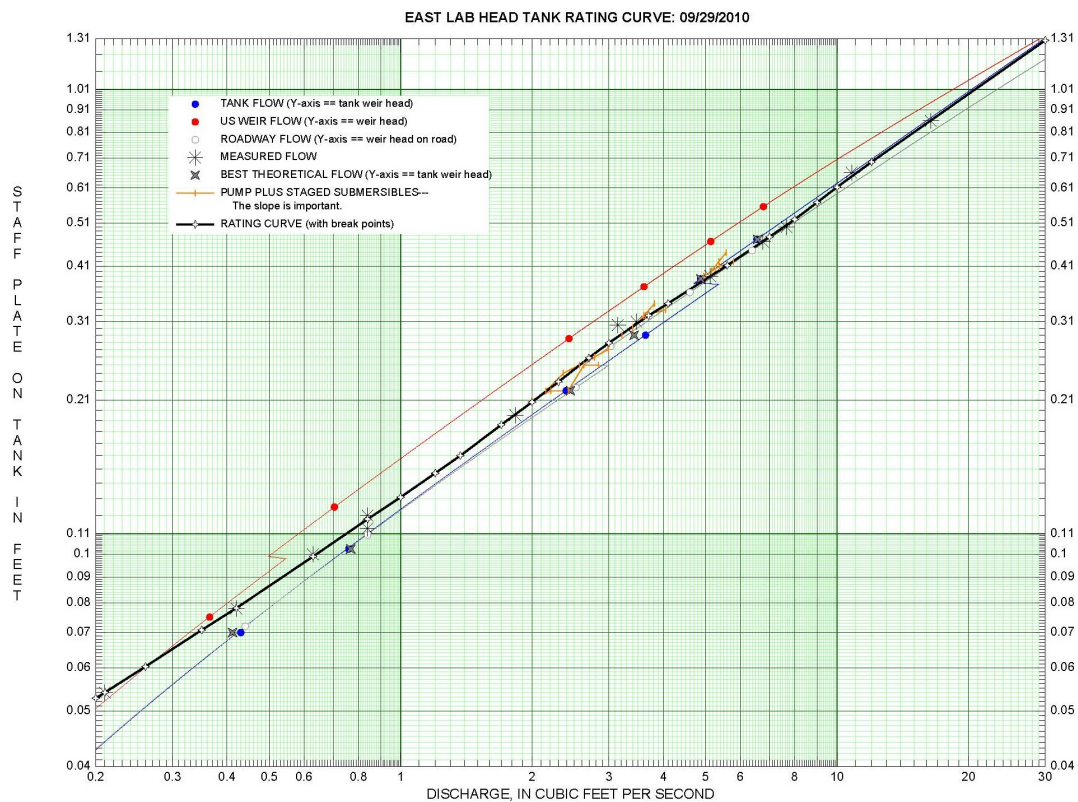
Figure 27: Head-Discharge Relation for the Head Tank

Stage in the tank was measured by a staff-plate mounted in proximity to a sight glass, shown in Figure 28, and by a radar-level-sensor aimed at the water surface in the tank.

The radar results were used except in cases where the radar was not functioning. The rating curve was developed by measuring the stage in the head tank and relating that stage to measurements of discharge in the flume made by different operators using SonTek flowtracker instruments[8].

Figure 28: Sight Glass Used to Measure Head in the Head Tank

The rating curve (William H. Asquith, U.S. Geological Survey written communication, 2010) converts stage readings into equivalent discharge by entering the graph on the vertical axis with the stage in the tank, finding the intersection of the rating curve with that value, and then reading the corresponding discharge value on the horizontal axis.

4.2.2   Velocity within the flume

SonTek Micro-Acoustic Doppler Velocimeters (ADVs) were used to measure the velocity in the channel. The ADVs were mounted on aluminum rods that spanned the width of the flume. The rods had an adjustable clamping system that allowed measurements to be collected in the same place, even after resetting from different locations[9].

During experiments, the ADVs were used for two purposes: to record entrance and exit

---

[8]The process of rating the head tank is identical to the process of rating a stream gaging station, including the same instrumentation and methodology.

[9]The repeatability of the locations was important for interpreting results.

velocities in the culvert barrels, and to determine when the culvert was clogged. In the sediment transport experiments, the middle barrel of the array was monitored at the inlet and outlet for velocity. If the array had multiple barrels, the third ADV was used to measure the outlet of the right bank-side barrel. If the array was a single barrel, the third ADV was used to monitor the velocity just above the streambed approximately eight feet downstream from the culvert outlet.

4.2.3   Flow depth within the flume

Flow depth within the flume was determined by staff gage direct measurements over reference monuments (nails) that were located upstream and down stream of the culvert models. These reference monuments were also used as part of the topographic registration of the survey instrument. Flow depth was also measured using another radar-level-sensor and two bubbler systems. At times during the experiments, the bubblers and radars would fail (usually a power issue), and these failures were not discovered until after the experimental runs. All experiments were conducted with the independent manual (staff gage) method, so those values were retained for data analysis.

4.2.4   Solids flux

The amount of solids that passed through the culvert array was a fundamental measurement (and driving goal) of the research. The amount of solids that was moved during an experiment was determined in two independent measurements: a direct measurement of volume that needed replacement upstream of the culvert for each experiment (bucket count) and a cut-and-fill computation based on a before-after topographic survey downstream of the culvert model.

The bucket counts provide a rough approximation of the volume of solids that are mobilized and moved into and past the culvert model. The upstream surface before each experiment is leveled and the volume of solids required to return the bed to the same level is recorded. Solids in the culvert are extracted and their volume determined, and the downstream volume change is measured by the topographic survey.

The purpose for measuring the solids stuck in the barrel was to be able to account for differences between the bucket-determined volume and the surveyed volume. The solids that remained upstream of the culvert after the experiment were measured to the nearest 1/4 bucket, and the difference between the measured upstream volume and the total bucket volume should approximate the volume transported to and through the culvert.

The measurements of the 5-gallon bucket and the survey results were compared for the larger rock size. The comparison shows 0.665 cubic feet per bucket and 0.668 as the defined conversion factor to cubic feet. The comparison was made only on the experimental results that did not have rocks trapped in the culvert barrel. The data are shown in Figure 29

and listed in Table 5.
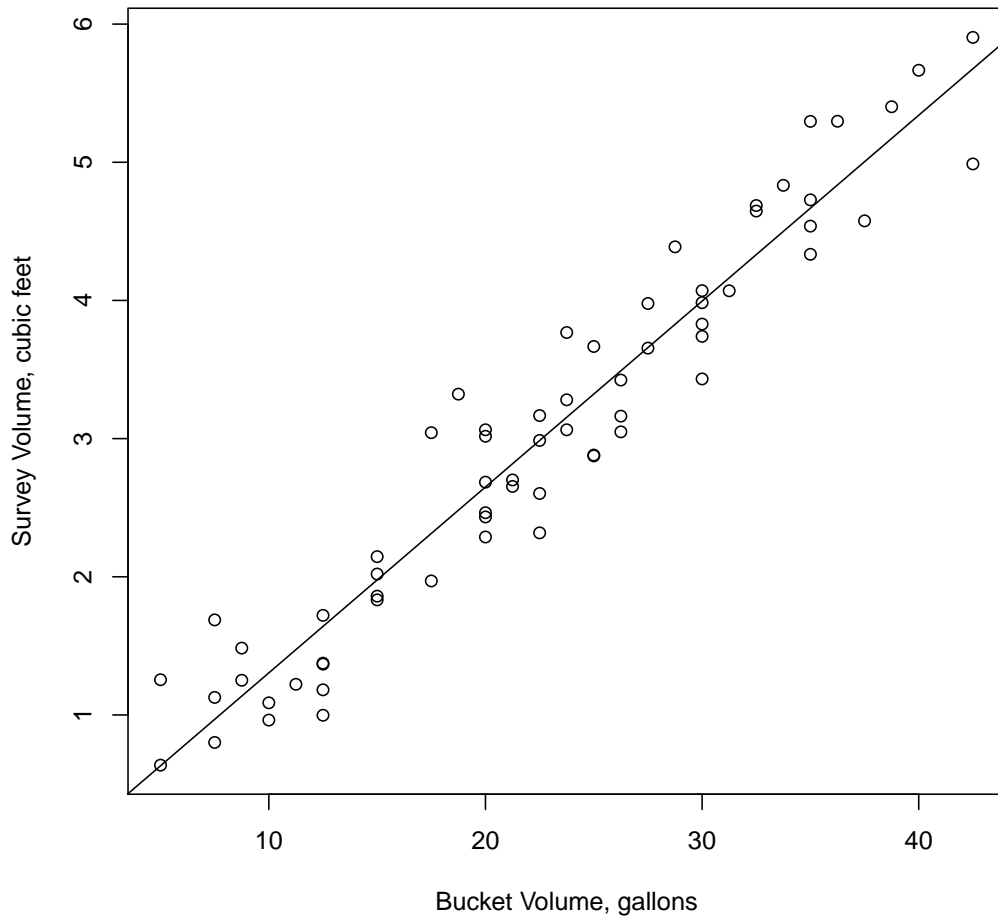
Figure 29: Relation Between Bucket-Determined Volume and Surveyed and Kriged Volume and a Superimposed Regression Line—Data are Listed in Table 5.

Table 5: Comparison Between Bucket-Determined Volume and Surveyed and Kriged Volume—Data are Shown in Figure 29

Buckets	Survey (ft^3)	Buckets	Survey (ft^3)	Buckets	Survey (ft^3)
4	2.464	4 1/4	2.654	6 1/2	4.687
5 3/4	4.388	6	3.984	6 3/4	4.833
8 1/2	5.904	4	2.288	6 1/4	4.070
8 1/2	4.988	1	1.255	7	4.728
8	5.666	2 1/2	0.998	5 1/4	3.163
7	4.334	2	1.088	4	2.685
7	5.296	2 1/2	1.375	5 1/4	3.049
7 1/2	4.576	1	0.637	1 3/4	1.484
5	2.881	1 1/2	1.127	3	1.860
4	3.064	2	0.963	3	1.833
4 1/2	2.987	2 1/2	1.721	4 3/4	3.281
4 1/2	2.318	2 1/2	1.182	4 1/4	2.701
4	3.017	5 1/2	3.655	4 3/4	3.064
5 1/4	3.424	7	4.538	2 1/4	1.222
3	2.146	7 1/4	5.297	1 1/2	0.801
3 1/2	1.970	7 3/4	5.402	1 1/2	1.688
3	2.020	6	3.740	4	2.433
6	4.071	4 3/4	3.768	2 1/2	1.368
6	3.829	6	3.432	1 3/4	1.251
4 1/2	3.167	5 1/2	3.978	3 1/2	3.043
4 1/2	2.603	5	3.667	3 3/4	3.322
5	2.875	6 1/2	4.647	--	--

4.2.5   Solids passed through the culvert.

A Sokkia total station was used to generate an appropriate resolution survey of the topography to estimate the solids passed through the culvert as a change in topography (aggregation or degradation). An x-y-z coordinate system was established within the lab with benchmarks. A Carlson Surveyor field computer was used to perform resection (3D triangulation) to bring each survey into vertical and horizontal control using approximately 4 to 6 points. Details of the survey protocol are presented in Dixon (2011).

Noncoincident topographic points were measured for each experiment, in two sets, the before and the after the experimental run. The region surveyed prior to an experimental run was entirely dependent upon how far the rocks were anticipated to move. The collected points were exported in a text file and imported into an Excel spreadsheet, which was subsequently converted into a Surfer grid file. By taking the difference between the before and after surfaces, an approximation of the volume of solids passed through the culvert models was calculated. Surveys were performed in accordance with the specifications and recommendations of Topcon (2009). Davis et al. (1981) also provides some useful commentary on topographic surveying theory.

An example of the survey method with the data points plotted and connected in the order with which they were collected is shown in Figure 30. The grid is not uniform, which is by design. The points were not surveyed in the same location for each survey. The portion at the bottom of the graph is where the survey grid alignment tool was turned sideways to extend the survey further downstream.

A comparison of the results is given in Table 6. The kriging method volume results were typically nearer to the bucket volume than the inverse distance results. Also, the kriging method produces the most faithful representation of the surface based on photographs taken just after the experiments. Figure 31 renders the surface output generated by Surfer. Figure 32 is a photograph of the actual surface model with yellow string simulating contour line. The surface forms are close, and this kind of similarity observed for other experiments supports that the surveying technique and interpolation methods are adequate.
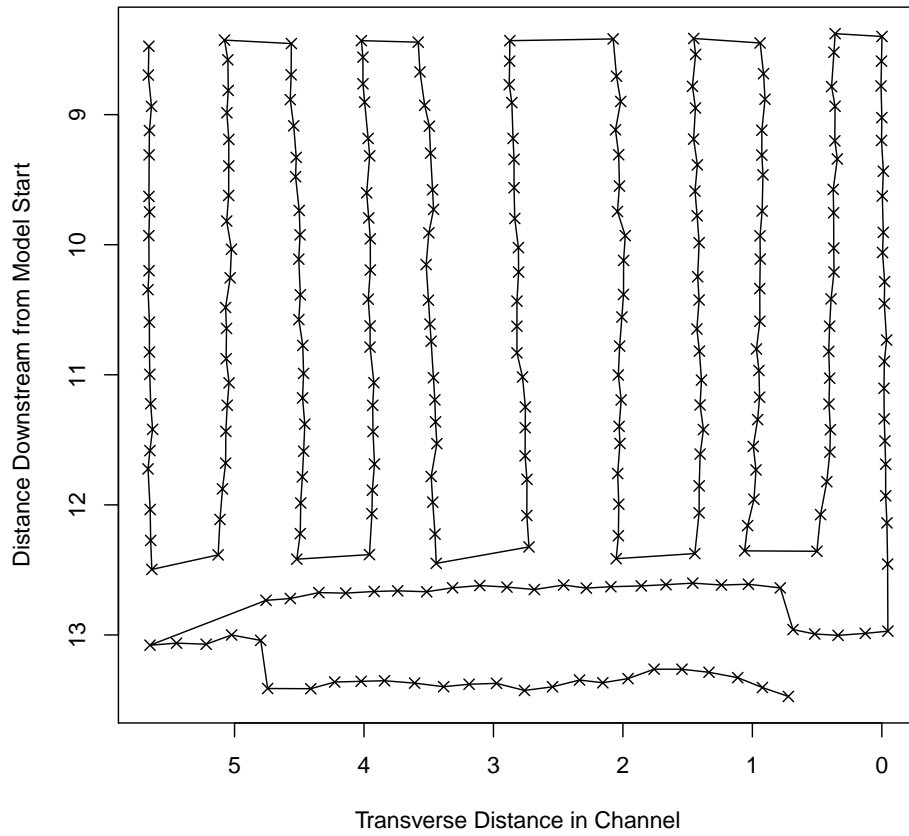
Figure 30: Example of the Initial Surveying Technique—Semi-Uniform spacing
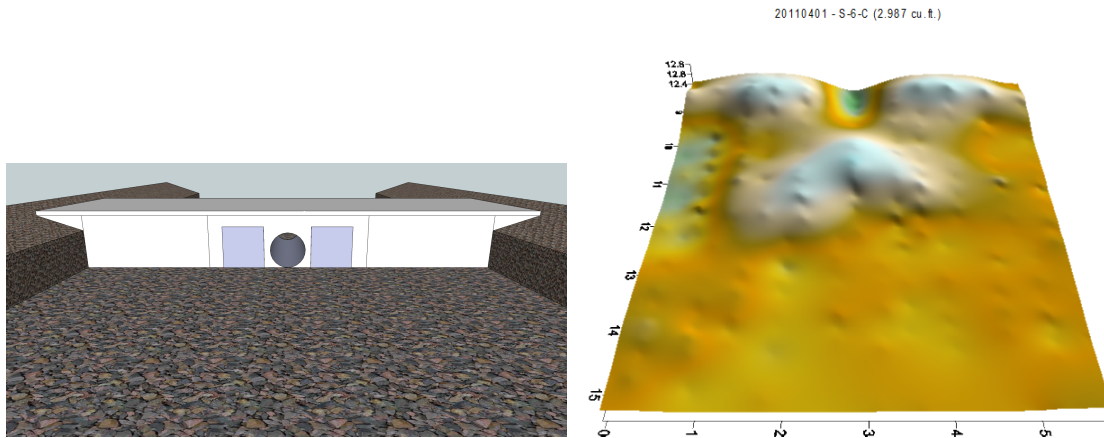
Figure 31: Surface Generated by Kriging Method for Experiment on 2011/04/01, Experimental Model S-6-C—Culvert Diagram Not to Scale

Figure 32: Photograph of Downstream Bedform Following Experiment on 2011/04/01, Experimental Model S-6-C

The bedform can be rendered in both modeling methods; the inverse distance method has a tendency to produce "bumps" where the data points were acquired, whereas the kriging surface produces less of that effect.

Table 6: Comparison of Calculated Volume Transported in Cubic Feet

Date	Model	Buckets	Kriging	Inverse Distance	Simple mean
2011/03/22	M-R	5.653	5.904	5.939	4.305
2011/04/01	S-6-C	2.993	2.987	3.110	2.749
2011/05/20	S-R	0.665	0.637	0.574	0.654
2011/07/22	M-R	3.658	3.655	3.709	3.118
2011/08/05	S-6-C	2.660	2.685	2.769	3.401

Summarizing these findings:

- The inverse distance method produces bumps in the surface,

- The kriging method has an overall smoother appearance, and

- The volumes represented in both methods are comparable.

Therefore, kriging is chosen as the selected method because it produces a more faithful representation of the surface.

4.2.6   Solids retained in the culvert

After each experiment, the rocks that are retained in the culvert barrel(s) are removed and weighed on a digital scale. The scale can read different values based on where the bucket is placed, so multiple readings are taken. If the readings match, then the weight of rocks is assumed to be correct at that value.

Table 7 lists selected experiments that had a substantial amount of rocks remaining in the culvert barrel(s), and these weights are used to relate the relative of the size of the clog in the barrels.

Table 7: Weights of Rocks Measured on Experiments with Substantial Volume Remaining in the Barrels

Date	Configuration	Weight	Date	Configuration	Weight
2011/01/24	SB-I	30.0	2011/05/12	M-6-C	24.8
2011/01/25	M-4-C	41.6	2011/05/13	M-6-C	16.8
2011/01/27	M-4-C	29.6	2011/05/14	M-6-C	13.0
2011/01/28	M-4-C	44.0	2011/05/16	M-R	24.2
2011/02/05	S-4-C	16.4	2011/05/17	M-R	36.2
2011/02/07	S-4-C	14.6	2011/05/18	M-R	14.4
2011/02/10	S-4-C	16.2	2011/08/11	M-4-C	7.6
2011/02/14	S-6-C	23.4	2011/08/12	M-4-C	6.2
2011/02/15	S-6-C	29.2	2011/08/13	M-4-C	8.0
2011/02/16	S-6-C	17.4	2011/08/17	SB-I	10.4
2011/02/17	M-6-C	18.6	2011/08/19	M-6-C	7.4
2011/02/18	M-6-C	50.8	2011/08/20	M-6-C	15.0
2011/02/19	M-6-C	42.8	2011/08/21	M-6-C	8.7
2011/02/21	M-R	35.4	2011/08/23	SB-C	6.4
2011/02/22	M-R	25.8	2011/08/25	M-R	32.2
2011/02/23	M-R	17.0	2011/08/25	M-R	35.4
2011/02/28	S-R	12.2	2011/08/26	M-R	35.2

4.3   Culvert Induced Bedforms

One of the results of the experiments was that there were specific bedforms created by each culvert arrangement. Single barrel arrangements tended to have two very pronounced scour pits downstream and to the outside of the main bedform that formed downstream of the culvert barrel. Multiple identical barrel arrangements tended to have one large mound that would nearly span the channel width. The staggered barrel arrangements showed a tendency for what appeared to be early stages of erosion of the built up formation.

The staggered barrel configurations exhibited bedforms that were not substantially different from the multiple barrel configurations with the exception that there seemed to be an orientation of the sediments. The orientation of the sediments would tend to indicate flow going around the largest portion of the bedform as the flow exits the culvert barrel.

The following set of images were generated in Surfer (Golden Software, 2002) using the survey data. The color ramp, shown in Figure 33, is normalized for all experiments, and the colors represent the same elevation in each picture. The numbers in the top of each picture show the difference in volume between the before surface and the after surface.
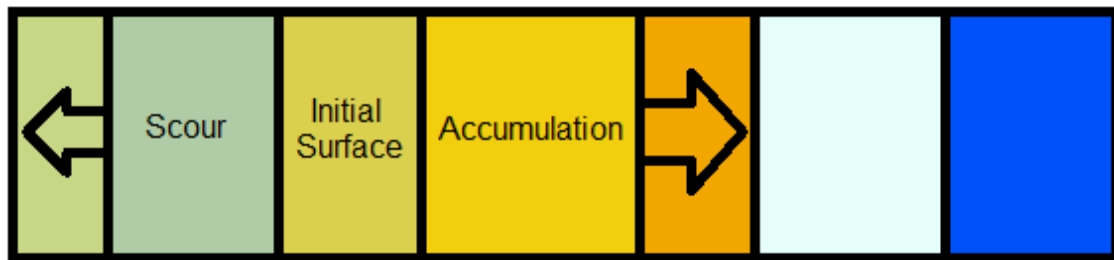

Figure 33: Color Ramp Used to Assist in the Evaluation of Surface Models

The different culvert systems are presented in the order of increasing culvert open area — that is the first images represent a system with the smallest hydraulic capacity, the last set of images represents a system with the largest hydraulic capacity. Only in-line results are presented, the skew experiments were not surveyed in the interest of time and only bucket counts were used.

4.3.1 Single 4-inch Circular Barrel (S-4-C)

Figure 34 shows two mounds, one just downstream of the culvert outlet near the centerline, and the other between the centerline and the left bank. This dual mounding is interesting because it presents evidence of an eddy near the culvert exit or that sediment is being transported over the roadway. Both situations were observed in the experiments, however the eddy is deemed by the researchers to be more significant.
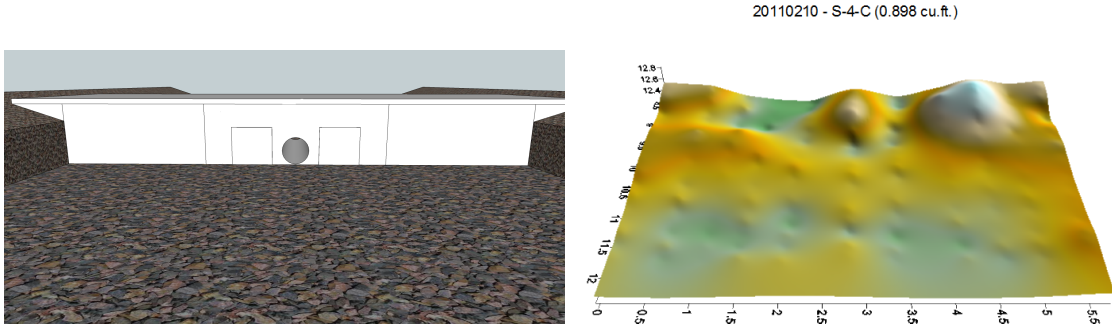

Figure 34: Typical Downstream Surface Model for Experimental Model S-4-C for 0.3 Percent Slope with Large Rocks

Figure 35 shows a U-shaped gravel bar with some scour on the outside banks. In this particular experiment, with steep slope and large rocks, the downstream bar creates a "dam" and clear water discharge is forced around this dam. If the experiments could have been operated long enough (weeks), the material would eventually migrate further downstream.
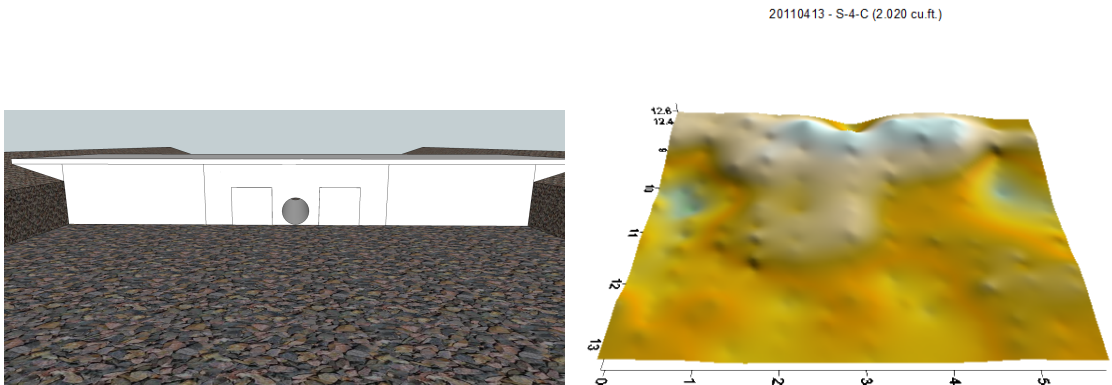

Figure 35: Typical Downstream Surface Model for Experimental Model S-4-C for 1.0 Percent Slope, with Large Rocks

Figure 36 shows a small mound downstream of the model, with smaller mounds against the model on the sides. These extra mounds further corroborate the evidence of local eddies near the culvert exit in Figure 34.
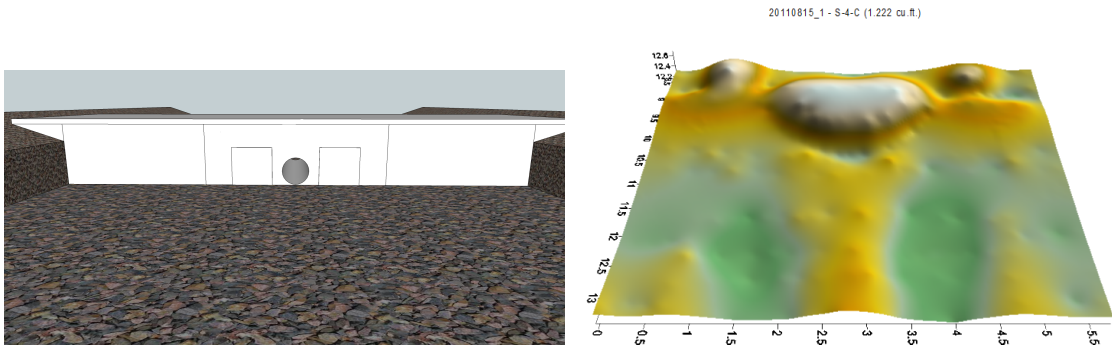
Figure 36: Typical Downstream Surface Model for Experimental Model S-4-C for 0.3 Percent Slope with Small Rocks

Figure 37 shows a flat mound the spans the channel, with scour downstream of the mound and at the culvert exit.
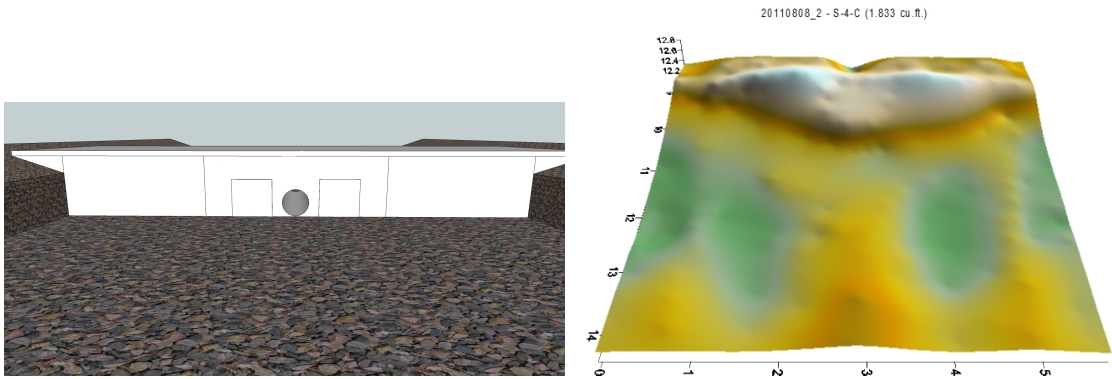

Figure 37: Typical Downstream Surface Model for Experimental Model S-4-C for 0.6 Percent Slope with Small Rocks

4.3.2   Single 6-inch Circular Barrel (S-6-C)

Figure 38 shows a mound just downstream of the culvert outlet.
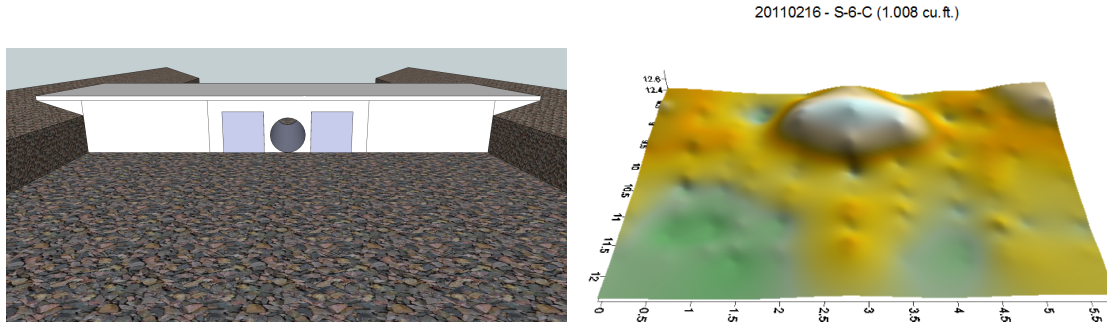
Figure 38: Typical Downstream Surface Model for Experimental Model S-6-C for 0.3 Percent Slope with Large Rocks

Figure 39 shows a flat gravel bar that nearly spans the channel and has mild scour downstream of the bar.
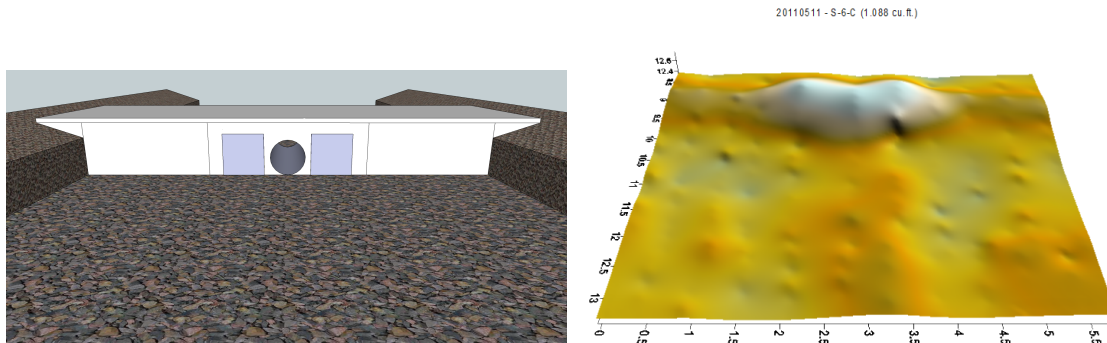

Figure 39: Typical Downstream Surface Model for Experimental Model S-6-C for 0.6 Percent Slope with Large Rocks

Figure 40 shows a gravel bar with a long wing and a some scour on the right bank. There are also mounds in the corners near the headwall.

Figure 41 shows a flat gravel bar with scour downstream and towards the banks. There is a continuous line of rocks from bank to bank on the upstream side of the gravel bar. This line is not an artifact of the survey or the interpolation method, but rather it was present in the bedform as observed.

Figure 42 shows a flat gravel bar with a wing towards the left bank and scour downstream on the right bank.
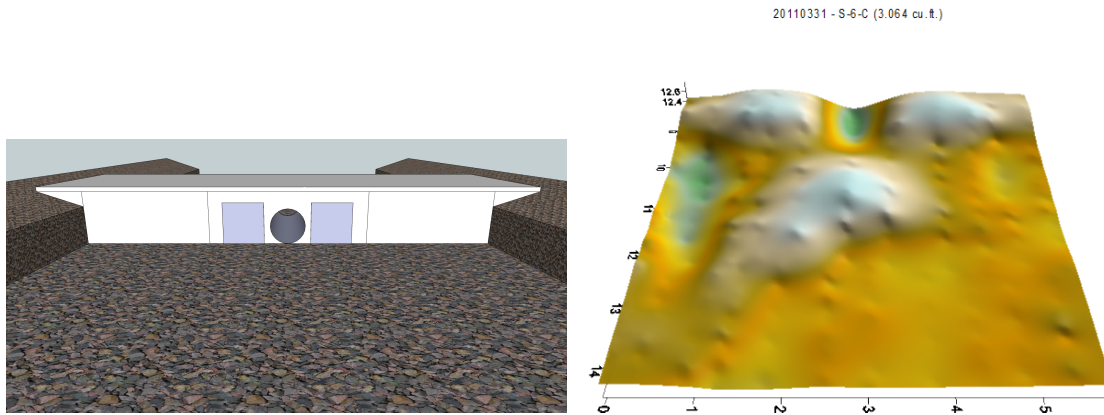
Figure 40: Typical Downstream Surface Model for Experimental Model S-6-C for 1.0 Percent Slope with Large Rocks
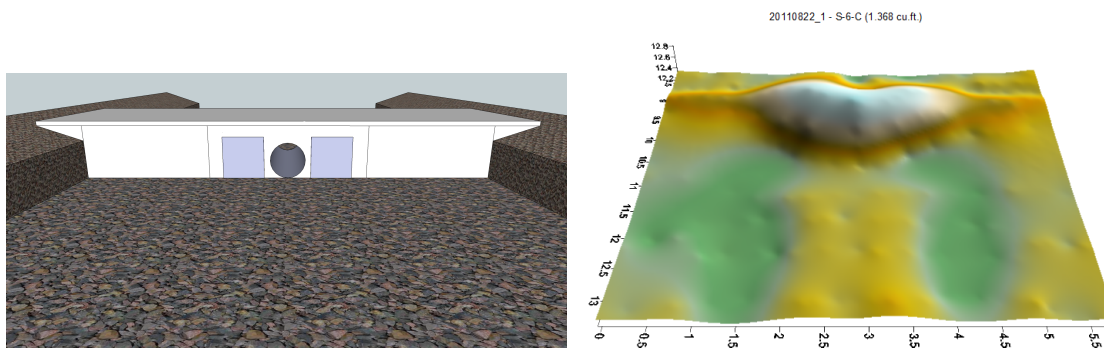
Figure 41: Typical Downstream Surface Model for Experimental Model S-6-C for 0.3 Percent Slope with Small Rocks
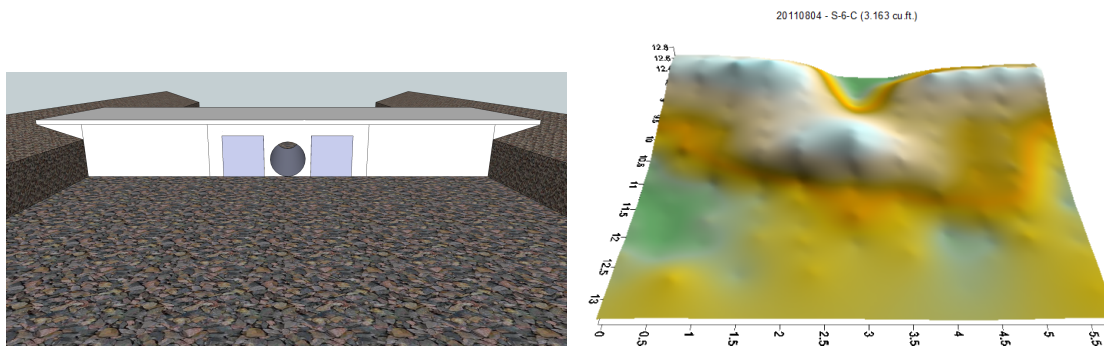
Figure 42: Typical Downstream Surface Model for Experimental Model S-6-C for 0.6 Percent Slope with Small Rocks

4.3.3 Multiple 4-inch Circular Barrels (M-4-C)

Figure 43 shows a slight mound with some scour immediately surrounding the mound.
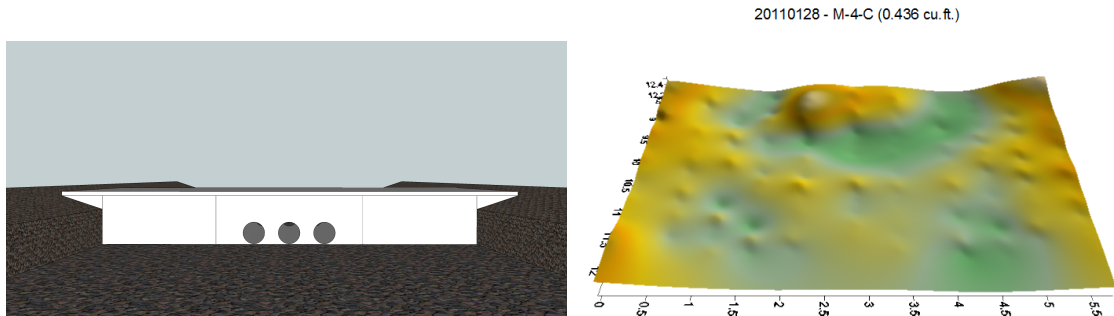
Figure 43: Typical Downstream Surface Model for Experimental Model M-4-C for 0.3 Percent Slope with Large Rocks

Figure 44 shows a flat gravel bar across the channel that has been built up significantly from the beginning of the experiment. Note the green shades near the culvert exit that signify scour.
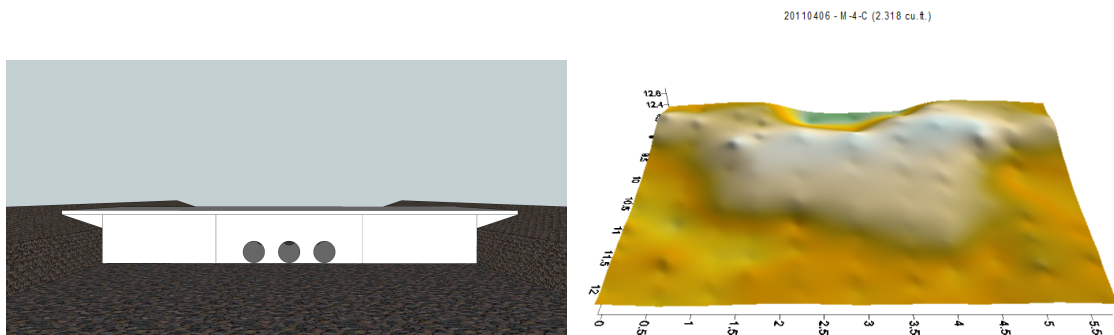
Figure 44: Typical Downstream Surface Model for Experimental Model M-4-C for 1.0 Percent Slope with Large Rocks

Figure 45 shows a flat gravel bar that spans most of the channel. There is also some significant scour present downstream.

Figure 46 also shows a flat gravel bar extending across the channel and scour is pronounced near the banks.
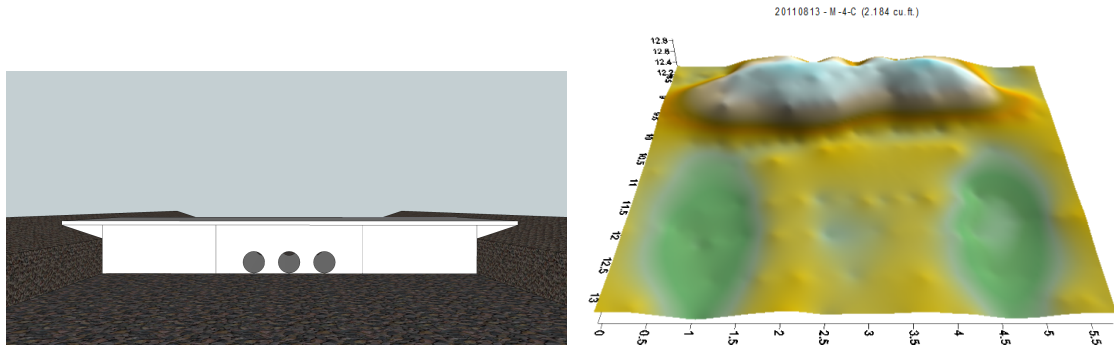
Figure 45: Typical Downstream Surface Model for Experimental Model M-4-C for 0.3 Percent Slope with Small Rocks
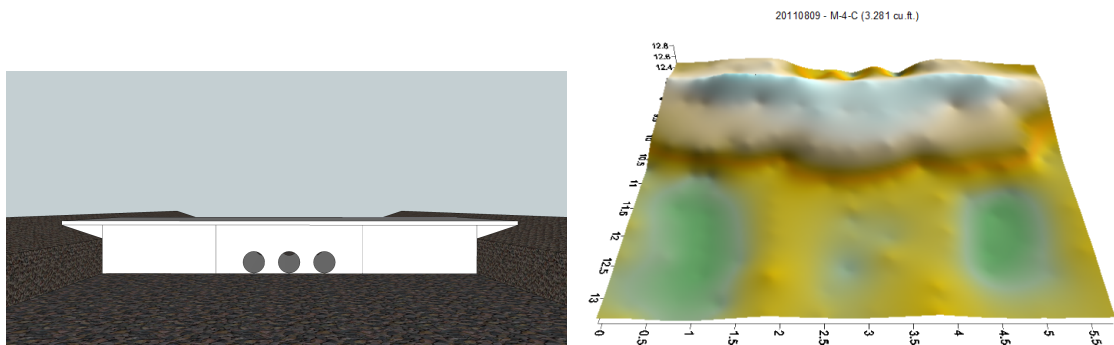
Figure 46: Typical Downstream Surface Model for Experimental Model M-4-C for 0.6 Percent Slope with Small Rocks

4.3.4 Single Rectangular Barrel (S-R)

Figure 47 shows a small mound downstream of the culvert with slight scour and mounds in the corner by the headwall
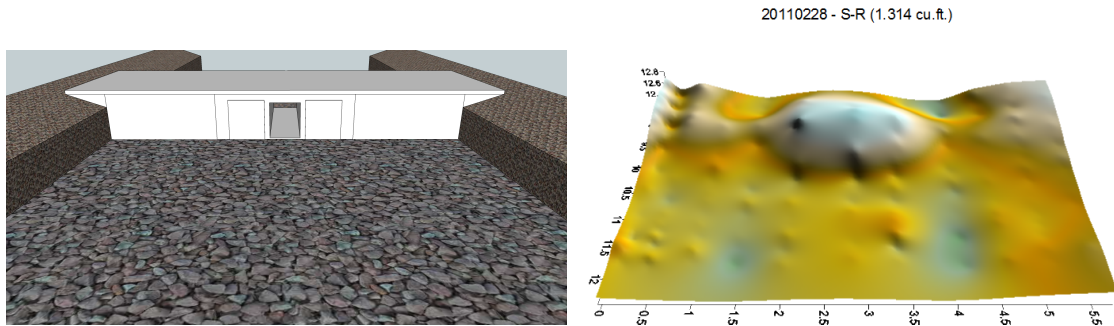
Figure 47: Typical Downstream Surface Model for Experimental Model S-R for 0.3 Percent Slope with Large Rocks

Figure 48 shows a small mound with little scour downstream of the mound.
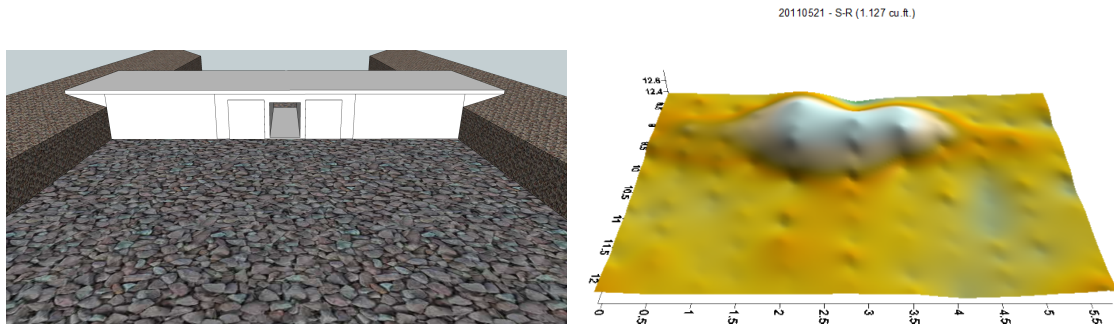
Figure 48: Typical Downstream Surface Model for Experimental Model S-R for 0.6 Percent Slope with Large Rocks

Figure 49 shows a U-shaped gravel bar with a wing on the left bank side and some minor scour at the culvert exit.

Figure 50 shows a U shaped gravel bar with a wing on the left bank side and some scour downstream of the culvert. Note the accumulation in the corners near the headwall.
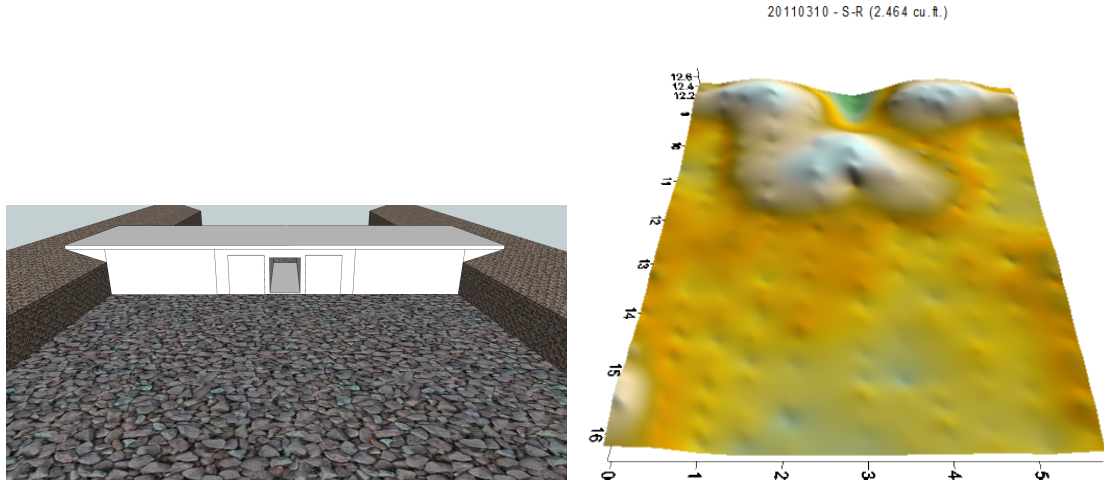
Figure 49: Typical Downstream Surface Model for Experimental Model S-R for 1.0 Percent Slope with Large Rocks
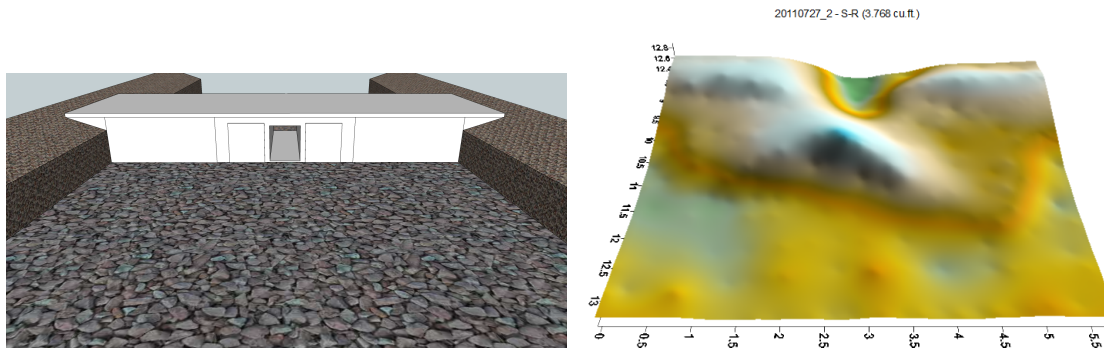
Figure 50: Typical Downstream Surface Model for Experimental Model S-R for 0.6 Percent Slope with Small Rocks

4.3.5   Staggered Barrels with Inverts Equal (SB-I)

Figure 51 shows that the surveyed bedform has very slight accumulation and there is mild scour evidence.
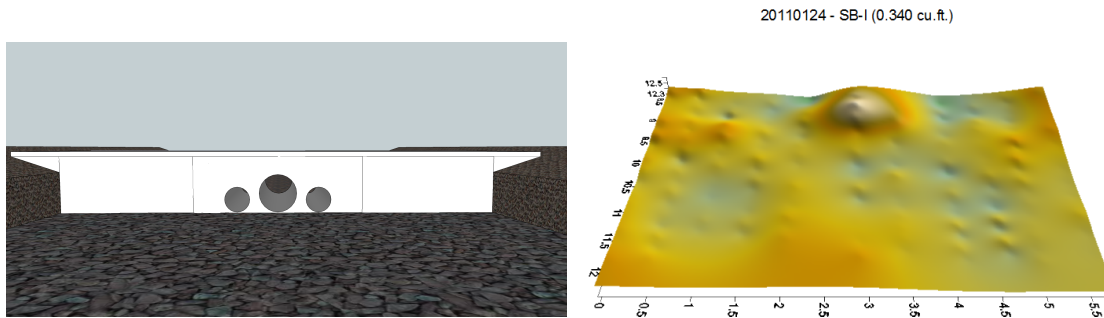
Figure 51: Typical Downstream Surface Model for Experimental Model SB-I for 0.3 Percent Slope with Large Rocks

Figure 52 shows a "U-shaped" gravel bar with a slight wing toward the right bank and a larger wing toward the left bank.
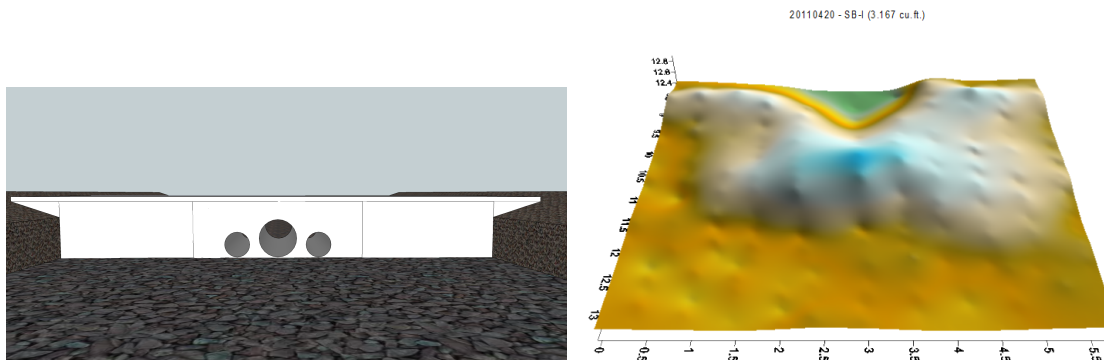

Figure 52: Typical Downstream Surface Model for Experimental Model SB-I for 1.0 Percent Slope with Large Rocks

Figure 53 shows a gravel bar just downstream of the culvert with noticeable scour downstream and towards the banks.

4.3.6   Staggered Barrels with Crowns Equal (SB-C)

Figure 54 shows a gravel bar with mild scour downstream of the bedform and some mild accumulation near the culvert headwall.

Figure 55 also shows a gravel bar, but has obvious evidence of scour along the left bank.
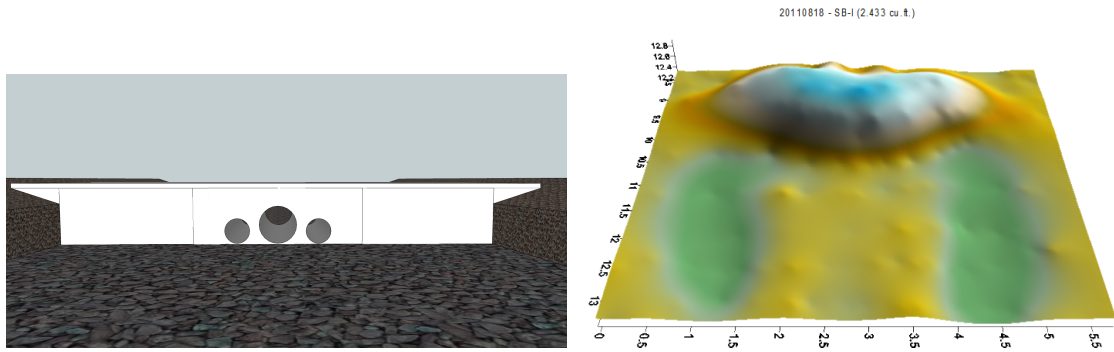
Figure 53: Typical Downstream Surface Model for Experimental Model SB-I for 0.3 Percent Slope with Small Rocks
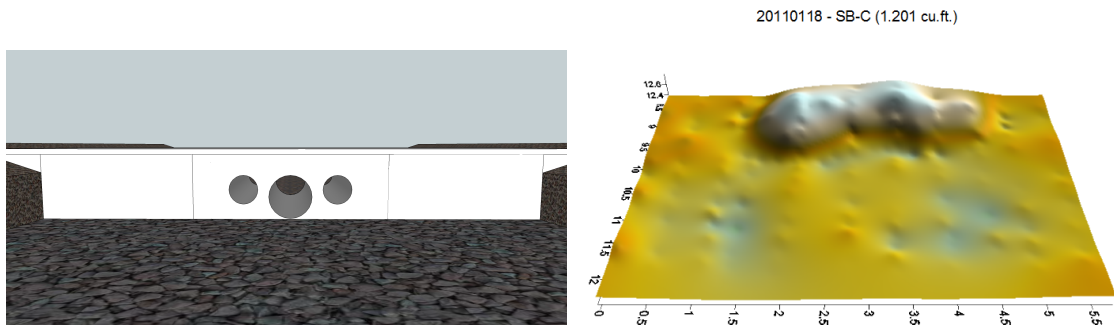

Figure 54: Typical Downstream Surface Model for Experimental Model SB-C for 0.3 Percent Slope with Large Rocks
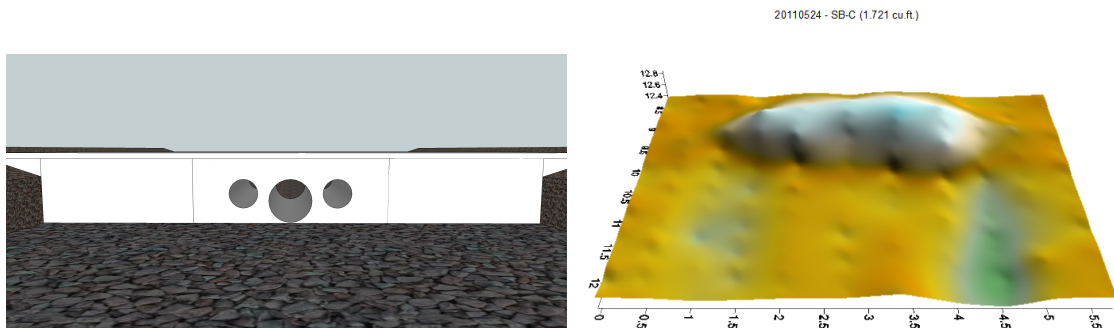
Figure 55: Typical Downstream Surface Model for Experimental Model SB-C for 0.6 Percent Slope with Large Rocks

Figure 56 shows a U-shaped gravel bar with the sides washed out into wings, as well as some accumulation near the culvert headwall.

Figure 57 shows a gravel bar with noticeable scour downstream and towards the banks.
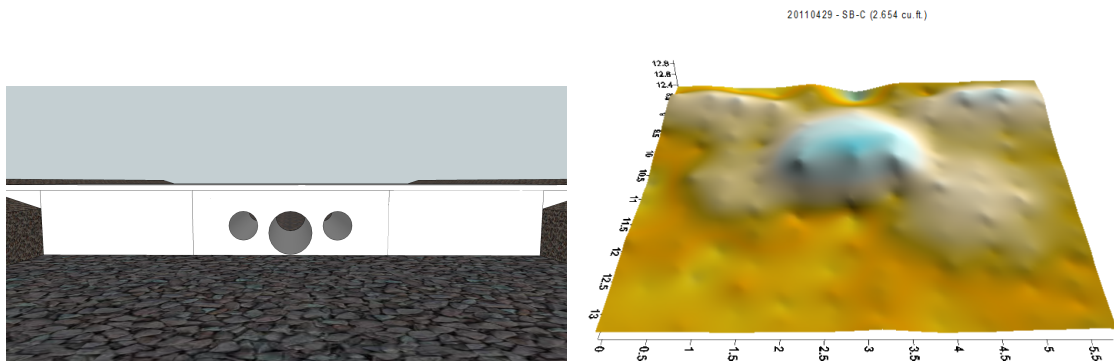
Figure 56: Typical Downstream Surface Model for Experimental Model SB-C for 1.0 Percent Slope with Large Rocks
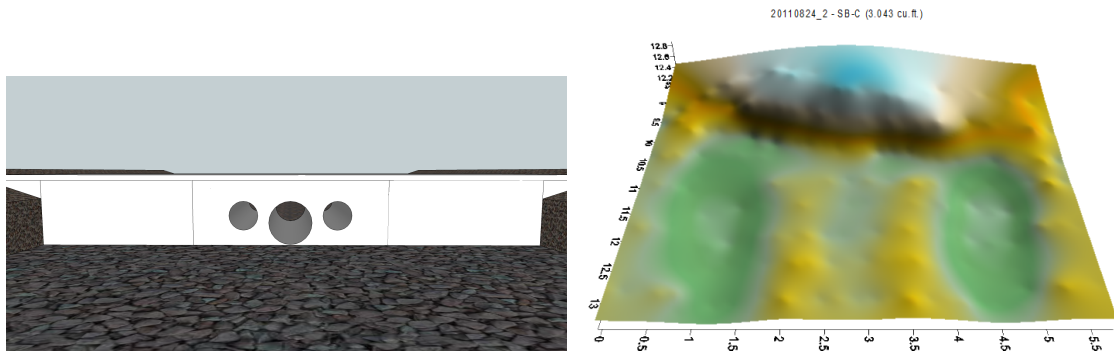
Figure 57: Typical Downstream Surface Model for Experimental Model SB-C for 0.3 Percent Slope with Small Rocks

Figure 58 shows an gravel bar with a pronounced wing on the left bank and a lesser wing on the right bank.
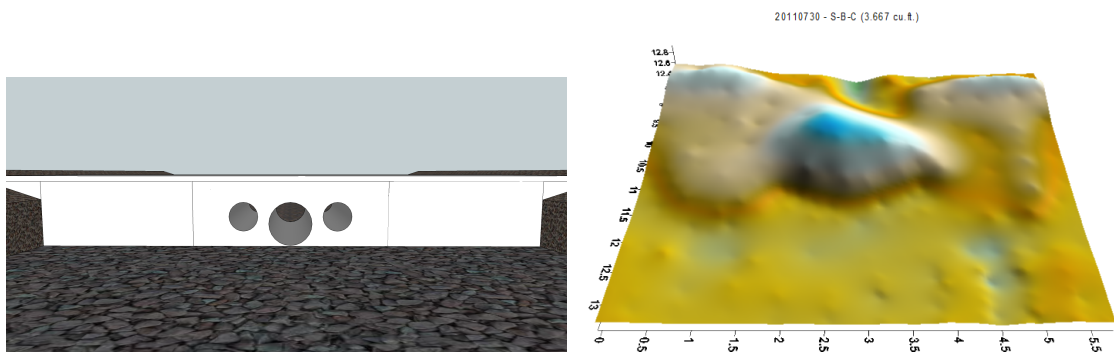
Figure 58: Typical Downstream Surface Model for Experimental Model SB-C for 0.6 Percent Slope, with Small Rocks

4.3.7   Multiple 6-inch Circular Barrels (M-6-C)

Figure 59 shows a small, flat gravel just downstream of the culvert near the headwall.
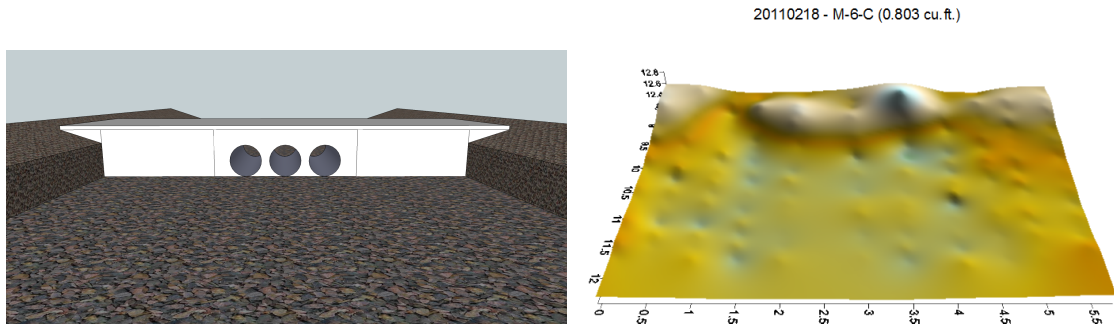

Figure 59: Typical Downstream Surface Model for Experimental Model M-6-C for 0.3 Percent Slope with Large Rocks

Figure 60 shows a flat gravel bar downstream of the culvert, but there is also some scour downstream of the bar and towards the right bank.
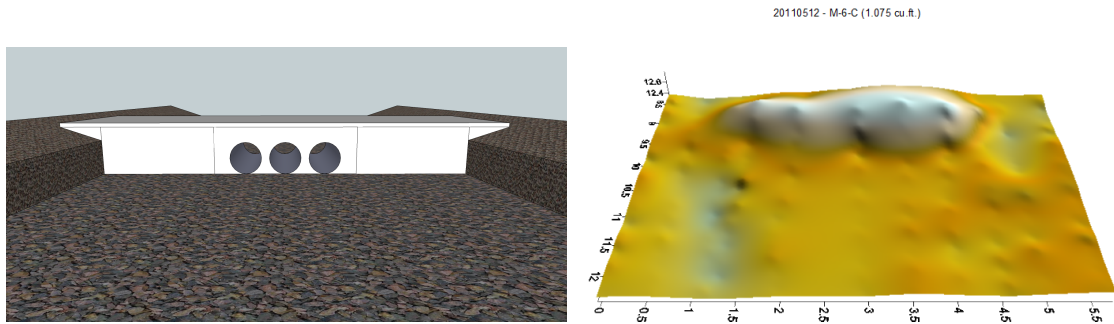
Figure 60: Typical Downstream Surface Model for Experimental Model M-6-C for 0.6 Percent Slope with Large Rocks

Figure 61 shows a U-shaped gravel bar that has notable scour at the culvert outlet and wings on both sides of the centerline. Note the accumulation in the corners by the headwall.

Figure 62 shows a flat gravel bar with three scour holes downstream.

Figure 63 shows a U-shaped gravel bar with slight scour downstream and at the culvert exit.
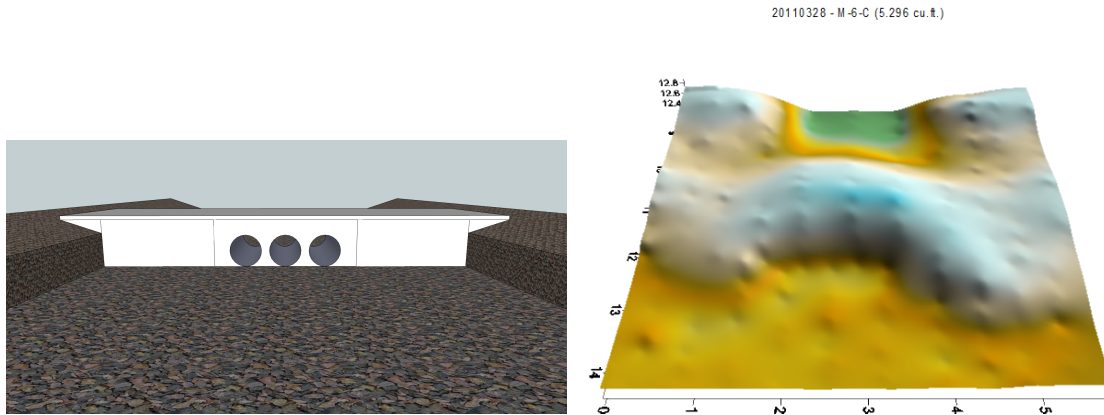
Figure 61: Typical Downstream Surface Model for Experimental Model M-6-C for 1.0 Percent Slope with Large Rocks
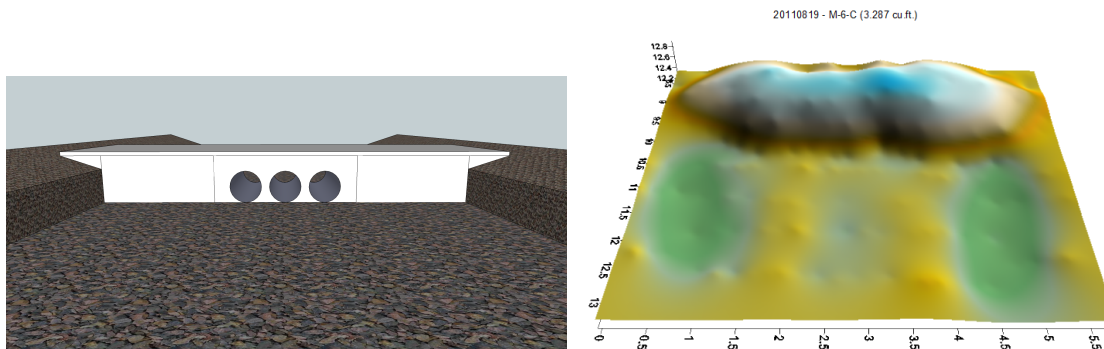

Figure 62: Typical Downstream Surface Model for Experimental Model M-6-C for 0.3 Percent Slope with Small Rocks
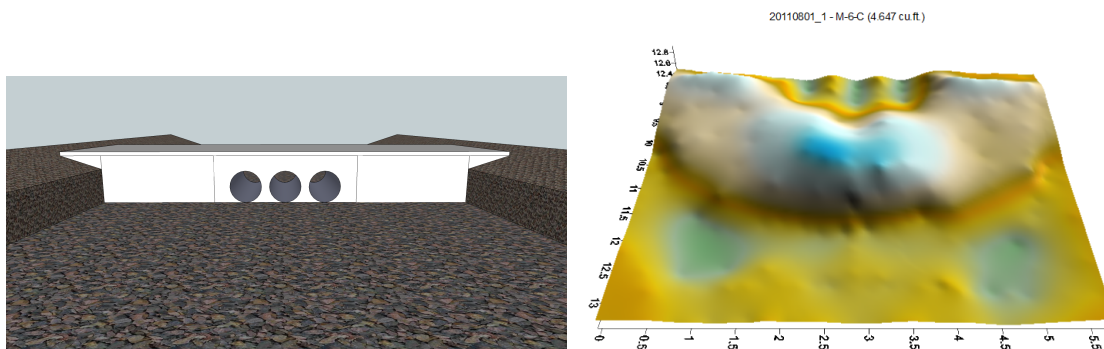
Figure 63: Typical Downstream Surface Model for Experimental Model M-6-C for 0.6 Percent Slope with Small Rocks

4.3.8 Multiple Rectangular Barrels (M-R)

Figure 64 shows a small mound immediately downstream of the outlet, with slight scour downstream of the mound and accumulation in the corners near the headwall.
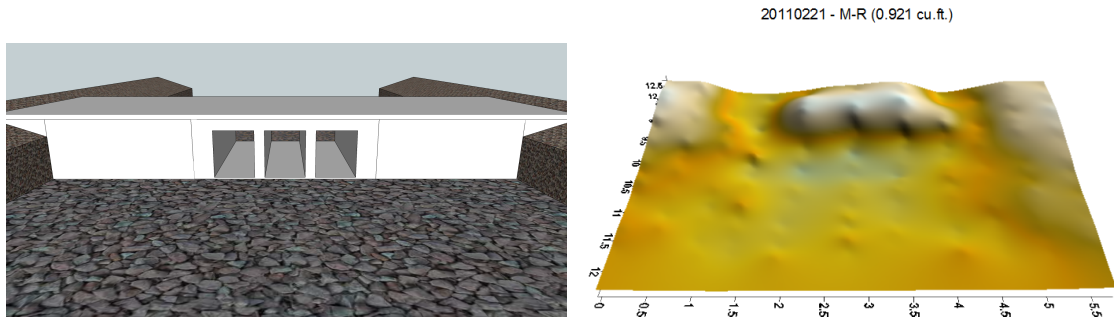
Figure 64: Typical Downstream Surface Model for Experimental Model M-R for 0.3 Percent Slope with Large Rocks

Figure 65 shows a gravel bar just downstream of the culvert outlet, with very slight scour.
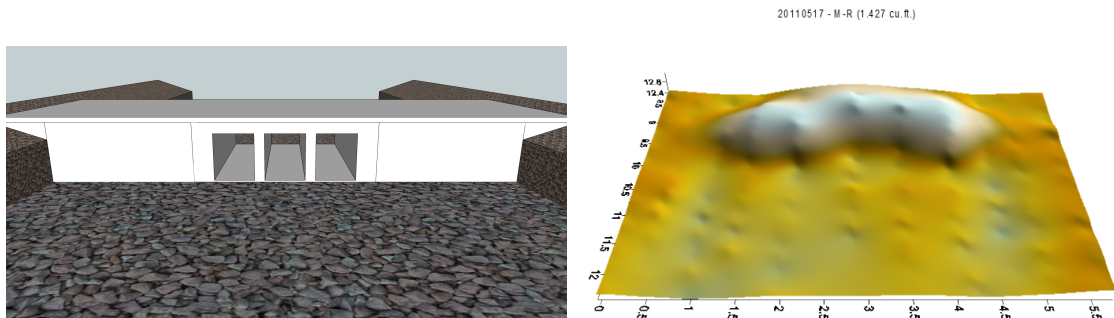
Figure 65: Typical Downstream Surface Model for Experimental Model M-R for 0.6 Percent Slope with Large Rocks

Figure 66 shows a U-shaped gravel bar with a wing on the left bank side of the bar. There is also scour near the culvert outlet.

Figure 67 shows a gravel bar just downstream of the outlet with scour holes downstream.

Figure 68 shows a U-shaped gravel bar with a wing on the left bank side of the bar. There is also scour near the culvert outlet.
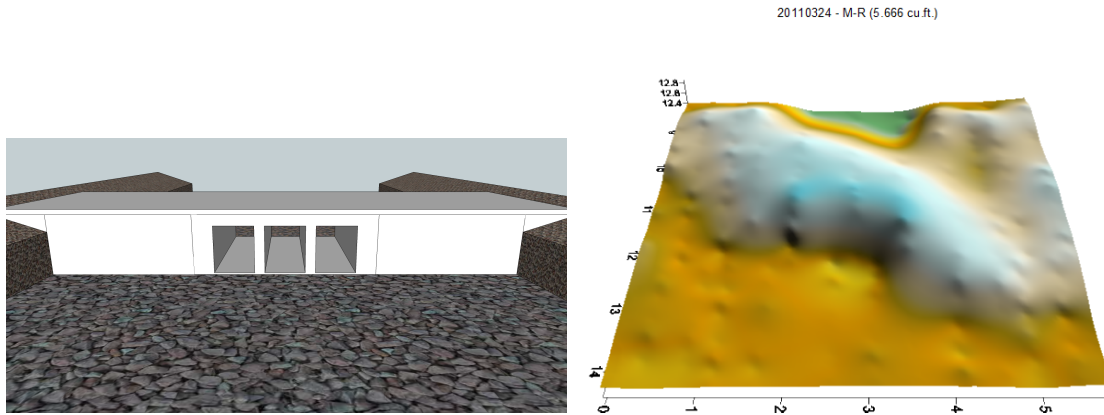
Figure 66: Typical Downstream Surface Model for Experimental Model M-R for 1.0 Percent Slope with Large Rocks
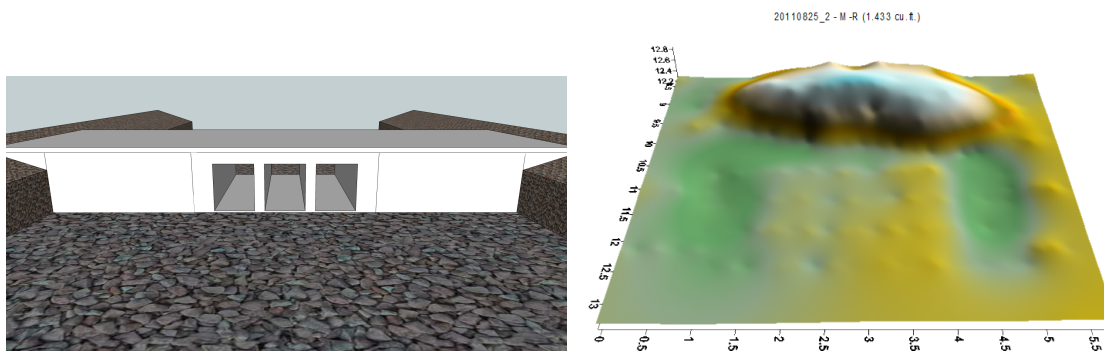
Figure 67: Typical Downstream Surface Model for Experimental Model M-R for 0.3 Percent Slope with Small Rocks
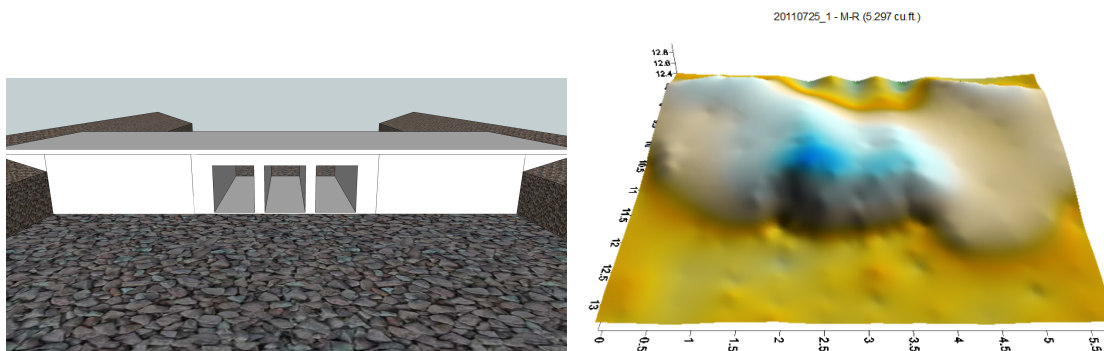
Figure 68: Typical Downstream Surface Model for Experimental Model M-R for 0.6 Percent Slope with Small Rocks

5 Results and Interpretation

5.1 Water Flow Behavior

The experimental program collected both flow field information as well as solids mobilization information. This sub-section presents results regarding the flow field, a subsequent sub-section addresses the solids mobilization.

5.1.1 Velocity Profiles

The experimental program collected velocity profiles upstream, just downstream, and further downstream of the culvert system models. Velocity profiles in this report are plots of the downstream component of velocity versus distance above the bed elevation at some location in the model. The shape of these profiles conveys information on the culvert system's ability to influence fluid and solids transport.
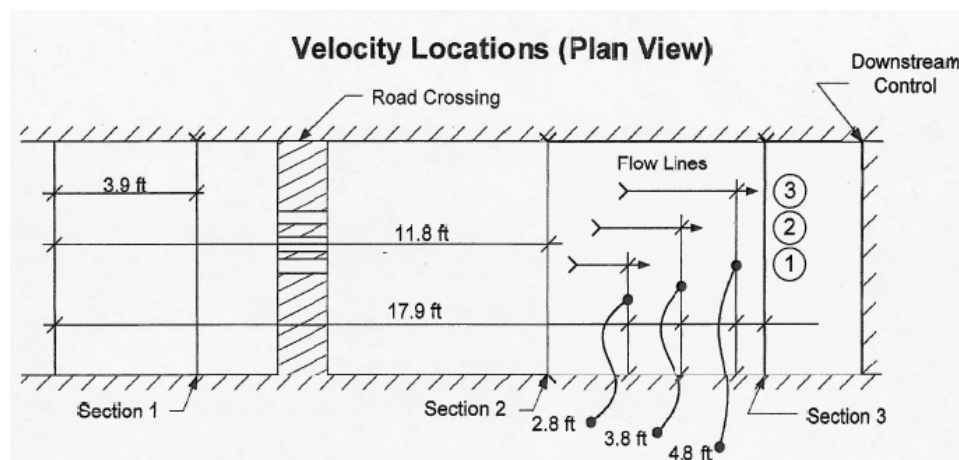
Figure 69: Locations of the three cross sections relative to the inlet head tank (left) and the West wall of the flume (bottom). Distances from the West wall to the three stations at each cross section are 2.8, 3.8, and 4.8 feet. The 3.8 foot distance is the distance from the wall to the centerline of the flume as configured for this research. The three cross section distances from the inlet, moving downstream, are 3.9, 11.8, and 17.9 feet.

Figure 69 is a plan view sketch of the location of three cross sections in the flume. The centerline and 1.0 feet left and right of this centerline were the stations in each cross section where velocity measurements were collected. At each station instantaneous velocities using the Micro-ADVs were collected at different depths during the experiments. The collection of these measurements for a particular experimental condition is the velocity profile. The stations were the same for all three cross sections, hence a line segment connecting the three cross sections at a particular station is called a "flowline." For example the centerline

stations at each cross section are the centerline flowline. Similarily the left and right bank flowlines are the lines left and right of center (looking downstream).
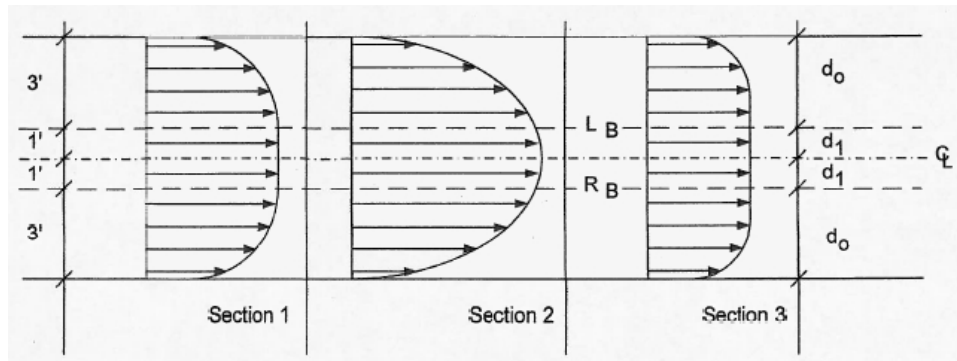
Figure 70: Approximate surface flow field in vicinity of each cross section.

The approximate surface velocity field at each section is depicted in Figure 70. The approach section is almost uniform across the flume, but just downstream of the culvert models, the culverts have accelerated the centerline flows and produce a flow field that has more curvature, with the largest velocity values at or near the centerline. Further downstream the flow field returns to an almost uniform condition.

Figure 71 is a typical velocity profile rendered in a 3-dimensional plotting routine. The culvert system models are located between the left and center profiles. The variation of flow velocity with depth is apparent in the plot. The mobile bed lies just below the bottom velocity vector at each location and has a non-zero thickness as implied by the plot.
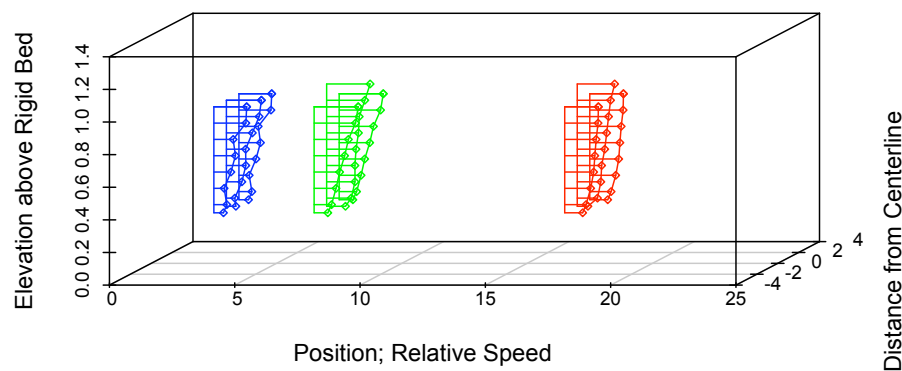
Figure 71: Typical velocity profiles at each section, station, and depth in 3-D rendering.

The plots like Figure 71 were studied and some general observations follow.

- Section 1 plots (upstream most section) have the same vertical profile on each flowline as the water approaches the culvert models. The profiles have vertical curvature that decreases (become straight) with increasing model slope. The shapes also change slightly with different culvert models — models with the most culvert open area (MR) are slightly convex indicating that a portion of the flow is through the culvert, whereas the small area systems, the curves are indistinguishable from intentionally blocked culverts.

  In small area models negative velocities were observed at the bed; the net discharge is still downstream, however there is a subtle "reverse" flow near the bed, near the culvert models. Such velocities would be anticipated to retard solids motion and contribute to solids deposition just upstream of the culvert model. As model slope is increased the magnitude of the negative velocities decreases.

  The near-surface velocities are proportional to model slope and are the highest magnitude velocity values in any profile.

- Section 2 plots (immediately downstream of the models) show the effects of the different model systems. The presence of the culvert models produced centerline velocities greater than the two off centerline velocities (an anticipated result). The near surface velocities were greater in the models with smaller open area, likely a consequence of more water being forced over the road and a requisite "contraction" to accommodate the added discharge with negligible change in flow depth.

 Negative velocities were observed in some of the non-centerline measurements suggesting reverse currents and eddies. Underwater video capture supports this interpretation — while these eddies eventually seem to move downstream (and new ones form), for practical purposes these are ineffective flow regions.

  The models with larger culvert area (e.g. MR) produced vertical profile nearly identical to the approach section in magnitude and shape. This result suggests that culvert open area dominates behavior, at least in our experiments, and if the area is large enough the presence of the hydraulic structure is undetectable using velocity measurements.

- Section 3 profiles are more uniform than the upstream sections suggesting that the effect of the hydraulic structure is a short-distance phenomenon. Our flume is too short for the effect of the models to be completely absent at the downstream section, but the profiles at Section 3 were remarkably similar (such that one cannot tell which upstream model was present).

Figure 72 is a sketch of the typical observed flow field — the sketch represents a composite of researcher observations for many experiments. The mound on the left side of the sketch is the mobile bed material that is initially mobilized by the water flow, builds up into a mound, and slowly approaches the culvert system. As materials are deposited on the

upstream side of the mound, other materials leave the downstream side of the mound and are carried through the culvert system, or are captured in the central eddy zone. Some materials are also trapped in the corner eddy zones (not depicted on the sketch, but are in the corners where the culvert model and the flume wall coincide).
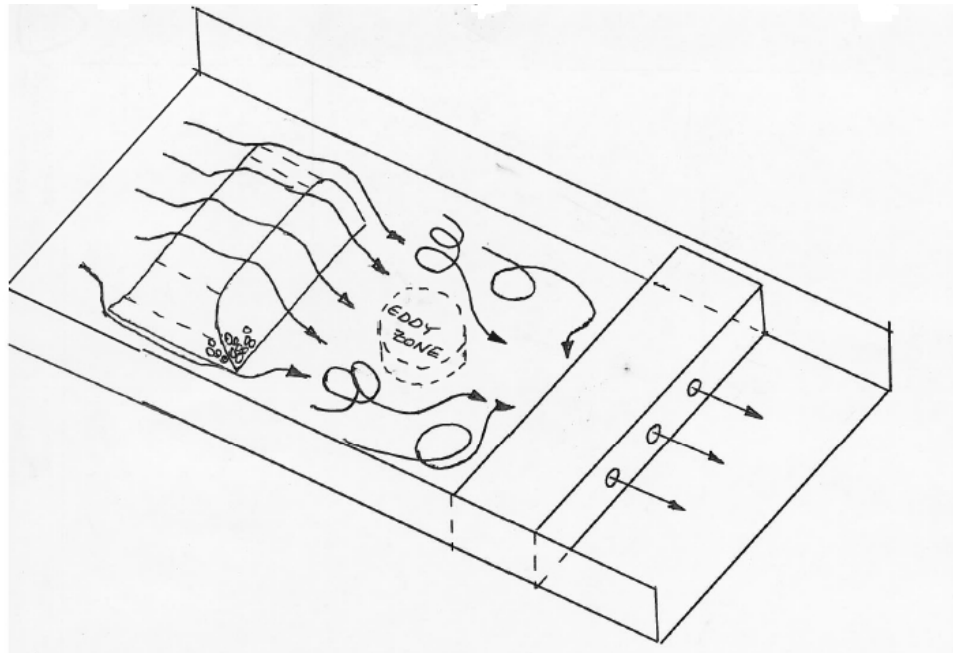
Figure 72: Sketch of typical observed flow fields for culvert systems arranged in-line with the approach flow axis.

The arrows represent typical pathlines in the experiments. The central eddy zone was common to all models, although it varied in size. This zone was subjected to occassional velocity measurements and generally there was no net downstream velocity component in a 40-second ADV interrogation. Solids would enter and leave this zone, so, over the several hour experiment duration, there was net downstream solids and liquid flow.

On the downstream side of the culvert model, the individual culverts produced straight pathlines close to the model. The roadway was submerged in all experiments, so these "jets" were identified by velocity measurements at the culvert outlet centerline as close to the culvert as the ADV probe could be placed.

Figure 73 is a photograph of a culvert system (multiple rectangular) near Junction, Texas in conditions similar to the experiments. Flow is through the system with flow over the road. The photograph shows that flow over the apron (close to the foreground) seems to go farther than flow through the culvert systems (which likely have debris). An explanation for this phenomenon is that the flow per unit width over the apron section is larger than over the section with culvert underflow. Similar behavior was observed in the laboratory experiments, although the effect was barely perceptible.

Figure 73: Photograph of a culvert system (multiple rectangular) in conditions similar to the experimental program.

The photograph also shows a mound of solids near the center of the stream on the downstream side of the culvert system. Similar mounds were observed in the experiments.

Figure 74 is an underwater photograph with hand-drawn contours that indicate the depression of the bed material just downstream of a culvert and flow arrows indicating the approximate direction of flow at the bed elevation. Near the right of the photograph is a hand drawn contour of the leading edge of the mound. The underwater photograph was made during one of the experiments represented in the previous chapter as Figure 49. In that figure, the mound and flow pattern is apparent from the post-experiment elevation survey.

Figure 75 is a sketch of the typical observed flow field in the skew experiments — the sketch represents a composite of researcher observations for many experiments. The skew angle was 15 degrees of arc. The researchers have visited actual skew systems with 30+ degrees of arc offset from the main axis of the channel.

The sketch depicts that the upstream mound assumes an angle similar to that of the culvert model. This orientation was observed in all experiments. The two eddy zones were prominent in the skew experiments with large deposition of material in these regions and essentially no further movement of that material within the experimental duration.
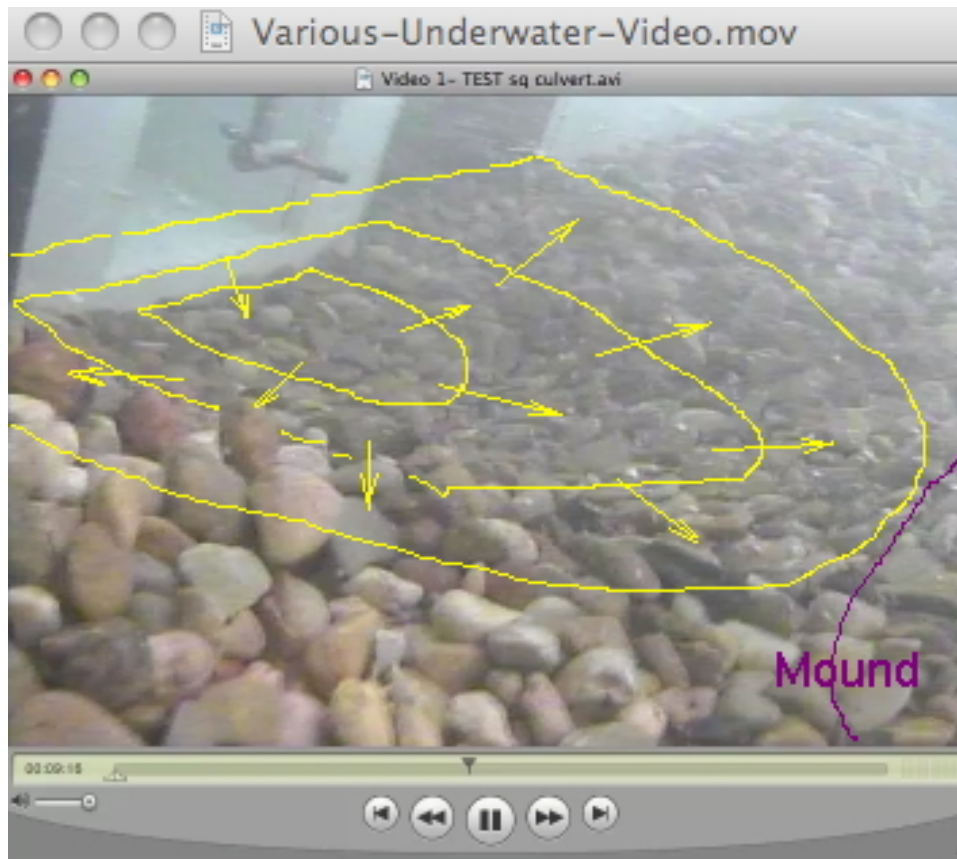
Figure 74: Underwater photograph downstream of culvert model. The ADV probe is visible. Yellow contours are hand drawn to help guide reader. There is a depression and a mound. Flow arrows are approximately the flow field at the bed-liquid interface. The system is a single rectangular culvert; the two side culverts are blocked by masonite panels in the experiment.

The velocity profiles along the three flowlines in Figure 69 were proportional to their position. In the skew experiments the highest magnitude velocity was at the inside of the skew induced turn and centerline, with smaller values on the outside of the skew induced turn.

In Figure 75 the skew system essentially forces water to turn (alternatively we can consider such systems in bends in streams where the roadway geometry requirements don't make sense to try a perpendicular crossing). Thus the near bank is on the inside of the turn, and the eddy zone is reasonably large as indicated in the sketch. The far bank is on the outside of the turn, the eddy zone is smaller in overall size but identical in impact; solids stop in this zone and stay there.

The relationship between culvert open area and velocity profiles, with the added consider-
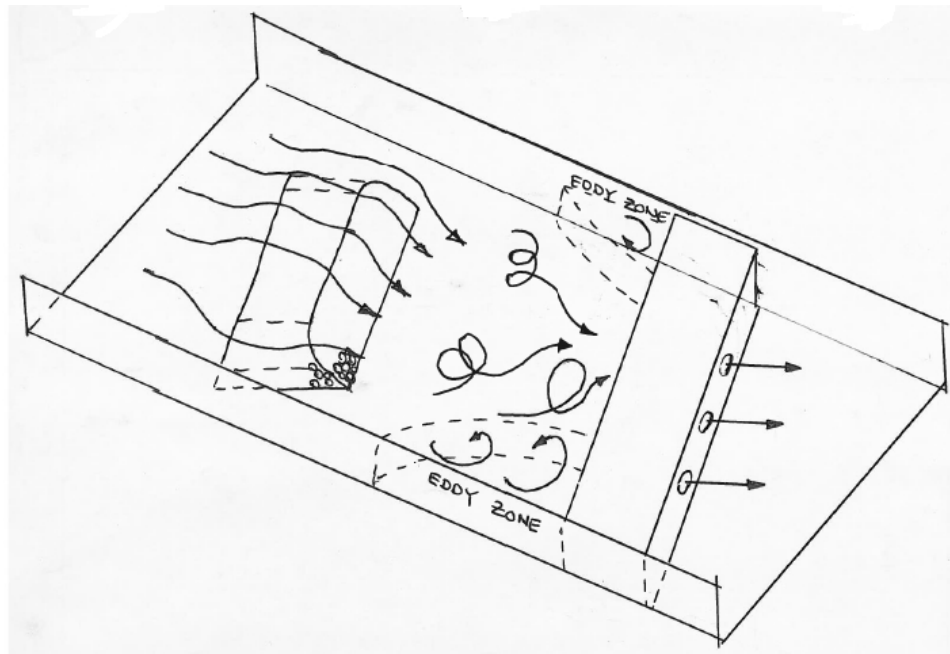
Figure 75: Sketch of typical observed flow fields for culvert systems arranged skew with the approach flow axis.

ation of asymmetry was preserved so in general skew systems behaved in a similar fashion as the in-line models although there is detectable asymmetry when comparing the left and right bank profiles. The eddy zones are different in size and shape, the central eddy zone in the upstream position just below the berm was not apparent. The culvert open area being related to velocity profile change was unanticipated, and the stage-conveyance was examined as a possible explanation.

Figure 76 is plot of the stage-conveyance relationship for the approach section (line with dots) and the various culvert models. The plot suggests why the larger area models are less detectable using velocity profiles (as well as better performance in solids transport) — the stage-conveyance of the larger area models is closer to the stage-conveyance of the approach section.

The result is essentially the stream-simulation concept restated and suggests culvert systems should be selected to match the stage-conveyance of the approach section. In our experiments we always had flow over the road so all systems departed from the concept, with the multiple rectangular being the closest in a practical sense to the approach condition.
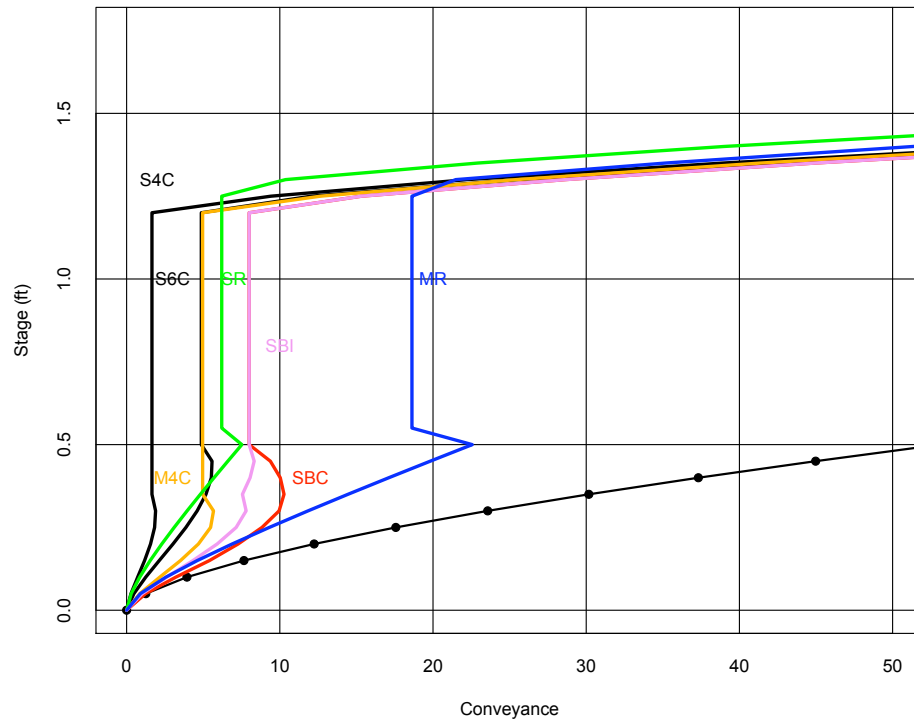
Figure 76: Stage-conveyance relationship for different culvert systems and the approach section

5.2   Solids Mobilization

Figure 77 is a plot of solids transport as a function of discharge for mobile bed experiments. The physical model experiments for the current study are plotted as circles, the prior literature as triangles.

Figure 77 uses proportional shading to indicate the quantity of data either recovered from the literature or created by the project. The plot represents nearly 12,000 different experimental values (from the literature). The plot indicates that the experimental results are consistent with prior studies.

5.2.1   Comparison to Screening Tool Estimates

The next two plots are comparisons of solids flux as predicted by the screening tool and as observed in the experiments just upstream and downstream of the culvert models. The observed values for the approach section were obtained from the product of solids density
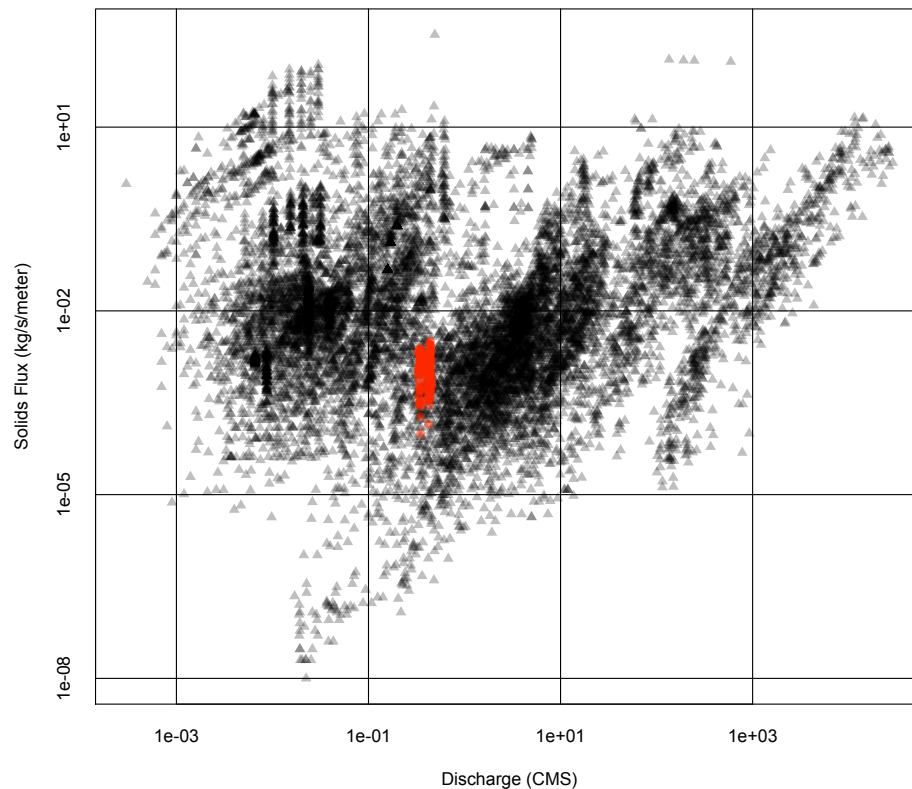
Figure 77: Solids transport ($\frac{kg}{m-s}$) versus discharge (m^3/s). Triangle markers are literature derived values. Circle markers are physical experiments conducted in this research.

and the volume transported divided by the experiment duration in seconds.

Figure 78 is the plot of solids flux in the approach section upstream of the culvert model. The equal value line indicates that the predicted values are generally greater than the observed values, however the order of magnitude is correct. The predicted values are generally no larger than one log cycle (factor of 10) than the observations. The literature values are sparse in the region of these experiment so these results are considered reasonable.

Figure 79 is the plot of solids flux in the exit section downstream of the culvert model. The predicted values from the screening tool are larger than in the approach section – reflective of the lower depth of flow, hence higher mean velocity for the cross section. The observed values for the exit section were obtained from the product of solids density and the volume transported less any volume remaining in the culvert barrels divided by the experiment duration in seconds.

In the plot the predicted and the observed values are still order of magnitude correct,
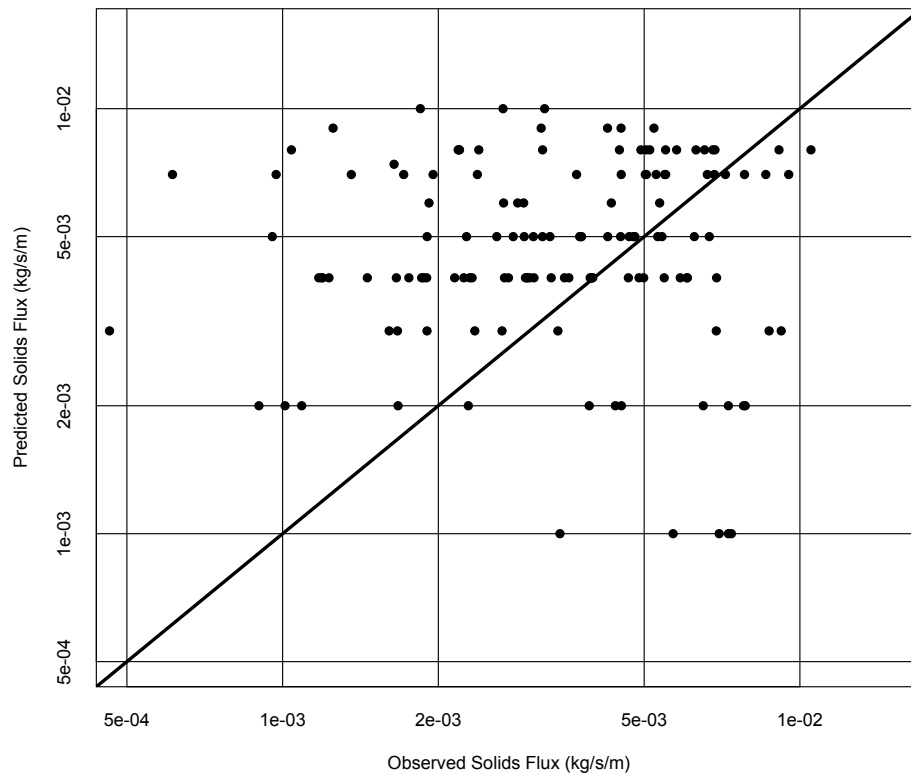
Figure 78: Solids transport flux as predicted by the screening tool and as observed at the **approach** section to the culvert models. The units are kg/s/m (mass flow per unit width). SI units are used for consistency with the literature derived database.

hence we conclude the screening tool is a reasonable predictor of solids flux approaching (and leaving) a culvert system.

5.2.2   Comparison by Solids Size, Culvert Area, and Culvert System Type

Figure 80 is a plot of solids transport as a function of solids size in the TTU experiments. Two materials were used, a large size and small size. The large material had a D_{50} of 19.1 millimeters, the small material had a D_{50} of 9.1 millimeters. The plot suggests that in the TTU experiments the size of material had minimal impact on the amount of solids mobilized and discharged through the culvert systems.
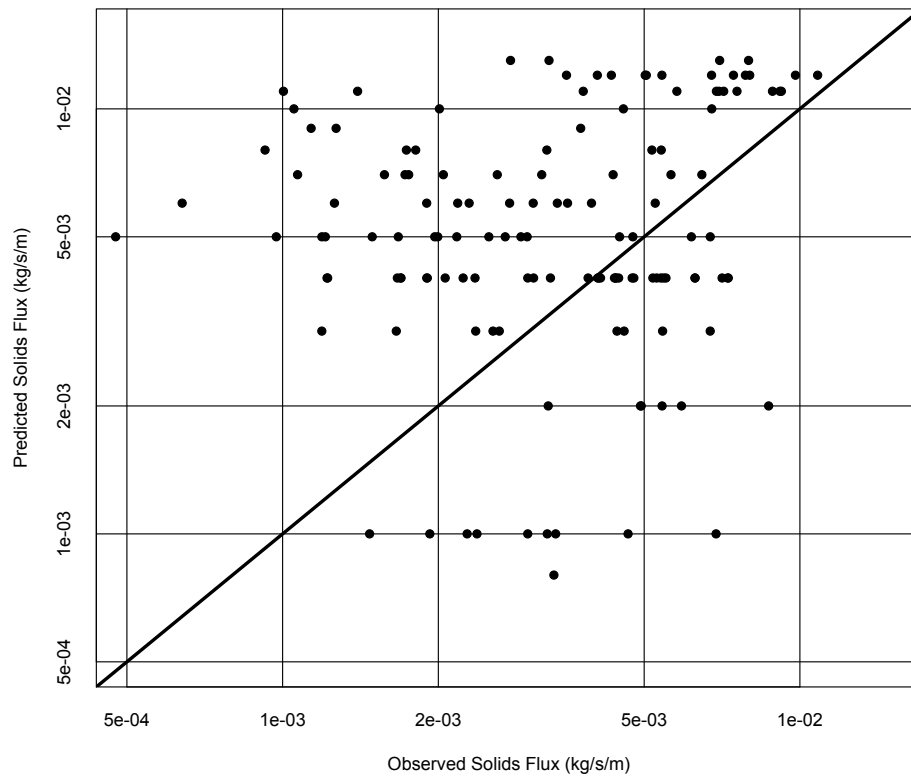
Figure 79: Solids transport flux as predicted by the screening tool and as observed at the **exit** section from the culvert models. The units are kg/s/m (mass flow per unit width). SI units are used for consistency with the literature derived database.
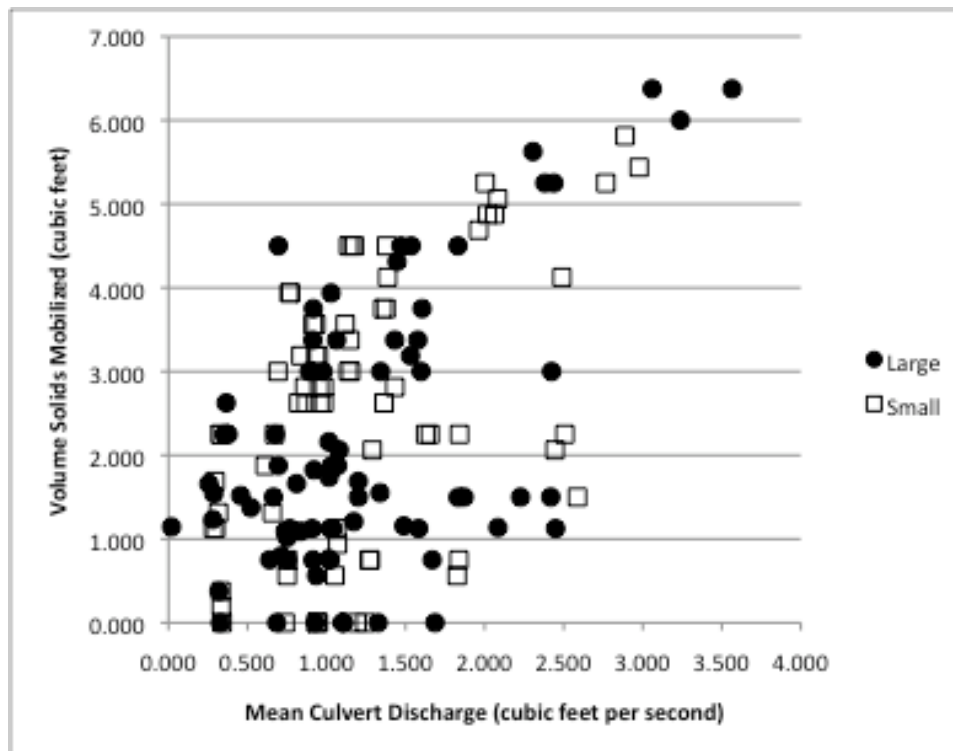
Figure 80: Solids transport ($\frac{kg}{m-s}$) versus discharge (m^3/s) for two different sized materials. Large has a $D_{50} \approx 19.1mm$, Small has a $D_{50} \approx 9.1mm$

Figure 81 is a two-panel boxplot comparing the discharge and the solids mobilized for the two different solids sizes. The boxplot as well as supporting two-sample Wilcoxon hypothesis tests indicates that the two sizes have no impact on either the requisite discharge to mobilize, nor on the solids volume actually moved. The experiments were all operated in a fashion to force mobilization and the upper limit of clear-water discharge is somewhat constrained by the flume, hence the researcher believes that the small solids should mobilize at lower flows and velocities, however these experimental conditions were not examined.

Figure 82 is a plot of solids volume transported through different culvert systems versus the clear water discharge (through the culvert, excluding the flow over the road). The plot indicates that the culvert systems with larger open area (multiple rectangular and multiple circular 6-inch) could convey more discharge as well as more solids volume. The plot includes skew experiments that are not distinguished in the plot.

The staggered barrel systems performed comparably to the larger open area systems in their discharge range, but because the larger systems could support larger culvert discharges, they could outperform the other systems in many experiments. Figure 82 does not distinguish channel slope, which is addressed in the next plot.
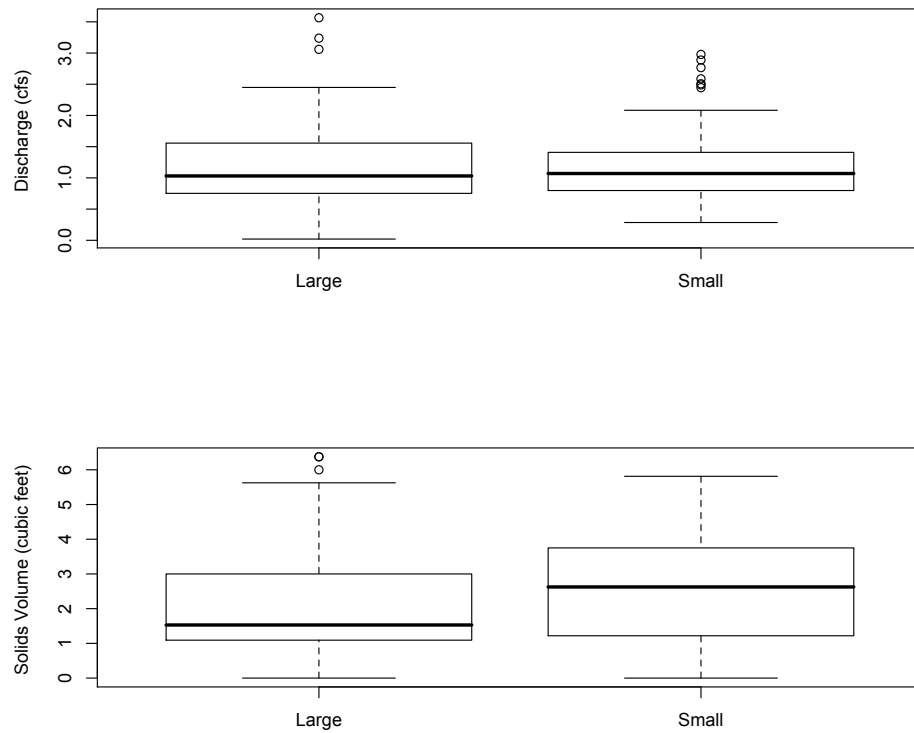
Figure 81: Discharge versus Mean Grain Diameter (Upper Panel) and Solids Mobilized versus Mean Grain Diameter (Lower Panel). Large mean grain diameter has $D_{50} \approx 19.1mm$, Small mean grain diameter has $D_{50} \approx 9.1mm$
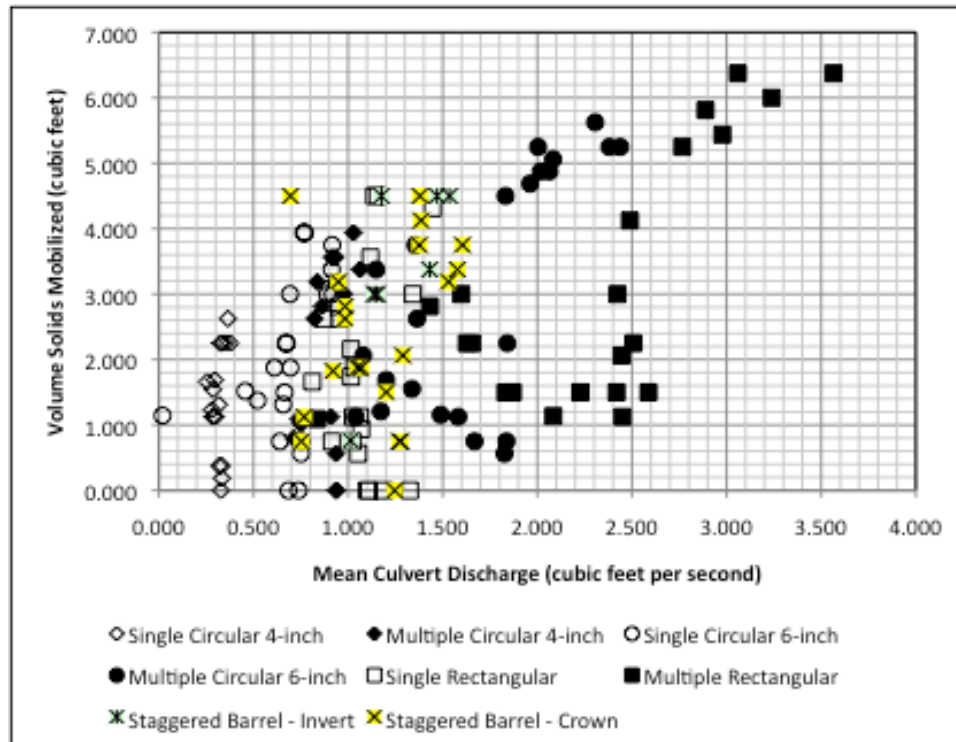
Figure 82: Solids transport $(\frac{kg}{m-s})$ versus discharge (m^3/s) for different culvert systems

Figure 83 is a plot of solids volume transported through different culvert systems versus the channel slope. The plot depicts three slopes for most of the models, and includes the skew experiments; these experiments are not separately distinguished in the figure. The lower values on the 0.006 slope line (middle set of markers) are generally the skew experiments — regardless of model type, the skew experiments mobilized less material.

Using the lower and upper values in each marker set to define an envelope of behavior the plot indicates that more solids are mobilized as the slope increases, an anticipated and literature supported finding.
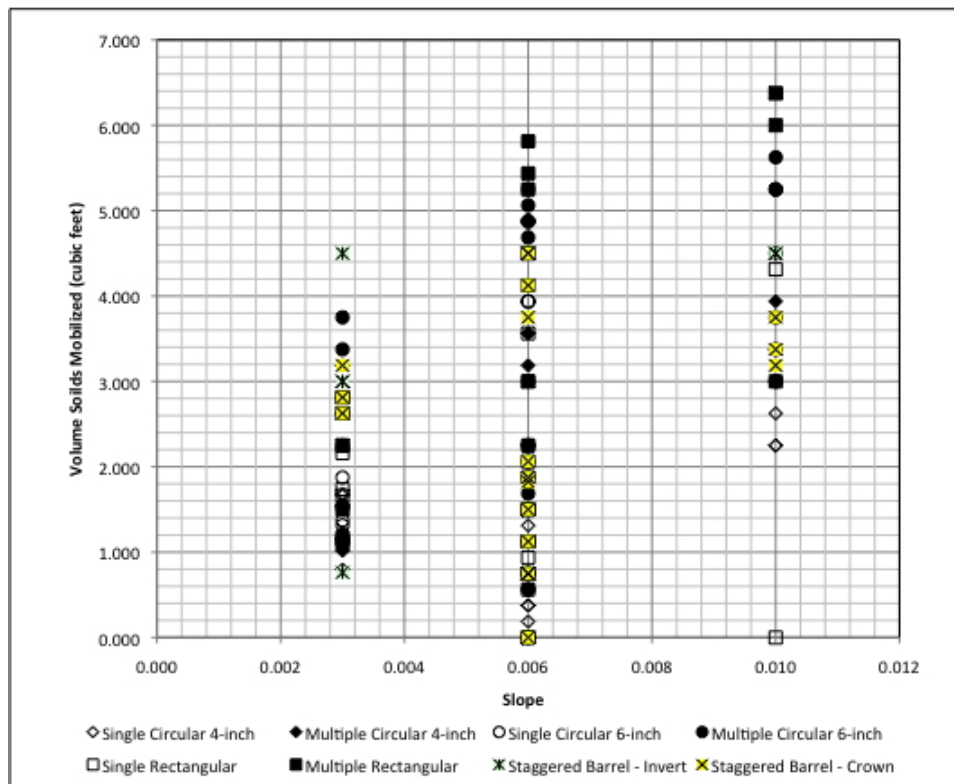
Figure 83: Solids volume transported (ft^3) versus channel slope for different culvert systems

Figure 84 is a plot of solids volume transported through different culvert systems versus the culvert open area. The plot includes both in-line and skew experiments (discussed later). The plot indicates that as culvert area is increased, the solids volume mobilized and discharged through the culvert system increases. The two largest area systems, the multiple circular 6-inch and the multiple rectangular, moved material in all experiments involving those two configurations.
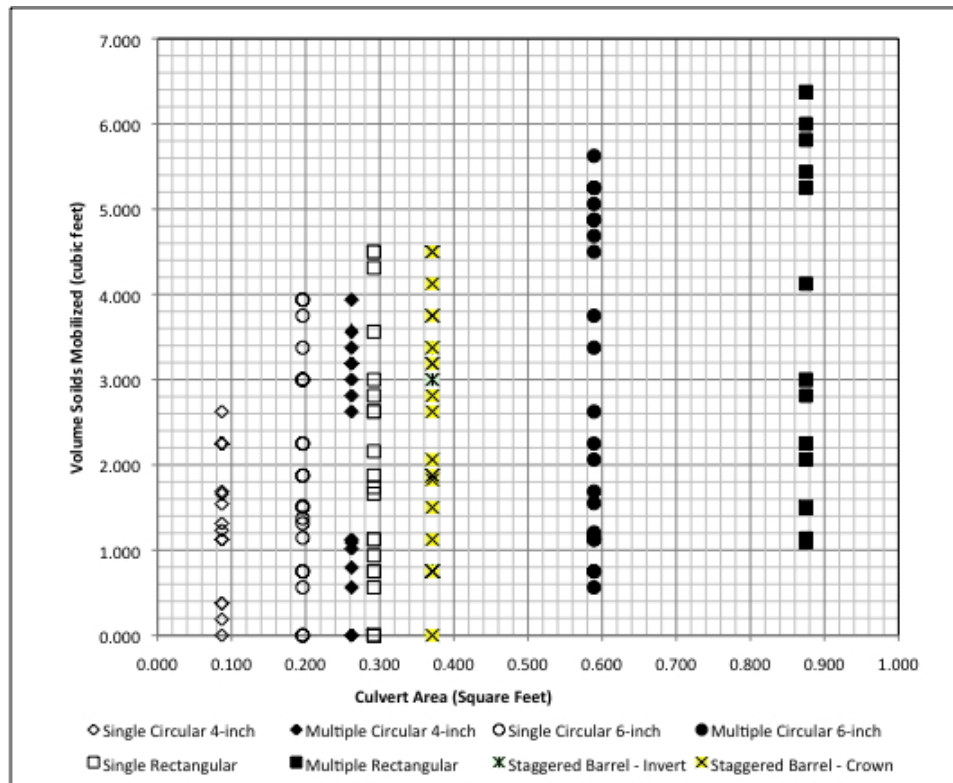
Figure 84: Solids volume transported (ft^3) versus culvert open area (ft^2) for different culvert systems

Figure 85 is a plot of solids volume transported through different culvert systems versus the product of slope and culvert open area. This particular plot is an attempt to incorporate the four variables in the screening tool, specifically the channel slope, the culvert area (which should be directly proportional to both the culvert discharge and velocity), and the solids transported.

The behavior is consistent with the screening tool (and with the Peterson (1975) charts) in that as slope is increased for a given discharge and presumably velocity, the solids mobilized increases. The plot includes the skew experiments; these experiments are not separately distinguished in the figure.
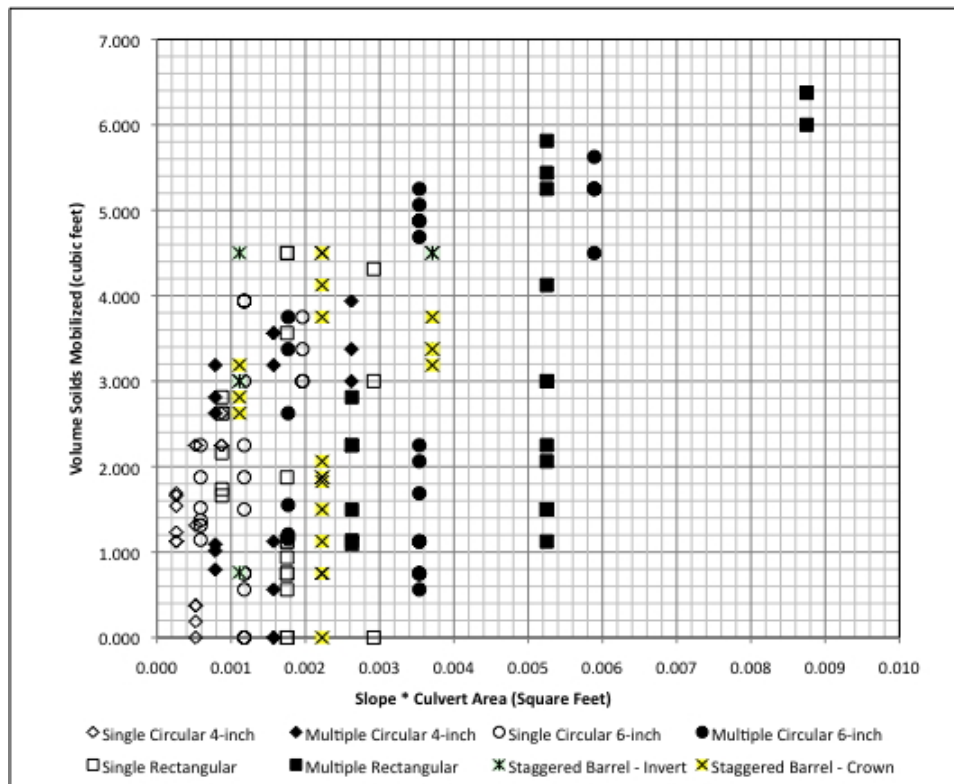
Figure 85: Solids volume transported (ft^3) versus product of channel slope and culvert open area (ft^2) for different culvert systems

The plot suggests that: (1) as the slope of the approach and exit sections is increased, more solids are mobilized (and moved through the culvert systems), and (2) as the culvert open area is increased, more solids are mobilized (and moved through the system).

5.2.3   Identification of Skew-Orientation Experiments

Figure 86 is a plot of solids volume transported through different culvert systems versus
the culvert open area, with the skew experiments identified. The values for the skew
experiments are identified by the ellipse drawings on the plot for the different culvert
configurations. The plot also has short horizontal line segments that identify upper support
for the skew experiments. Generally, experiments below these line segments are skew
experiments, while those above the line segments are the in-line results.
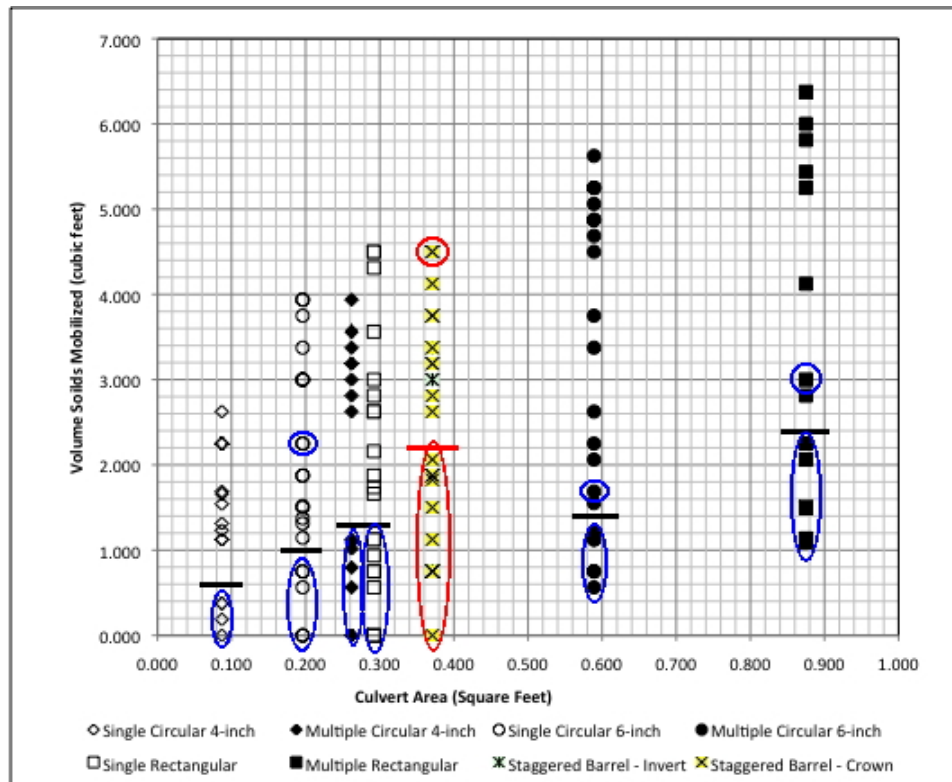
Figure 86: Solids volume transported (ft^3) versus culvert open area (ft^2) for different
culvert systems, with skew experiments identified

Figure 86 suggests that the staggered barrel systems may perform better than anticipated
based on culvert open area trend, although the evidence is weak.

Figure 87 is a boxplot of the different configurations for the skew experiments. The figure
supports the observation that staggered barrel systems seem to perform better than an-
ticipated on culvert open area alone, but only slightly — in general the solids transported
through a system in the skew configuration is roughly proportional to the culvert system
open area.
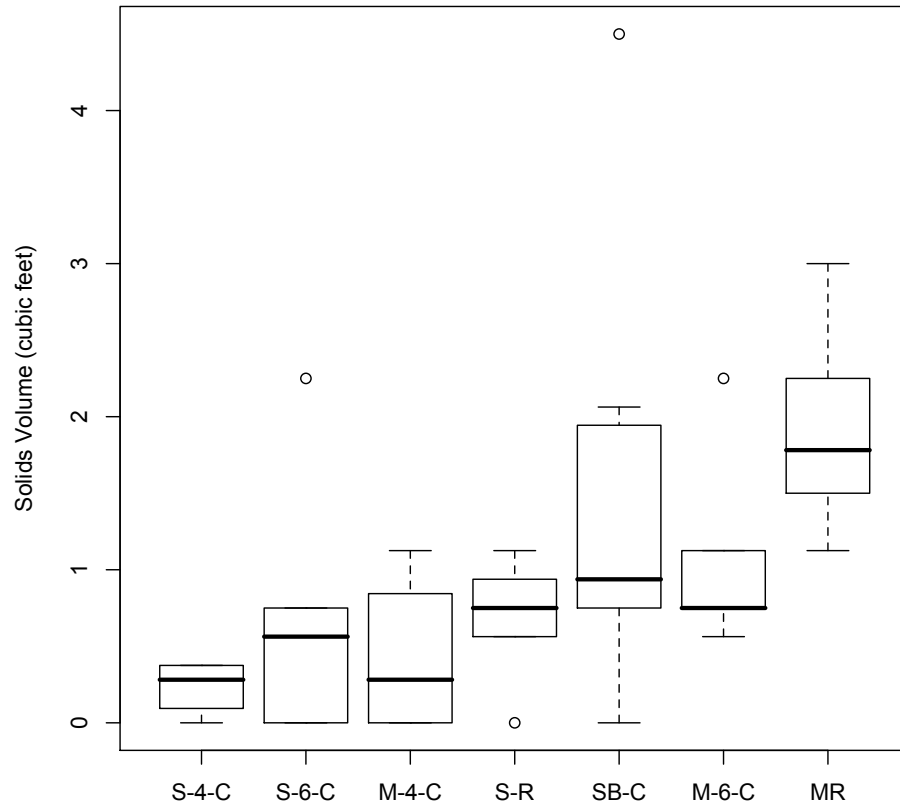
Figure 87: Boxplot of solids mobilized in skew setting by culvert type. Plot is arranged in increasing culvert open area order, consistent with presentation in Figure 86

Figure 88 is a boxplot of the different configurations for the in-line experiments; 6 experiments with zero mobilization are omitted from the plot. The figure supports the observation that in general the solids transported through a system is roughly proportional to the culvert system open area. This finding is somewhat logical, but does raise the question of how that open area is presented to the mobile bed stream.

In the laboratory experiments the culverts were all spaced close to each other (spacing proportional to the web spacing in typical specifications) and in the center for the stream — quite unlike the spacing depicted in Figure 1. Thus the water is accelerated through a contracting-type situation and that is why the systems performed about the same when normalized for culvert open area.
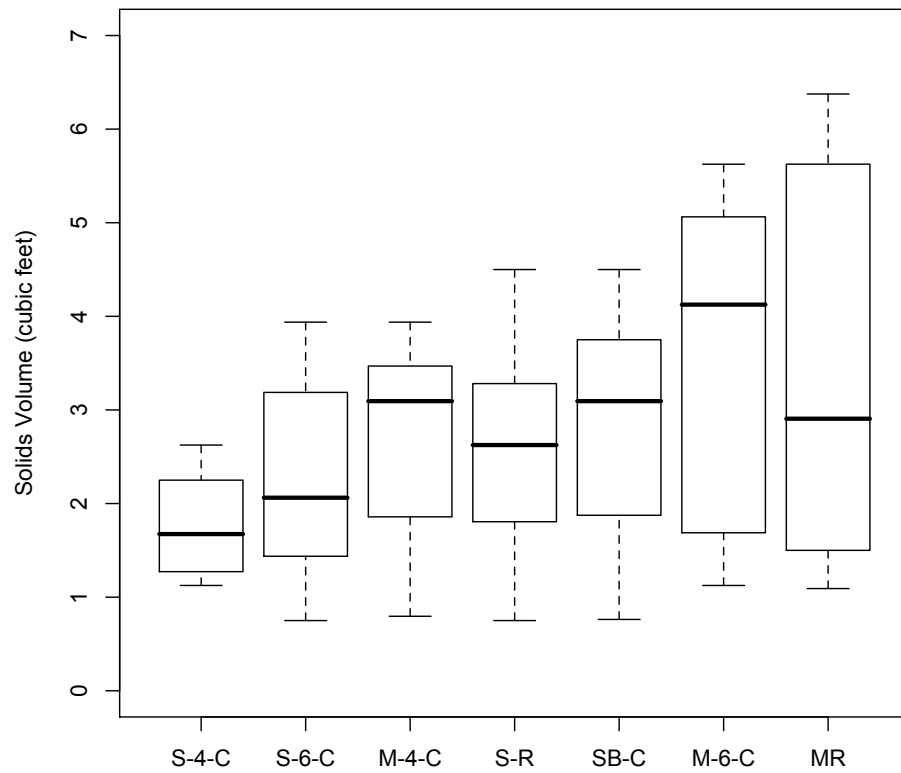
Figure 88: Boxplot of solids mobilized in in-line setting by culvert type. Plot is arranged in increasing culvert open area order, consistent with presentation in Figure 86

6   Guidelines and Summary

This section presents guidelines for using the findings of this research in solids management by culverts in areas of mobile beds, and summarizes the overall project.

The guidelines are largely extrapolated from observations in the laboratory study and principles from the literature review. The screening tool is also discussed as a way to estimate the solids that might be moved in a system and to use that estimate to produce a combined flow (water and solids) volume that could be considered in analysis of culvert systems.

6.1   Guidelines from Physical Modeling

The physical model suggests the following:

1. Our models needed to be in flood stage (flow over the road) to mobilize and transport solids in the time frame of the experiments – about 5 hours. How this time frame is related to real-world processes is unknown — but we believe it is long.

2. As the slope of the approach and exit increase, more solids are mobilized and moved through the system.

3. As the area of culverts is increased, more solids are mobilized and moved through the system.

4. The staggered-barrel systems performed as anticipated based on culvert open area. Hence our experiments showed no particular advantage to these systems, except in skew settings where the systems transported more solids than anticipated based on culvert open area.

5. Stage-conveyance plots showed that our largest open area systems to have a curve closest to the approach section stage-conveyence until submergence (of the culvert). We interpreted this finding as supportive of the hypothesis that matching the approach section conveyance and the culvert system conveyance is a way to build a system that can maintain solids continuity through the system.

6. As a practical matter, slope is dictated by the location of the system and engineered adjustments are likely to be ineffective and costly over any reasonable time frame. However, culvert open area is an engineering decision that is likely to be effective with the following considerations

    (a) The culvert system should be near the centerline of the stream to create the necessary acceleration to carry solids through the system. The contraction of such an arrangement based upon the literature review is important for solids continuity across the system. Spreading the culverts across the channel, even if it creates large culvert open areas, allows the approach flow to decelerate too

much and deposition to occur.

(b) Within the guidance above, the culvert system should match the stage-conveyance of the approach section at the desired clear-water discharge. Different culvert shapes could be used — our experiments found the rectangular to work best, but our approach section was essentially a wide rectangular approach section. Circular arrays are likely to be more useful in incised streams. Different diameters like that of the staggered barrel system make sense in such a matching exercise.

(c) The main barrel should be at grade or slightly below the stream grade so that the solids do not have to move vertically to get through the system. In our experiments there was sufficient force to lift the solids up a small step, but initial conditions in the experiment were solids slightly above the culvert invert (bottom) elevation.

7. Our experiments did not show performance differences in solids size; the mean grain diameter of our solids differed by only a factor of 2 (about 1/3 of a log cycle). The literature spans a greater range of sizes than the experiments and the researchers believe size difference surely matters. Sand sized experiments were omitted because these solids could not be kept in the experimental flume — thus our own anecdotal evidence is that solids size contributes to mobilization and hence culvert system solids transport performance.

6.2   Using the Screening Tool to Assist in Culvert Analysis

There was limited guidance in existing design manuals for estimating solids transport through a culvert system for analysis or design. Chapter 9 of the Utah DOT Manual of Instruction contains several procedures for estimating the volume of material moved through a culvert, which while decidedly more straightforward than the numerous equations presented in the second chapter is unsatisfying. The screening tool is a convenient alternative, data based and reasonably straightforward to apply.

The screening tool is useful for making two estimates, an estimate of the volume of solids approaching the culvert system, and an estimate of solids that can be transported through the system. A third estimate, the downstream solids volume transported, could be estimated. This discussion assumes the upstream and downstream would behave the same in the absence of the culvert system and this estimate is not considered.

6.2.1   Approach Solids Estimate

The approach section estimate is the amount of solids that the stream has to transport to maintain solids continuity. If the culvert system cannot accommodate this amount,

then deposition upstream of the culvert system is anticipated.

The actual use of the screening tool involves the following procedure:

(a) Estimate/specify the approach section water discharge. This value could be from a hydrologic study or observations or a design value. The screening tool is SI only, so the discharge would need to be converted into SI units (e.g. $1 ft^3/s * \frac{m^3}{35.31\ ft^3} = 0.02832 m^3/s$).

(b) Estimate the cross-sectional flow area for the water discharge based on the approach channel geometry and anticipated, or specified hydraulic conditions. The screening tool is SI only, so the area would need to be converted into SI units (e.g. $1 ft^2 * \frac{m^2}{10.76\ ft^2} = 0.0929 m^2$).

(c) Determine the approach section velocity as the ratio of the discharge and flow area.

(d) Determine the D_{50} of the mobile solids. Field samples, a photograph, or even a textural description should be sufficient. The database search engine is reasonably sensitive to this value, so a range is suggested — the example uses two orders of magnitude in the size entry.

(e) Determine the approach section channel slope.

(f) Determine the approach section equivalent width, W_{eq} — the ratio of flow area and hydraulic radius for the section.

(g) Use the screening tool to estimate the approach solids mass flow, $\dot{M}_{solids}$. The screening tool reports values in kilograms per meter width per second ($kg/m/s$).

(h) Convert to solids volume flow by

$$Q_{solids} = \dot{M}_{solids} * W_{eq} * \frac{m^3}{2650 kg} * \frac{35.31\ ft^3}{m^3} \qquad (19)$$

The estimate of solids volume is the volumetric flow rate of solids that the approach channel transports to the hydraulic structure. For solids transport continuity, the volume is the volume the structure has to transport so as to be transparent to the channel in terms of solids transport impact.

6.2.2   Culvert Solids Estimate

The culvert section estimate is the amount of solids that the culvert can transport assuming it behaves as an equivalent section in the screening tool database. The database, and indeed much of the literature, does not contain culvert specific information; however, borrowing from the UDOT manual a concept of equivalent section is useful for the solids flow estimates. In the equivalent section, the flow area is the

area of the culvert system. The equivalent width is the square root of this area. The discharge is the discharge through the culvert system. The approach discharge in our experiments was large relative to that actually conveyed by the culvert; all the experiments had flow over the road. In the culvert capacity estimate, only the culvert discharge is considered.

The actual use of the screening tool involves the following procedure:

(a) Estimate/specify the culvert water discharge. The value will either be the same as the approach discharge (culvert conveys all water) or smaller than the approach discharge (there is discharge over the top of the system). The screening tool is SI only, so the discharge would need to be converted into SI units (e.g. $1 ft^3/s * \frac{m^3}{35.31\ ft^3} = 0.02832 m^3/s$).

(b) Estimate the cross-sectional flow area for the water discharge based on the culvert system geometry and specified hydraulic conditions. The screening tool is SI only, so the area would need to be converted into SI units (e.g. $1 ft^2 * \frac{m^2}{10.76\ ft^2} = 0.0929 m^2$)

(c) Determine the culvert section velocity as the ratio of the discharge and flow area.

(d) Determine the D_{50} of the mobile solids. The same value as the approach section is sufficient. Again a range of one order of magnitude above and below the D_{50} is suggested.

(e) Determine the culvert slope. A broken-back system is beyond the scope of this procedure.

(f) Determine the culvert section equivalent width, W_{eq} — the ratio of flow area and hydraulic radius for the section.

(g) Use the screening tool to estimate the approach solids mass flow, $\dot{M}_{solids}$. The screening tool reports values in kilograms per meter width per second ($kg/m/s$).

(h) Convert to solids volume flow by

$$Q_{solids} = \dot{M}_{solids} * W_{eq} * \frac{m^3}{2650 kg} * \frac{35.31\ ft^3}{m^3} \tag{20}$$

The estimate of solids volume is the volumetric flow rate of solids that the culvert system should be able to transport. The estimate is made as if the culvert system is just a channel with the equivalent hydraulic properties and assumes that solids can readily enter the culvert system from upstream. If this value is about the same as the approach section value, then the system should function as desired and solids move through the system as dictated by hydraulics. If the value is substantially smaller than the approach section value, then upstream deposition is anticipated. If

the value is substantially larger than the approach section value, then upstream and downstream depressions (erosion pits) are anticipated.

6.2.3   Example 1: Experiment 24

An example is presented on use of the screening tool based on an arbitrary experiment (Experiment 24). In that experiment the following measurements and data were collected:

$Q_{approach} = 15.510\ ft^3/sec\ (0.440\ m^3/s)$;

$A_{approach} = 11.321\ ft^2\ (1.052\ m^2)$;

$V_{approach} = 1.37\ ft/s\ (0.418\ m/s)$;

$D_{50} = 19.05$mm (0.06248 ft);

$S_0 = 0.003$;

$\text{Depth}_{approach} = 1.649 ft$;

$W_{approach} = \frac{11.321 ft^2}{1.649 ft} = 6.865\ ft\ (2.03\ m)$;

These measurements and values are sufficient to use the screening tool to estimate the volumetric solids transport towards the culvert system.

Figure 89 is a screen capture of the screening tool with the requisite values input and the search result for the conditions using a median diameter one order of magnitude larger than the target value, Figure 90 is a screen capture of the screening tool with the requisite values input and the search result using a median diameter one order of magnitude smaller than the target value. Bracketing is suggested to avoid zero returns in the searches.

The two values from these two searches, converted into solids volume are:

$Q_{solids} = 4.315 \times 10^{-5}(kg/m/s) * 2.03m * \frac{m^3}{2650kg} * \frac{35.31\ ft^3}{m^3} = 1.16 \times 10^{-6}\ cfs$

$Q_{solids} = 8.501 \times 10^{-3}(kg/m/s) * 2.03 * \frac{m^3}{2650kg} * \frac{35.31\ ft^3}{m^3} = 0.000229\ cfs.$

Thus the anticipated range of solids transport is from almost zero to 0.0002 cubic feet per second.

Continuing the example, the culvert values are then used in the screening tool to identify how much, if any solids the culvert system could be anticipated to transport.

$Q_{culvert} = 0.457\ ft^3/s\ (0.193\ m^3/s)$;

$A_{culvert} = 0.196\ ft^2\ (0.018\ m^2)$;

$V_{culvert} = 2.33\ ft/s\ (0.710\ m/s)$;

$W_{culvert} = \sqrt{0.196 ft^2} = 0.442\ ft\ (0.135\ m)$;

As before using a range of the median size is suggested to avoid zero returns in the searches. The same two searches are conducted, but the discharge and velocity are changed to reflect the culvert hydraulics rather than the entire channel hydraulics.
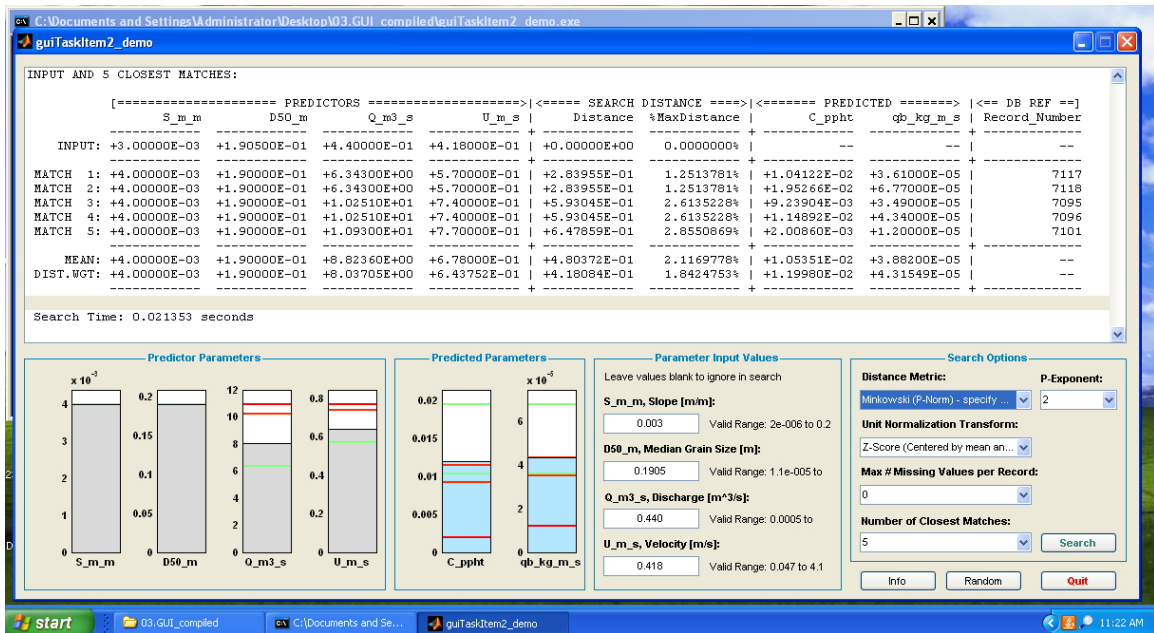
Figure 89: Screen capture of screening tool with approach values in input panel and search results displayed.
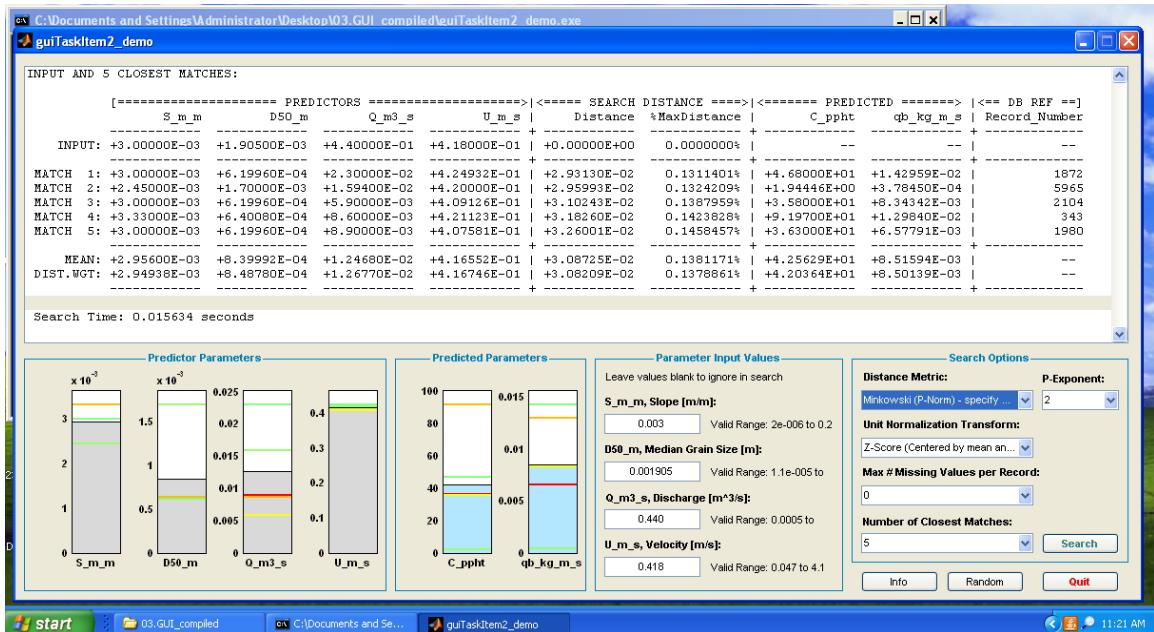
Figure 90: Screen capture of screening tool with approach values in input panel and search results displayed.

Figures 91 and 92 are screen captures of the screening tool with the requisite values input and the search result.

The two values from these two searches, converted into solids volume are:
$Q_{solids} = 3.42 \times 10^{-5}(kg/m/s) * 0.135m * \frac{m^3}{2650kg} * \frac{35.31\ ft^3}{m^3} = 6.15 \times 10^{-8}\ cfs$
$Q_{solids} = 3.22 \times 10^{-2}(kg/m/s) * 0.135m * \frac{m^3}{2650kg} * \frac{35.31\ ft^3}{m^3} = 0.00005\ cfs.$

Comparison of the two ranges suggests that the culvert system should be able to convey a fraction of solids transported to it by the approach section, but deposition is anticipated. The higher magnitude approach estimate is 0.0002 cubic feet per second of solids, while the higher magnitude capacity is 0.00005 cubic feet per second — about a factor of four less.

In the actual experiment the solids transported were $Q_{solids;observed} = \frac{1.518 ft^3}{15120 sec} = 0.0001004\ ft^3/s$[10]. The screening tool, when using the size bracketing suggested captures the observed value in the approach section, an encouraging outcome, but underestimates the culvert capacity by about a factor of two.

6.2.4   Example 2: Experiment 54

An example is presented on use of the screening tool based on an arbitrary experiment (Experiment 54). In that experiment the following measurements and data were collected:
$Q_{approach} = 15.510\ ft^3/sec\ (0.440\ m^3/s)$;
$A_{approach} = 10.767\ ft^2\ (1.001\ m^2)$;
$V_{approach} = 1.44\ ft/s\ (0.439\ m/s)$;
$D_{50} = 19.05$mm (0.06248 ft);
$S_0 = 0.010$;
$\text{Depth}_{approach} = 1.578 ft$;
$W_{approach} = \frac{10.767 ft^2}{1.578 ft} = 6.823\ ft\ (2.08\ m).$
These measurements and values are sufficient to use the screening tool to estimate the volumetric solids transport towards the culvert system.

The result of these two searches (screen captures are omitted) are:
$Q_{solids} = 4.13 \times 10^{-5}(kg/m/s) * 2.08m * \frac{m^3}{2650kg} * \frac{35.31\ ft^3}{m^3} = 1.14 \times 10^{-6}\ cfs$
$Q_{solids} = 7.48 \times 10^{-3}(kg/m/s) * 2.08m * \frac{m^3}{2650kg} * \frac{35.31\ ft^3}{m^3} = 0.0002078\ cfs.$

The range is again from almost zero to 0.0002 cfs solids are transported. The change in this experiment is a different slope (steeper) and a different culvert system. The solids are the same (hence the size range is the same).

---

[10]The implied precision is greater than actual precision — only one significant digit at best, hence volumetric rate is 0.0001 cfs.
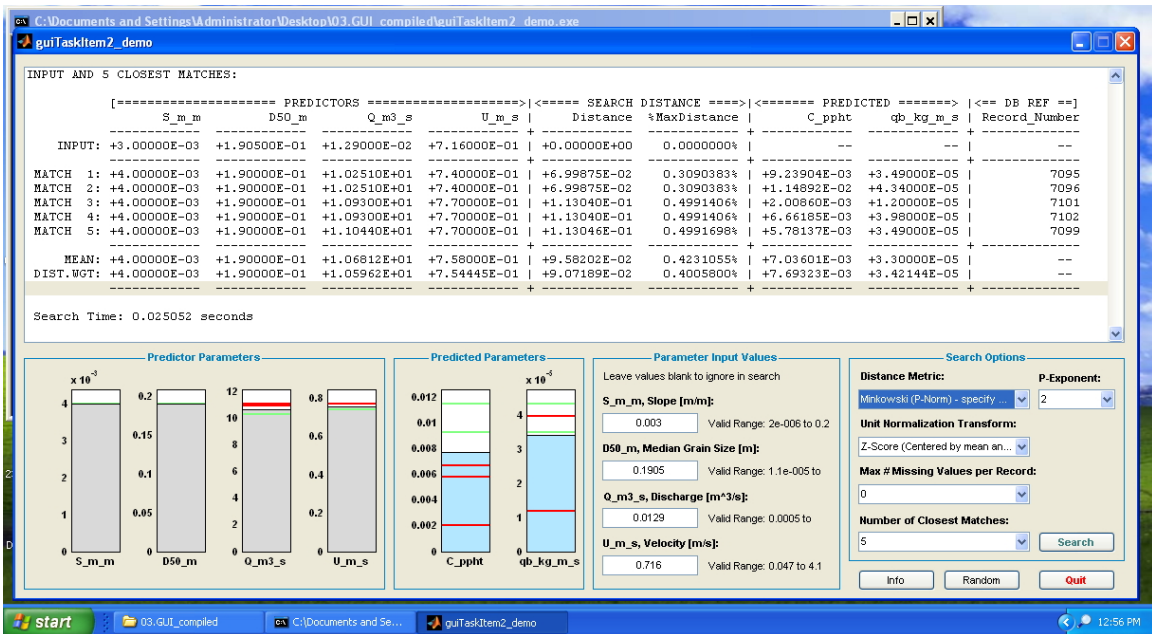
Figure 91: Screen capture of screening tool with approach values in input panel and search results displayed.
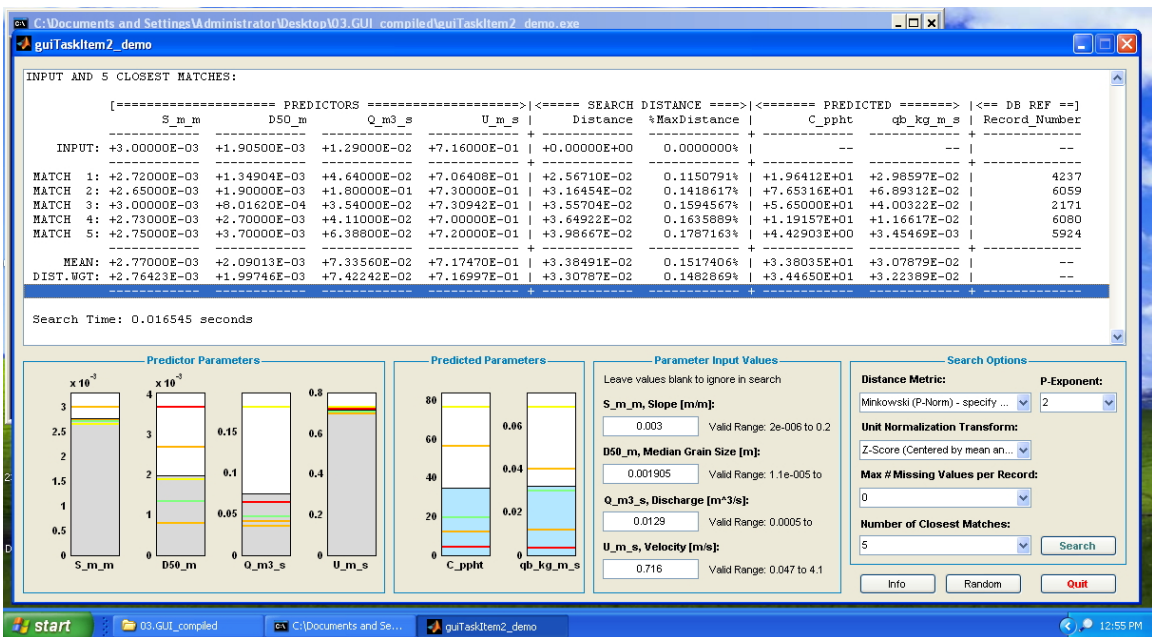
Figure 92: Screen capture of screening tool with approach values in input panel and search results displayed.

Continuing the example, the culvert values are then used in the screening tool to identify how much, if any solids the culvert system could be anticipated to transport.
$Q_{culvert} = 1.02 \ ft^3/s \ (0.029 \ m^3/s)$;
$A_{culvert} = 0.262 \ ft^2 \ (0.024 \ m^2)$;
$V_{culvert} = 3.89 \ ft/s \ (1.16 \ m/s)$;
$W_{culvert} = \sqrt{0.262 ft^2} = 0.511 \ ft \ (0.156 \ m)$;
As before using a range of the median size is suggested to avoid zero returns in the searches. The same two searches are conducted, but the discharge and velocity are changed to reflect the culvert hydraulics rather than the entire channel hydraulics.

The two values from these two searches, converted into solids volume are

$$Q_{solids} = 1.96 \times 10^{-4}(kg/m/s) * 0.156m * \frac{m^3}{2650kg} * \frac{35.31 \ ft^3}{m^3} = 4.07 \times 10^{-7} \ cfs$$
$$Q_{solids} = 6.214 \times 10^{-1}(kg/m/s) * 0.156m * \frac{m^3}{2650kg} * \frac{35.31 \ ft^3}{m^3} = 0.00129 \ cfs.$$

In this example, comparing the anticipated solids from the approach section and culvert capacity (expressed as an equivalent channel) the culvert should accommodate the solids without impact on the channel system (hence the screening approach suggests little deposition).

In the actual experiment the solids transported were $Q_{solids;observed} = \frac{3.938 ft^3}{11640 sec} = 0.0003383 \ ft^3/s$[11]. The screening tool, when using the size bracketing suggested captures the observed value in the approach section, an encouraging outcome, but underestimates the culvert capacity by about a factor of two.

6.2.5   Example 3: Experiment 67

An example is presented on use of the screening tool based on an arbitrary experiment (Experiment 67). This particular experiment is a staggered barrel system, but otherwise the only change from the previous example is the culvert model area and minor changes in flow values as measured in the experiment.

In the experiment the following measurements and data were collected:
$Q_{approach} = 15.240 \ ft^3/sec \ (0.432 \ m^3/s)$;
$A_{approach} = 10.513 \ ft^2 \ (0.977 \ m^2)$;
$V_{approach} = 1.45 \ ft/s \ (0.442 \ m/s)$;
$D_{50} = 19.05mm \ (0.06248 \ ft)$;
$S_0 = 0.010$;
$\text{Depth}_{approach} = 1.546 ft$;
$W_{approach} = \frac{10.513 ft^2}{1.546 ft} = 9.857 \ ft \ (3.005 \ m)$;

---

[11]The implied precision is greater than actual precision — only one significant digit at best, hence volumetric rate is 0.0003 cfs.

These measurements and values are sufficient to use the screening tool to estimate the volumetric solids transport towards the culvert system.

The result of these two searches (screen captures are omitted) are $Q_{solids} = 4.13 \times 10^{-5}(kg/m/s) * 3.005m * \frac{m^3}{2650kg} * \frac{35.31\ ft^3}{m^3} = 1.65 \times 10^{-6}\ cfs$
$Q_{solids} = 6.82 \times 10^{-3}(kg/m/s) * 3.005m * \frac{m^3}{2650kg} * \frac{35.31\ ft^3}{m^3} = 0.000273\ cfs.$

The range is again from almost zero to 0.0002 cfs solids are transported. The change in this experiment is a different culvert system. The solids are the same (hence the size range is the same).

Continuing the example, the culvert values are then used in the screening tool to identify how much, if any solids the culvert system could be anticipated to transport.
$Q_{culvert} = 1.531\ ft^3/s\ (0.0434\ m^3/s);$
$A_{culvert} = 0.371\ ft^2\ (0.03448\ m^2);$
$V_{culvert} = 4.12\ ft/s\ (1.258\ m/s)\ ;$
$W_{culvert} = \sqrt{0.371 ft^2} = 0.609\ ft\ (0.186\ m)\ ;$
As before using a range of the median size is suggested to avoid zero returns in the searches. The same two searches are conducted, but the discharge and velocity are changed to reflect the culvert hydraulics rather than the entire channel hydraulics.

The two values from these two searches, converted into solids volume are

$Q_{solids} = 3.25 \times 10^{-4}(kg/m/s) * 0.186m * \frac{m^3}{2650kg} * \frac{35.31\ ft^3}{m^3} = 8.04 \times 10^{-7}\ cfs$
$Q_{solids} = 3.29 \times 10^{0}(kg/m/s) * 0.186m * \frac{m^3}{2650kg} * \frac{35.31\ ft^3}{m^3} = 0.00814\ cfs.$

In this example, comparing the anticipated solids from the approach section and culvert capacity (expressed as an equivalent channel) the culvert should accommodate the solids without impact on the channel system (hence the screening approach suggests little deposition).

In the actual experiment the solids transported were $Q_{solids;observed} = \frac{3.188 ft^3}{12660 sec} = 0.000251\ ft^3/s^{12}$. The screening tool, when using the size bracketing suggested captures the observed value in the approach section, an encouraging outcome, but underestimates the culvert capacity by about a factor of two.

---

[12]The implied precision is greater than actual precision — only one significant digit at best, hence volumetric rate is 0.0002 cfs.

6.3   Summary and Suggestions for Future Work

The research conducted a literature review, compiled a literature derived database for solids transport in channels, and conducted computational and physical model experiments in an attempt to assess the hydraulic properties of a staggered barrel culvert system as compared to other typical systems in use.

The literature-derived database was incorporated into a screening tool that uses a searching algorithm to estimate solids transport given clear water discharge, velocity, slope, and median grain diameter. Subsequent use of the tool during the research led the researchers to conclude the search engine is particularly sensitive to the median grain diameter, and they used the tool to bracket behavior by searching with grain diameters one order of magnitude smaller and larger than the target value.

The research identified that culvert open area was correlated to solids transport capability and in our studies the geometric shapes seemed to have little impact. This common sense finding needs to be qualified with the requirement that the culvert area, when possible, should be concentrated near the channel centerline — the systems work because the flow is accelerated through the culvert and the acceleration is needed to maintain the solids flow. The researchers think that spreading out the area across a stream is counter-productive. This spreading forces a ponding that while hydraulically simple, wastes any momentum the system has developed in the approach and allows solids to fall out of suspension. Future studies should consider field surveys to confirm or refute this conjecture.

Staggered barrel systems performed better than anticipated (based on culvert open area) in the skew experiments, but otherwise were unremarkable as compared to the rectangular and conventional circular systems. The approach section was essentially a wide rectangular channel, and in retrospect that single decision may have impacted the entire study. Incised channels could be expected to behave differently. The skew experiments in this research were conducted in a hasty fashion and future work should consider a more systematic study of the skew conditions. The researchers believe that many real systems exhibit the skew conditions in practice, and again field surveys would be productive.

Conveyance matching was briefly examined in the study. There is evidence that this simple approach has merit, and future studies should consider conveyance matching as the principal research question in cases where the culvert system carries the entire flow (not over the road as in our studies).

The experiments suggest that multiple culverts are preferable to single systems. A few experiments were conducted with the culverts pre-packed with solids. The multiple barrel systems self-cleared; the single barrel systems did not. These experiments were conducted without benefit of the entire measurement system, so outside of this anecdotal statement are otherwise unreported. In addition to these unrecorded

experiments a set of unrecorded experiments where the downstream side of the system was allowed to run free (instead of discharge into a "pool") was able to convey any solids flow once the head cut from the downstream side reached the culvert system. In general, when deposition formed on the downstream side (as it did in nearly every experiment) the deposition formed downstream and moved towards the culvert system until an equilibrium was established or the experiment terminated. Future studies should consider the downstream conditions in greater detail than this study — it controls the deposition behavior far more than anticipated.

The screening tool was illustrated in several examples to show how it might be used to assess the impact of a culvert system in a solids transport situation. Solids size bracketing was used in the examples and using the bracketing, assuming the other variables are more precisely known, the tool returned values consistent with experimental results.

While the results are inconclusive, the researchers suggest that in skew settings staggered barrel systems have advantages, and should be employed where practical. The common crown design (as in the original problem statement) is the most favorable in our opinion. Existing systems should not be replaced with staggered systems until they fail or routine replacement is scheduled. The invert (flowline) of the culvert should be at or slightly below the existing natural stream gradient so that solids do not have to move uphill to traverse the culvert system. Systems that join two ditches where the ditch axis is at a right angle to the culvert axis are outside the scope of this study, but the researchers believe such system will not benefit from staggered barrel considerations. The abrupt direction change wastes any momentum in the solids flow and deposition should be expected in such cases.

References

Abida, H. and R. Townsend (1991). Local scour downstream of box-culvert outlets. *Journal of Irrigation and Drainage Engineering 117*(3), 425–441.

Abt, S., R. Kloberdanz, and C. Mendoza (1984). Unified culvert scour determination. *Journal of Hydraulic Engineering 110*(10), 1475–1479.

Abt, S., J. Ruff, and F. Doehring (1985). Culvert slope effects on outlet scour. *Journal of Hydraulic Engineering 111*(10), 1363–1367.

Ashida, K. and M. Michiu (1972). Study on hydraulic resistance and bed load transport rate in alluvial streams. *Transactions, Japan Society of Civil Engineering 206*, 59–69.

Babcock, H. A. (1970). The sliding bed flow regime. In *1st International Conference on Hydraulic Transportation of Solids in Pipes*, Number Paper H1 in Hydrotransport 1. British Hydromechanics Research Association.

Bathurst, J. C., W. H. Graf, and H. H. Cao (1987). Bed load discharge equations for steep mountain rivers. In C. R. Thorne, J. C. Bathurst, and R. D. Hey (Eds.), *Sediment Transport in Gravel-bed Rivers*, pp. 453–491. John Wiley & Sons Ltd.

Biedenharn, D. S., R. R. Copeland, C. R. Thorne, P. J. Soar, R. D.Hey, and C. C. Watson (2000). Effective discharge calculation: A practical guide. ERDC/CHL TR-00-15, U.S. Army Engineer Research and Development Center, Coastal and Hydraulics Laboratory.

Brownlie, W. R. (1981). Prediction of flow depth and sediment discharge in open channels. Report KH-R-43A, W. M. Keck Laboratory of Hydraulics and Water Resources, California Institute of Technology, Pasadena, California, USA.

Buffington, J. M. and D. R. Montgomery (1997). A systematic analysis of eight decades of incipient motion studies, with special reference to gravel-bedded rivers. *Water Resources Research 33*(8), 1993–2029.

Chang, H. (1988). *Fluvial Processes in River Engineering*. Krieger.

Chien, N. and Z. Wan (1999). *Mechanics of Sediment Transport*. Reston, Va: ASCE Press.

Chiu, C. L. and J. J. Seman (1971). Head loss in spiral-liquid flow in pipes. In I. Zandi (Ed.), *Advances in Solid-Liquid Flow in Pipes and its Application*. Pergamon Press Inc.

Church, M. (2006). Bed material transport and the morphology of alluvial river channels. *Annual Review of Earth and Planetary Sciences 34*, 325–354.

Crookston, B. M. (2008). A laboratory study of streambed stability in bottomless culverts. Master's thesis, Utah State University, Logan, Utah.

Crookston, B. M. and B. P. Tullis (2006). Preliminary study of scour in bottomless culverts. Technical Report FHWA-AK-RD-06-05, Alaska Department of Transportation.

Davis, R. E., F. S. Foote, J. M. Anderson, and E. M. Mikail (1981). *Surveying: Theory and Practice*. McGraw-Hill, Sixth Edition.

Dietrich, W. E., J. W. Kirchner, H. Ikeda, and F. Iseya (1989). Sediment supply and the development of the coarse surface layer in gravel-bedded rivers. *Nature 340*(6230), 215–217.

Dixon, J. (2011). *A Relation Between Select Hydraulic Properties and Sediment Transport Volume Through Experimental Culvert Configurations and Techniques for Measuring Sediment Transport Volumes*. Ph. D. thesis, Texas Tech University.

Dodd, C. K., W. J. Barichivich, and L. L. Smith (2004). Effectiveness of a barrier wall and culverts in reducing wildlife mortality on a heavily traveled highway in florida. *Biological Conservation 118*(5), 619–631.

Egiazaroff, I. V. (1965). Calculation of nonuniform sediment concentration. *Journal of the Hydraulics Division, Proceedings of the ASCE 91*(4), 225–248.

Einstein, H. A. (1950). The bed load function for sediment transport in open channels. Technical Bulletin 1026, U.S. Department of Agriculture.

Emmett, W. and M. Wolman (2001). Effective discharge and gravel-bed rivers. *Earth Surface Processes and Landforms 26*(13), 1369–1380.

Eriksson, A. and A. van den Hengel (2010). Efficient computation of robust low-rank matrix approximations in the presence of missing data using the L_1 norm. *http:// acutech. files. wordpress. com/ 2010/ 06/ robustl1_ eriksson. pdf*.

Fenton, J. D. and J. E. Abbott (1977). Initial movement of grains on a stream bed: the effect of relative protrusion. *Proceedings of the Royal Society of London. Series A 352*, 523–537.

Ferguson, R. and M. Church (2004). A simple universal equation for grain settling velocity. *Journal of Sedimentary Research 74*(6), 933–937.

García, M. H. (Ed.) (2008a). *Sedimentation Engineering: Processes, Measurements, Modeling, and Practice*. ASCE Manuals and Reports on Engineering Practice No. 110. ASCE.

García, M. H. (Ed.) (2008b). *Sedimentation Engineering: Processes, Measurements, Modeling, and Practice*, Chapter 3, pp. 165–251. ASCE Manuals and Reports on Engineering Practice No. 110. American Society of Civil Engineering.

Gilbert, R. (1960). Transport hydraulique et refoulement des mixtures en conduit. *Anals des Pontes et Chaussees 130*(3.4), 307–373,437–494.

Golden Software, I. (2002). Surfer 8 User's Guide. Golden Software, Inc.

Goodridge, W. H. (2009). *Sediment Transport Impacts Upon Culvert Hydraulics*. Ph. D. thesis, Utah State University, Logan, Utah.

Graf, W. H. (1971). *Hydraulics of Sediment Transport*. McGraw-Hill.

Graf, W. H. and E. R. Acaroglu (1968). Sediment transport in conveyance systems. *Bulletin of the International Association of Scientific Hydrology 13*(2).

Haderlie, G. and B. Tullis (2008). Hydraulics of multibarrel culverts under inlet control. *Journal of Irrigation and Drainage Engineering 134*, 507.

Ho, H.-C. and M. Muste (2009, August). Sedimentation of multi-barrel culverts. In *Proceedings of the 2009 Mid-Continent Transportation Research Symposium*, Ames, Iowa.

Hofland, B. and J. A. Battjes (2006). Probability density function of instantaneous drag forces and shear stresses on a bed. *Journal of Hydraulic Engineering 132*(11), 1169–1175.

Hofland, B., J. A. Battjes, and R. Booij (2005). Measurement of fluctuating pressures on coarse bed material. *Journal of Hydraulic Engineering 131*(9), 770–781.

House, M., M. Pyles, and D. White (2005). Velocity distributions in streambed simulation culverts used for fish passage. *Journal of the American Water Resources Association 41*(1), 209–217.

Howard, G. W. (1939). Transportation of sand and gravel in a four-inch pipe. *Transactions ASCE 104*(2039), 1334–1348.

Howard, G. W. (1941). Effects of rifling on four-inch pipe transporting solids. *Transactions ASCE 106*(2101), 135–137.

Johnson, P. and E. Brown (2000). Stream assessment for multicell culvert use. *Journal of Hydraulic Engineering-Reston 126*(5), 381–386.

Julien, P. Y. (1998). *Erosion and Sedimentation*. Cambridge University Press.

Kerenyi, K., J. Jones, and S. Stein (2003). Bottomless culvert scour study: Phase 1 laboratory report. Research Report FHWA–RD–02–078, Federal Highway Administration, 6300 Georgetown Pike, McLean VA 22101-2296.

Kerenyi, K., J. Jones, and S. Stein (2007). Bottomless culvert scour study: Phase 2 laboratory report. Research Report FHWA–HRT–07–026, Federal Highway Administration, 6300 Georgetown Pike, McLean VA 22101-2296.

King, J., W. Emmett, P. Whiting, R. Kenworthy, and J. Barry (2004). Sediment transport data and related information for selected coarse-bed streams and rivers in idaho. General Technical Report RMRS-GTR-131, USDA Forest Service, Rocky Mountain Research Station, Fort Collins, CO.

Lamb, M. P., W. E. Dietrich, and J. G. Venditti (2008). Is the critical Shields stress for incipient sediment motion dependent on channel-bed slope. *Journal of Geophysical Research 113*, F02008.

Laursen, E. (1956). The hydraulics of a storm-sewer system for sediment-transporting flow.

Technical Report Bulletin 5, Iowa Highway Research Board.

Lee, K. T., Y.-L. Liu, and K.-H. Cheng (2004). Experimental investigation of bedload transport processes under unsteady flow conditions. *Hydrological Processes 18*, 2439–2454.

Liriano, S., R. Day, and W. White (2002). Scour at culvert outlets as influenced by the turbulent flow structure. *Journal of Hydraulic Research 40*(3), 367–376.

Math Works, Inc. (2008). MatLab Version 7.6.

Maxwell, A., A. Papanicolaou, R. Hotchkiss, M. Barber, and J. Schafer (2001). Step-pool morphology in high-gradient countersunk culverts. *Transportation Research Record 1743*(01-2304), 49–56.

McEwan, I. and J. Heald (2001). Discrete particle modeling of entrainment from flat uniformly sized sediment beds. *Journal of Hydraulic Engineering 127*(7), 588–597.

Meyer-Peter, E. and R. Müller (1948). Formulas for bed-load transport. In *Proceedings of the Second Meeting*, Stockholm, Sweden, pp. 39–64. IAHR.

Monteith, H. and G. Pender (2005). Flume investigations into the influence of shear stress history on a graded sediment bed. *Water Resources Research 41*(12), W12401.

Muste, M., H.-C. Ho, and D. Mehl (2010). Insights into the origin and characteristics of the sedimentation process at multi-barrel culverts in iowa. Technical Report IHRB Project TR-596, The Iowa Highway Research Board.

Neill, C. R. (1968). A re-examination of the beginning of movement for coarse granular bed material. Technical Report Report INT 68, Hydraulics Research Station, Wallingford, UK.

Newitt, D. M., J. F. Richardson, M. Abbott, and R. B. Turtle (1955). Hydraulic conveying of solids in horizontal pipes. *Transactions Institution of Chemical Engineers 33*(2), 93–113.

Oldmeadow, D. F. and M. Church (2006). A field experiment on streambed stabilization by gravel structures. *Geomorphology 78*, 335–350.

Paintal, A. S. (1971). Concept of critical shear stress in loose boundary open channels. *Journal of Hydraulic Research 9*(1), 91–113.

Papanicolaou, A. N., P. Diplas, N. Evaggelopoulos, and S. Fotopoulos (2002). Stochastic incipient motion criterion for spheres under various bed packing conditions. *Journal of Hydraulic Engineering 128*(4), 369–380.

Parker, G. (1990). Surface-based bedload transport relation for gravel rivers. *Journal of Hydraulic Research 28*(4), 417–436.

Parker, G. and P. C. Klingeman (1982). On why gravel bed streams are paved. *Water*

Resources Research 18(5), 1409–1423.

Parker, G., P. C. Klingeman, and D. G. McLean (1982). Bedload and size distribution in paved gravel-bed streams. *Journal of Hydraulic Engineering 108*(4), 544–571.

Parker, G. and A. J. Sutherland (1990). Fluvial armouring. *Journal of Hydraulic Research 28*(5), 529–544.

Peake, S. (2004). An evaluation of the use of critical swimming speed for determination of culvert water velocity criteria for smallmouth bass. *Transactions of the American Fisheries Society 133*(6), 1472–1479.

Peterson, A. (1975). Universal flow diagrams for mobile boundary channels. *Canadian Journal of Civil Engineering 2*, 549–557.

Peterson, A. W. and R. F. Howells (1973). A compendium of solids transport data for mobile boundary channels. Technical report, Inland Waters Directorate, Envrionment Canada.

Recking, A. (2010). A comparison between flume and field bed load transport data and consequences for surface-based bed load transport prediction. *Water Resources Research 46*(3), W03518.

Recking, A., P. Frey, A. Paquier, P. Belleudy, and J. Y. Champagne (2008a). Bed-load transport flume experiments on steep slopes. *Journal of Hydraulic Engineering 134*(9), 1302–1310.

Recking, A., P. Frey, A. Paquier, P. Belleudy, and J. Y. Champagne (2008b). Feedback between bed load transport and flow resistance in gravel and cobble bed rivers. *Water Resources Research 44*(5), W05412.

Schoklitsch, A. (1949). Berechnung der geschiebefracht. *Wasser und Energiewirtschaft 1*.

Shields, A. (1936). *Anwendung der Aehnlichkeitsmechanik und der Turbulenz Forschung auf die Geschiebebewegung*. Ph. D. thesis, Mitt. der Preussische Versuchanstalt für Wasserbau und Schiffbau,, Berlin, Germany.

Strom, K., A. N. Papanicolaou, N. Evangelopoulos, and M. Odeh (2004). Microforms in gravel bed rivers: Formation, disintegration, and effects on bedload transport. *Journal of Hydraulic Engineering 130*(6), 554–567.

Thompson, D. B., T. G. Cleveland, K.-H. Wang, and X. Fang (2009). Design guidance for areas of extreme bed mobility. Technical Report FHWA/TX–08/0–4695–4, TechMRT, Texas Tech University.

Topcon, S. (2009). Series 50RX Operator's Manual. Sokkia Topcon.

Vanoni, V. A. (Ed.) (1975). *Sedimentation Engineering*. ASCE Manuals and Reports on Engineering Practice No. 54. ASCE.

Wargo, R. S. and R. N. Weisman (2006). A comparison of single-cell and multicell culverts for stream crossings. *Journal of the American Water Resources Association 42*(4), 989–995.

Warren, M. and M. Pardew (1998). Road crossings as barriers to small-stream fish movement. *Transactions of the American Fisheries Society 127*(4), 637–644.

Whiting, P. J., J. F. Stamm, and D. B. Moog (1999). Sediment-transporting flows in headwater streams. *Geological Society of America Bulletin 111*(3), 450–466.

Wilcock, P. R. and J. C. Crowe (2003). Surface-based transport model for mixed-size sediment. *Journal of Hydraulic Engineering 129*(2), 120–128.

Wilcock, P. R., S. T. Kenworthy, and J. C. Crowe (2001). Experimental study of the transport of mixed sand and gravel. *Water Resources Research 37*(12), 3349–3358.

Wolman, M. G. and J. C. Miller (1960). Magnitude and frequency of forces in geomorphic processes. *Journal of Geology 68*, 54–74.

Wong, M. and G. Parker (2006). Reanalysis and correction of bed-load relation of meyer-peter and müller using their own database. *Journal of Hydraulic Engineering 132*(11), 1159–1168.

Wong, M., G. Parker, P. DeVries, T. M. Brown, and S. J. Burges (2007). Experiments on dispersion of tracer stones under lower-regime plane-bed equilibrium bed load transport. *Water Resources Research 43*, W03440.

Wu, F. C. and Y. J. Chou (2003). Rolling and lifting probabilities for sediment entrainment. *Journal of Hydraulic Engineering 129*(2), 110–119.

Yang, C. T. (1996). *Sediment Transport: Theory and Practice.* McGraw-Hill Series in Water Resources and Environmental Engineering. McGraw-Hill.

Zenz, F. A. and D. F. Othmer (1960). *Fluidization and Fluid-Particles Systems.* New York, NY: Reinhold Publishing Corp.

7 Appendix-I Texas Tech Experiment Database

The Texas Tech experimental program conducted over 160 experiments. Table 8 lists the identification codes, and descriptive codes used to identify experimental conditions. These condition codes are identified in the report body.

Table 9 is a list of the discharge values extracted and/or derived by calculation from the experiments listed in Table 8.

Table 10 is a list of the hydraulic conditions at the approach, culvert, and downstream sections for the experiments listed in Table 8. The width values are hydraulic equivalent widths to be consistent with the literature derived database.

Table 11 is a list of the solids behavior for the experiments listed in Table 8.

Table 8: Cross-Reference Identification Codes for Texas Tech Experiments.

[ID: An experiment identification code, unique to each experiment. Repeated in subsequent tables; ORIENTATION: Classification of In-Line (Not Skew) or Skew orientation of culvert sysatem relative to flume channel centerline; MODEL: A code that identifies the model type; SLOPE: Dimensionless slope of the channel ; ROCK: Classification of large or small. Size metrics reported in other tables

ID	ORIENTATION	MODEL	SLOPE	ROCK
5	NotSkew	SB-I	0.003	Large
T	NotSkew	SB-C	0.003	Large
6	NotSkew	SB-C	0.003	Large
7	NotSkew	SB-C	0.003	Large
8	NotSkew	SB-C	0.003	Large
9	NotSkew	SB-C	0.003	Large
10	NotSkew	SB-C	0.003	Large
12	NotSkew	SB-I	0.003	Large
13	NotSkew	M-4-C	0.003	Large
14	NotSkew	M-4-C	0.003	Large
15	NotSkew	M-4-C	0.003	Large
18	NotSkew	S-4-C	0.003	Large
19	NotSkew	S-4-C	0.003	Large
20	NotSkew	S-4-C	0.003	Large
23	NotSkew	S-6-C	0.003	Large
24	NotSkew	S-6-C	0.003	Large
25	NotSkew	S-6-C	0.003	Large
26	NotSkew	M-6-C	0.003	Large
27	NotSkew	M-6-C	0.003	Large

Continued on next page

Table 8: Cross-Reference Identification Codes for Texas Tech
Experiments — Continued

ID	ORIENTATION	MODEL	SLOPE	ROCK
28	NotSkew	M-6-C	0.003	Large
29	NotSkew	M-R	0.003	Large
30	NotSkew	M-R	0.003	Large
31	NotSkew	M-R	0.003	Large
32	NotSkew	S-R	0.003	Large
33	NotSkew	S-R	0.003	Large
34	NotSkew	S-R	0.003	Large
38	NotSkew	S-R	0.010	Large
39	NotSkew	S-R	0.010	Large
40	NotSkew	S-R	0.010	Large
41	NotSkew	M-R	0.010	Large
42	NotSkew	M-R	0.010	Large
43	NotSkew	M-R	0.010	Large
44	NotSkew	M-6-C	0.010	Large
45	NotSkew	M-6-C	0.010	Large
46	NotSkew	M-6-C	0.010	Large
47	NotSkew	S-6-C	0.010	Large
48	NotSkew	S-6-C	0.010	Large
49	NotSkew	S-6-C	0.010	Large
52	NotSkew	M-4-C	0.010	Large
53	NotSkew	M-4-C	0.010	Large
54	NotSkew	M-4-C	0.010	Large
55	NotSkew	S-4-C	0.010	Large
56	NotSkew	S-4-C	0.010	Large
57	NotSkew	S-4-C	0.010	Large
60	NotSkew	SB-I	0.010	Large
61	NotSkew	SB-I	0.010	Large
62	NotSkew	SB-I	0.010	Large
65	NotSkew	SB-C	0.010	Large
66	NotSkew	SB-C	0.010	Large
67	NotSkew	SB-C	0.010	Large
68	NotSkew	M-6-C	0.010	Large
69	NotSkew	S-6-C	0.010	Large
70	NotSkew	S-6-C	0.006	Large
71	NotSkew	S-6-C	0.006	Large
72	NotSkew	S-6-C	0.006	Large
73	NotSkew	M-6-C	0.006	Large
74	NotSkew	M-6-C	0.006	Large
75	NotSkew	M-6-C	0.006	Large

Continued on next page

Table 8: Cross-Reference Identification Codes for Texas Tech
Experiments — Continued

ID	ORIENTATION	MODEL	SLOPE	ROCK
78	NotSkew	M-R	0.006	Large
79	NotSkew	M-R	0.006	Large
80	NotSkew	M-R	0.006	Large
82	NotSkew	S-R	0.006	Large
83	NotSkew	S-R	0.006	Large
84	NotSkew	S-R	0.006	Large
85	NotSkew	SB-C	0.006	Large
86	NotSkew	SB-C	0.006	Large
87	NotSkew	SB-C	0.006	Large
91	Skew	M-R	0.006	Large
92	Skew	M-R	0.006	Large
93	Skew	M-R	0.006	Large
94	Skew	S-R	0.006	Large
95	Skew	S-R	0.006	Large
96	Skew	S-R	0.006	Large
101	Skew	S-6-C	0.006	Large
102	Skew	S-6-C	0.006	Large
103	Skew	M-6-C	0.006	Large
104	Skew	M-6-C	0.006	Large
105	Skew	M-6-C	0.006	Large
106	Skew	SB-C	0.006	Large
107	Skew	SB-C	0.006	Large
108	Skew	SB-C	0.006	Large
109	Skew	SB-C	0.006	Large
113	Skew	S-4-C	0.006	Large
114	Skew	S-4-C	0.006	Large
115	Skew	M-4-C	0.006	Large
116	Skew	M-4-C	0.006	Large
117	Skew	M-4-C	0.006	Large
118	Skew	M-4-C	0.006	Small
119	Skew	M-4-C	0.006	Small
120	Skew	M-4-C	0.006	Small
121	Skew	S-4-C	0.006	Small
122	Skew	S-4-C	0.006	Small
123	Skew	S-4-C	0.006	Small
125	Skew	M-6-C	0.006	Small
126	Skew	M-6-C	0.006	Small
127	Skew	M-6-C	0.006	Small
128	Skew	S-6-C	0.006	Small

Continued on next page

Table 8: Cross-Reference Identification Codes for Texas Tech
Experiments — Continued

ID	ORIENTATION	MODEL	SLOPE	ROCK
129	Skew	S-6-C	0.006	Small
130	Skew	S-6-C	0.006	Small
131	Skew	SB-C	0.006	Small
132	Skew	SB-C	0.006	Small
133	Skew	SB-C	0.006	Small
134	Skew	SB-C	0.006	Small
135	Skew	M-R	0.006	Small
136	Skew	M-R	0.006	Small
137	Skew	M-R	0.006	Small
138	Skew	S-R	0.006	Small
139	Skew	S-R	0.006	Small
140	Skew	S-R	0.006	Small
141	Not Skew	M-R	0.006	Small
142	Not Skew	M-R	0.006	Small
143	Not Skew	M-R	0.006	Small
144	Not Skew	M-R	0.006	Small
145	Not Skew	S-R	0.006	Small
146	Not Skew	S-R	0.006	Small
147	Not Skew	S-R	0.006	Small
148	Not Skew	S-R	0.006	Small
149	Not Skew	SB-C	0.006	Small
150	Not Skew	SB-C	0.006	Small
151	Not Skew	SB-C	0.006	Small
152	Not Skew	M-6-C	0.006	Small
153	Not Skew	M-6-C	0.006	Small
154	Not Skew	M-6-C	0.006	Small
155	Not Skew	M-6-C	0.006	Small
156	Not Skew	M-6-C	0.006	Small
157	Not Skew	S-6-C	0.006	Small
158	Not Skew	S-6-C	0.006	Small
159	Not Skew	S-6-C	0.006	Small
160	Not Skew	S-4-C	0.006	Small
161	Not Skew	S-4-C	0.006	Small
162	Not Skew	S-4-C	0.006	Small
163	Not Skew	M-4-C	0.006	Small
164	Not Skew	M-4-C	0.006	Small
165	Not Skew	M-4-C	0.006	Small
166	Not Skew	M-4-C	0.003	Small
167	Not Skew	M-4-C	0.003	Small

Continued on next page

Table 8: Cross-Reference Identification Codes for Texas Tech
Experiments — Continued

ID	ORIENTATION	MODEL	SLOPE	ROCK
168	Not Skew	M-4-C	0.003	Small
169	Not Skew	S-4-C	0.003	Small
170	Not Skew	S-4-C	0.003	Small
171	Not Skew	S-4-C	0.003	Small
172	Not Skew	SB-I	0.003	Small
173	Not Skew	SB-I	0.003	Small
174	Not Skew	SB-I	0.003	Small
175	Not Skew	M-6-C	0.003	Small
176	Not Skew	M-6-C	0.003	Small
177	Not Skew	M-6-C	0.003	Small
178	Not Skew	S-6-C	0.003	Small
179	Not Skew	S-6-C	0.003	Small
180	Not Skew	S-6-C	0.003	Small
181	Not Skew	SB-C	0.003	Small
182	Not Skew	SB-C	0.003	Small
183	Not Skew	SB-C	0.003	Small
184	Not Skew	M-R	0.003	Small
185	Not Skew	M-R	0.003	Small
186	Not Skew	M-R	0.003	Small
187	Not Skew	S-R	0.003	Small
188	Not Skew	S-R	0.003	Small
189	Not Skew	S-R	0.003	Small

Table 9: Measured and computed clear-water discharge for
Texas Tech Experiments

[ID: An experiment identification code, unique to each experiment. Repeated in subsequent tables; Q_{rating}: Approach discharge in cubic feet per second from the rating curve; $Q_{culvert}$: Culvert discharge in cubic feet per second computed as product of culvert area and measured velocity at culvert outlet; Q_{road}: Discharge over the road (culvert system) in cubic feet per second computed as difference between Q_{rating} and $Q_{culvert}$; RUN TIME: Classification of large or small. Size metrics reported in other tables

ID	Q_{rating}	$Q_{culvert}$	Q_{road}	RUN TIME
5	15.240	–	–	13260
T	–	–	–	–
6	15.510	–	–	15480
7	17.470	–	–	16800
8	16.060	–	–	13020
9	16.060	–	–	15480
12	14.970	1.014	13.956	13080
13	15.510	0.751	14.759	13200
14	15.510	0.713	14.797	12900
15	15.510	0.739	14.771	12900
18	16.060	0.287	15.773	14400
19	16.060	0.256	15.804	13500
20	16.060	0.281	15.779	12600
23	15.510	0.020	15.490	15660
24	15.510	0.457	15.053	15120
25	15.510	0.522	14.988	16140
26	15.510	1.173	14.337	14520
27	15.240	1.338	13.902	12180
28	15.240	1.489	13.751	12000
29	14.970	1.832	13.138	13320
30	14.970	2.084	12.886	12840
31	14.970	0.837	14.133	13320
32	15.510	1.015	14.495	13920
33	15.510	1.016	14.494	13140
34	15.510	0.811	14.699	12900
38	15.240	1.327	13.913	13380
39	15.510	1.342	14.168	12720
40	15.510	1.446	14.064	13620
41	15.510	3.059	12.451	13920
42	15.510	3.565	11.945	12060
43	15.240	3.238	12.002	12540

Continued on next page

Table 9: Measured and computed clear-water discharge for
Texas Tech Experiments — Continued

ID	Q_{rating}	$Q_{culvert}$	Q_{road}	RUN TIME
44	15.510	2.381	13.129	12120
45	15.510	2.438	13.072	11940
46	15.510	2.306	13.204	12120
47	15.240	0.916	14.324	12240
48	15.790	0.919	14.871	12120
49	15.510	0.913	14.597	12300
52	14.700	1.064	13.636	11040
53	14.970	0.978	13.992	12480
54	15.510	1.029	14.481	11640
55	15.790	0.378	15.412	11820
56	15.510	0.365	15.145	12180
57	15.240	0.352	14.888	12660
60	15.790	1.471	14.319	12240
61	15.790	1.536	14.254	12420
62	14.970	1.431	13.392	12600
65	15.240	1.578	13.636	12240
66	15.240	1.604	13.636	12660
67	15.240	1.531	13.709	12660
68	15.240	1.832	13.408	12960
69	15.240	0.891	14.349	12360
70	15.240	0.640	14.600	12420
71	14.970	0.695	14.275	12480
72	14.970	0.665	14.305	13800
73	14.970	1.201	13.769	13140
74	15.240	1.080	14.160	12420
75	14.700	1.040	13.660	10920
78	14.430	2.419	12.011	8940
79	14.970	2.227	12.743	12480
80	15.790	1.598	14.192	11400
82	14.970	1.033	13.937	12120
83	14.430	1.023	13.407	12660
84	14.430	1.025	13.405	13440
85	14.700	1.202	13.498	12780
86	15.790	1.051	14.739	13020
87	15.510	1.070	14.440	12660
91	14.700	1.870	12.830	10020
92	15.240	2.423	12.817	13200
93	14.970	2.449	12.521	9840
94	14.700	1.110	13.590	10320

Continued on next page

Table 9: Measured and computed clear-water discharge for
Texas Tech Experiments — Continued

ID	Q_{rating}	$Q_{culvert}$	Q_{road}	RUN TIME
95	14.700	1.100	13.600	11940
96	14.700	0.914	13.786	12480
101	14.970	0.685	14.285	13080
102	15.510	0.676	14.834	13500
103	14.700	1.668	13.032	10200
104	15.240	1.583	13.657	9900
105	14.970	1.687	13.283	11400
106	15.510	0.920	14.590	12360
107	14.970	0.768	14.202	11700
108	14.970	0.753	14.217	12060
109	14.700	0.696	14.004	12900
113	14.700	0.328	14.372	11400
114	14.970	0.320	14.650	15960
115	14.970	0.909	14.061	11880
116	15.510	0.929	14.581	11520
117	15.240	0.936	14.304	11640
118	12.330	0.939	11.391	10920
119	12.080	0.948	11.132	13380
120	11.590	0.937	10.653	13740
121	12.330	0.333	11.997	12540
122	12.330	0.334	11.996	11940
123	12.330	0.339	11.991	11400
125	11.830	1.827	10.003	11940
126	11.830	1.841	9.989	12540
127	11.830	1.837	9.993	11400
128	12.080	0.751	11.329	11100
129	11.830	0.739	11.091	11700
130	11.830	0.753	11.077	12300
131	12.080	1.246	10.834	11940
132	12.330	1.277	11.053	14160
133	12.330	1.272	11.058	15240
134	11.830	1.289	10.541	13320
135	11.830	2.508	9.322	11880
136	11.830	2.445	9.385	12420
137	11.590	2.587	9.003	11640
138	12.080	1.063	11.017	11820
139	12.330	1.070	11.260	11520
140	12.330	1.053	11.277	12840
141	11.590	2.489	9.101	12420

Continued on next page

Table 9: Measured and computed clear-water discharge for
Texas Tech Experiments — Continued

ID	Q_{rating}	$Q_{culvert}$	Q_{road}	RUN TIME
142	12.080	2.766	9.314	13800
143	12.080	2.978	9.102	14400
144	12.080	2.888	9.192	15300
145	12.330	1.192	11.138	
146	12.330	1.156	11.174	13920
147	12.080	1.118	10.962	14820
148	12.330	1.139	11.191	14640
149	12.590	1.386	11.204	14880
150	12.330	1.376	10.954	14580
151	12.330	1.379	10.951	14100
152	12.330	2.064	10.266	14340
153	12.080	2.017	10.063	14760
154	12.330	2.083	10.247	14100
155	12.080	1.962	10.118	14100
156	12.330	2.004	10.326	14820
157	12.330	0.772	11.558	14640
158	12.080	0.693	11.387	14460
159	12.080	0.765	11.315	15420
160	12.080	0.317	11.763	14520
161	12.330	0.331	11.999	14280
162	12.330	0.328	12.002	14520
163	12.330	0.914	11.416	14460
164	12.080	0.932	11.148	14460
165	12.330	0.933	11.397	14220
166	12.080	0.838	11.242	14760
167	11.590	0.823	10.767	16620
168	12.080	0.862	11.218	13440
169	12.080	0.296	11.784	15060
170	12.080	0.299	11.781	14220
171	12.080	0.285	11.795	14100
172	11.830	1.176	10.654	14160
173	13.360	1.138	12.222	14100
174	13.100	1.153	11.947	14220
175	13.100	1.356	11.744	14280
176	12.840	1.364	11.476	12780
177	13.100	1.148	11.952	13260
178	12.840	0.611	12.229	14280
179	12.840	0.657	12.183	14460
180	13.100	0.671	12.429	14460

Continued on next page

Table 9: Measured and computed clear-water discharge for
Texas Tech Experiments — Continued

ID	Q_{rating}	$Q_{culvert}$	Q_{road}	RUN TIME
181	13.100	0.949	12.151	14220
182	12.840	0.984	11.856	14520
183	12.840	0.984	11.856	13560
184	12.840	1.432	11.408	11220
185	12.840	1.655	11.185	10740
186	13.100	1.627	11.473	10680
187	12.840	0.873	11.967	14280
188	12.840	0.956	11.884	14220
189	13.100	0.954	12.146	14400

Table 10: Flow Areas, Depths, and Widths for Texas Tech
Experiments

[ID: An experiment identification code, unique to each experiment. Repeated in subsequent tables; $A_{culvert}$: Culvert open area in square feet; $A_{approach}$: Approach section cross sectional flow area in square feet (depth dependent); A_{exit}: Exit section (downstream) cross sectional flow area in square feet (depth dependent); $D_{approach}$: Approach section flow depth in feet ; D_{exit}: Exit section flow depth in feet ; $W_{approach}$: Approach section flow width in feet (equivalent rectangular width) ; W_{exit}: Exit section flow depth in feet (equivalent rectangular width)

ID	$A_{culvert}$	$A_{approach}$	A_{exit}	$D_{approach}$	D_{exit}	$W_{approach}$	W_{exit}
5	0.371	–	–	–	–	–	–
T	0.371	–	–	–	–	–	–
6	0.371	–	–	–	–	–	–
7	0.371	–	–	–	–	–	–
8	0.371	–	–	–	–	–	–
9	0.371	–	–	–	–	–	–
12	0.371	10.608	9.987	1.558	1.514	6.810	6.594
13	0.262	10.675	9.972	1.566	1.513	6.816	6.593
14	0.262	10.421	10.069	1.534	1.525	6.795	6.603
15	0.262	10.843	10.202	1.588	1.543	6.828	6.612
18	0.087	10.882	10.170	1.593	1.538	6.831	6.613
19	0.087	10.891	10.342	1.594	1.563	6.832	6.617
20	0.087	11.084	10.225	1.619	1.548	6.846	6.605
23	0.196	11.124	10.232	1.624	1.548	6.849	6.608
24	0.196	11.321	10.406	1.649	1.573	6.865	6.616
25	0.196	11.157	10.321	1.628	1.561	6.853	6.612
26	0.589	10.593	10.170	1.556	1.536	6.808	6.621
27	0.589	10.720	10.151	1.572	1.538	6.818	6.601
28	0.589	10.406	9.900	1.532	1.501	6.791	6.595
29	0.875	10.587	10.108	1.555	1.531	6.808	6.602
30	0.875	10.452	10.170	1.538	1.542	6.796	6.596
31	0.875	10.306	9.909	1.519	1.501	6.785	6.602
32	0.292	11.082	10.141	1.619	1.537	6.847	6.598
33	0.292	11.373	10.372	1.656	1.568	6.867	6.613
34	0.292	11.144	10.335	1.626	1.563	6.852	6.613
38	0.292	10.765	9.739	1.578	1.485	6.821	6.556
39	0.292	10.738	9.931	1.575	1.485	6.820	6.685
40	0.292	10.830	10.165	1.586	1.494	6.827	6.805
41	0.875	10.191	10.193	1.505	1.511	6.773	6.746
42	0.875	10.270	9.952	1.515	1.512	6.781	6.583

Continued on next page

Table 10: Flow Areas, Depths, and Widths for Texas Tech
Experiments — Continued

ID	$A_{culvert}$	$A_{approach}$	A_{exit}	$D_{approach}$	D_{exit}	$W_{approach}$	W_{exit}
43	0.875	10.214	9.931	1.507	1.510	6.776	6.577
44	0.589	10.425	10.094	1.535	1.505	6.794	6.709
45	0.589	10.446	10.108	1.537	1.510	6.795	6.694
46	0.589	10.455	10.207	1.538	1.503	6.797	6.792
47	0.196	10.897	10.011	1.595	1.496	6.832	6.692
48	0.196	10.843	9.860	1.588	1.485	6.827	6.642
49	0.196	10.895	10.058	1.595	1.483	6.832	6.784
52	0.262	10.476	9.611	1.541	1.463	6.797	6.571
53	0.262	10.449	9.913	1.538	1.461	6.796	6.784
54	0.262	10.767	10.129	1.578	1.491	6.823	6.794
55	0.087	10.957	10.122	1.603	1.487	6.837	6.806
56	0.087	10.900	10.016	1.595	1.490	6.832	6.722
57	0.087	10.865	10.009	1.591	1.485	6.830	6.738
60	0.371	10.632	10.200	1.561	1.493	6.811	6.833
61	0.371	10.524	10.087	1.547	1.502	6.801	6.716
62	0.371	10.468	9.804	1.540	1.474	6.797	6.651
65	0.371	10.475	10.200	1.541	1.486	6.798	6.863
66	0.371	10.483	10.051	1.542	1.486	6.799	6.762
67	0.371	10.513	10.258	1.546	1.492	6.801	6.877
68	0.589	10.365	10.160	1.527	1.495	6.789	6.796
69	0.196	10.709	9.803	1.571	1.474	6.818	6.650
70	0.196	10.632	9.999	1.561	1.486	6.811	6.729
71	0.196	10.683	10.154	1.568	1.493	6.815	6.799
72	0.196	10.638	10.069	1.562	1.493	6.812	6.746
73	0.589	10.510	10.165	1.545	1.498	6.801	6.785
74	0.589	10.586	10.212	1.555	1.503	6.808	6.793
75	0.589	10.383	9.959	1.529	1.479	6.790	6.733
78	0.875	9.944	9.829	1.473	1.454	6.752	6.759
79	0.875	10.348	10.129	1.525	1.485	6.788	6.819
80	0.875	10.591	10.362	1.556	1.518	6.807	6.824
82	0.292	10.610	10.158	1.558	1.489	6.809	6.821
83	0.292	10.454	9.881	1.538	1.474	6.796	6.705
84	0.292	10.482	10.065	1.542	1.480	6.798	6.801
85	0.371	10.555	10.009	1.551	1.495	6.805	6.697
86	0.371	10.695	10.115	1.569	1.505	6.816	6.719
87	0.371	10.610	10.044	1.558	1.495	6.809	6.721
91	0.875	10.327	10.061	1.522	1.485	6.785	6.775
92	0.875	10.525	9.860	1.547	1.498	6.802	6.581
93	0.875	10.445	10.280	1.537	1.490	6.796	6.899

Continued on next page

Table 10: Flow Areas, Depths, and Widths for Texas Tech
Experiments — Continued

ID	$A_{culvert}$	$A_{approach}$	A_{exit}	$D_{approach}$	D_{exit}	$W_{approach}$	W_{exit}
94	0.292	10.593	9.905	1.556	1.483	6.808	6.679
95	0.292	10.616	9.888	1.559	1.487	6.809	6.649
96	0.292	10.687	10.122	1.568	1.527	6.815	6.628
101	0.196	10.735	9.706	1.574	1.496	6.819	6.489
102	0.196	10.891	9.991	1.594	1.511	6.832	6.613
103	0.589	10.455	10.122	1.538	1.505	6.797	6.728
104	0.589	10.947	10.431	1.601	1.549	6.836	6.736
105	0.589	10.486	9.779	1.542	1.494	6.799	6.543
106	0.371	10.558	9.816	1.552	1.505	6.805	6.522
107	0.371	10.802	10.158	1.583	1.489	6.825	6.821
108	0.371	10.721	10.173	1.573	1.479	6.818	6.878
109	0.371	10.645	9.952	1.563	1.497	6.812	6.647
113	0.087	10.893	9.909	1.595	1.488	6.831	6.659
114	0.087	11.032	10.018	1.612	1.505	6.842	6.658
115	0.262	10.695	9.980	1.569	1.489	6.816	6.702
116	0.262	10.734	9.929	1.574	1.500	6.820	6.619
117	0.262	10.720	9.943	1.572	1.484	6.818	6.698
118	0.262	10.199	9.415	1.506	1.459	6.774	6.453
119	0.262	10.028	9.315	1.484	1.429	6.759	6.518
120	0.262	9.937	9.230	1.472	1.419	6.752	6.504
121	0.087	10.147	9.064	1.499	1.398	6.769	6.484
122	0.087	10.043	9.165	1.486	1.396	6.761	6.567
123	0.087	10.336	9.399	1.523	1.423	6.787	6.605
125	0.589	9.633	9.345	1.433	1.436	6.722	6.507
126	0.589	9.625	9.337	1.432	1.431	6.721	6.525
127	0.589	9.587	9.322	1.427	1.427	6.718	6.533
128	0.196	9.985	9.353	1.478	1.423	6.756	6.573
129	0.196	9.923	9.197	1.470	1.426	6.750	6.449
130	0.196	9.954	9.408	1.474	1.412	6.753	6.663
131	0.371	9.672	9.236	1.438	1.422	6.726	6.495
132	0.371	9.866	9.308	1.463	1.439	6.745	6.468
133	0.371	9.915	9.407	1.469	1.450	6.749	6.488
134	0.371	9.907	9.485	1.468	1.446	6.748	6.558
135	0.875	9.463	9.205	1.411	1.423	6.707	6.469
136	0.875	9.392	9.259	1.402	1.423	6.699	6.507
137	0.875	9.376	9.205	1.400	1.421	6.697	6.478
138	0.292	9.968	9.376	1.476	1.428	6.753	6.566
139	0.292	9.915	9.166	1.469	1.424	6.749	6.437
140	0.292	9.915	9.306	1.469	1.417	6.749	6.567

Continued on next page

Table 10: Flow Areas, Depths, and Widths for Texas Tech
Experiments — Continued

ID	$A_{culvert}$	$A_{approach}$	A_{exit}	$D_{approach}$	D_{exit}	$W_{approach}$	W_{exit}
141	0.875	9.602	9.431	1.429	1.433	6.719	6.581
142	0.875	9.674	9.514	1.438	1.443	6.726	6.594
143	0.875	9.694	9.613	1.441	1.441	6.727	6.672
144	0.875	9.803	9.591	1.455	1.449	6.739	6.619
145	0.292	10.319	9.514	1.521	1.429	6.785	6.657
146	0.292	10.128	9.506	1.496	1.433	6.769	6.635
147	0.292	10.077	9.471	1.490	1.435	6.763	6.602
148	0.292	10.114	9.506	1.495	1.442	6.767	6.593
149	0.371	10.014	9.606	1.482	1.445	6.758	6.645
150	0.371	10.064	9.478	1.488	1.438	6.762	6.590
151	0.371	10.071	9.471	1.489	1.445	6.763	6.556
152	0.589	9.949	9.606	1.474	1.452	6.751	6.616
153	0.589	9.865	9.549	1.463	1.438	6.745	6.640
154	0.589	9.951	9.556	1.474	1.451	6.753	6.586
155	0.589	9.858	9.549	1.462	1.445	6.744	6.606
156	0.589	9.957	9.584	1.475	1.452	6.753	6.602
157	0.196	10.262	9.507	1.514	1.436	6.780	6.618
158	0.196	10.164	9.379	1.501	1.420	6.772	6.605
159	0.196	10.255	9.407	1.513	1.434	6.779	6.562
160	0.087	10.347	9.294	1.525	1.428	6.787	6.507
161	0.087	10.560	9.662	1.552	1.443	6.805	6.697
162	0.087	10.454	9.464	1.538	1.431	6.796	6.614
163	0.262	10.213	9.450	1.507	1.432	6.776	6.600
164	0.262	10.199	9.599	1.505	1.432	6.775	6.704
165	0.262	10.219	9.535	1.508	1.442	6.776	6.613
166	0.262	10.425	9.503	1.535	1.452	6.793	6.547
167	0.262	10.363	9.351	1.526	1.440	6.789	6.494
168	0.262	10.422	9.518	1.534	1.453	6.793	6.549
169	0.087	10.460	9.422	1.539	1.428	6.796	6.597
170	0.087	10.816	9.740	1.584	1.480	6.827	6.581
171	0.087	10.288	9.436	1.551	1.445	6.634	6.532
172	0.371	10.198	9.499	1.505	1.446	6.774	6.568
173	0.371	10.169	9.478	1.502	1.440	6.771	6.582
174	0.371	10.143	9.542	1.498	1.439	6.770	6.630
175	0.589	9.972	9.486	1.476	1.435	6.754	6.608
176	0.589	9.805	9.275	1.455	1.427	6.739	6.500
177	0.589	10.098	9.485	1.493	1.448	6.765	6.553
178	0.196	10.262	9.471	1.514	1.429	6.780	6.627
179	0.196	10.226	9.422	1.509	1.422	6.777	6.626

Continued on next page

Table 10: Flow Areas, Depths, and Widths for Texas Tech
Experiments — Continued

ID	$A_{culvert}$	$A_{approach}$	A_{exit}	$D_{approach}$	D_{exit}	$W_{approach}$	W_{exit}
180	0.196	10.325	9.528	1.522	1.432	6.784	6.654
181	0.371	10.288	9.492	1.517	1.448	6.782	6.557
182	0.371	10.247	9.563	1.512	1.448	6.779	6.602
183	0.371	10.221	9.531	1.508	1.449	6.776	6.577
184	0.875	9.787	9.513	1.453	1.447	6.737	6.573
185	0.875	9.751	9.492	1.448	1.439	6.733	6.596
186	0.875	9.735	9.384	1.446	1.434	6.732	6.544
187	0.292	10.164	9.344	1.501	1.428	6.772	6.542
188	0.292	10.078	9.195	1.490	1.421	6.764	6.471
189	0.292	10.623	9.763	1.560	1.484	6.810	6.577

Table 11: Solids behavior for Texas Tech Experiments

[ID: An experiment identification code, unique to each experiment. Repeated in subsequent tables; ρ: Dry density of mobile solids in pounds per cubic foot; D_{50}: 50th percentile grain diameter in millimeters. Determined by mechanical sieving; D_{84}: 84th percentile grain diameter in millimeters. Determined by mechanical sieving; D_{90}: 90th percentile grain diameter in millimeters. Determined by mechanical sieving; $V_{solids-exit}$: Volume of solids transported to exit (downstream) side of model in cubic feet. Determined by elevation survey and/or bucket count ; $V_{solids-barrel}$: Volume of solids remaining in barrel(s) at end of experiment in cubic feet. Determined by bucket count.

ID	ρ	D_{50}	D_{84}	D_{90}	$V_{solids-exit}$	$V_{solids-barrel}$
5	90.389	19.05	23.3	24.6	1.644	0.000
T	90.389	19.05	23.3	24.6	0.000	0.000
6	90.389	19.05	23.3	24.6	1.110	0.000
7	90.389	19.05	23.3	24.6	0.000	0.000
8	90.389	19.05	23.3	24.6	0.000	0.000
9	90.389	19.05	23.3	24.6	1.380	0.000
12	90.389	19.05	23.3	24.6	0.762	0.323
13	90.389	19.05	23.3	24.6	1.016	0.448
14	90.389	19.05	23.3	24.6	0.796	0.319
15	90.389	19.05	23.3	24.6	1.091	0.474
18	90.389	19.05	23.3	24.6	1.541	0.177
19	90.389	19.05	23.3	24.6	1.660	0.157
20	90.389	19.05	23.3	24.6	1.232	0.175
23	90.389	19.05	23.3	24.6	1.144	0.252
24	90.389	19.05	23.3	24.6	1.518	0.315
25	90.389	19.05	23.3	24.6	1.374	0.188
26	90.389	19.05	23.3	24.6	1.207	0.200
27	90.389	19.05	23.3	24.6	1.551	0.547
28	90.389	19.05	23.3	24.6	1.156	0.461
29	90.389	19.05	23.3	24.6	1.497	0.381
30	90.389	19.05	23.3	24.6	1.136	0.278
31	90.389	19.05	23.3	24.6	1.092	0.183
32	90.389	19.05	23.3	24.6	2.160	0.000
33	90.389	19.05	23.3	24.6	1.737	0.000
34	90.389	19.05	23.3	24.6	1.661	0.131
38	90.389	19.05	23.3	24.6	0.000	0.000
39	90.389	19.05	23.3	24.6	3.000	0.000
40	90.389	19.05	23.3	24.6	4.313	0.000
41	90.389	19.05	23.3	24.6	6.375	0.000
42	90.389	19.05	23.3	24.6	6.375	0.000

Continued on next page

Table 11: Solids behavior for Texas Tech Experiments —
Continued

ID	ρ	D_{50}	D_{84}	D_{90}	$V_{solids-exit}$	$V_{solids-barrel}$
43	90.389	19.05	23.3	24.6	6.000	0.000
44	90.389	19.05	23.3	24.6	5.250	0.000
45	90.389	19.05	23.3	24.6	5.250	0.000
46	90.389	19.05	23.3	24.6	5.625	0.000
47	90.389	19.05	23.3	24.6	3.750	0.000
48	90.389	19.05	23.3	24.6	3.000	0.000
49	90.389	19.05	23.3	24.6	3.375	0.000
52	90.389	19.05	23.3	24.6	3.375	0.000
53	90.389	19.05	23.3	24.6	3.000	0.000
54	90.389	19.05	23.3	24.6	3.938	0.000
55	90.389	19.05	23.3	24.6	2.250	0.000
56	90.389	19.05	23.3	24.6	2.625	0.000
57	90.389	19.05	23.3	24.6	2.250	0.000
60	90.389	19.05	23.3	24.6	4.500	0.000
61	90.389	19.05	23.3	24.6	4.500	0.000
62	90.389	19.05	23.3	24.6	3.375	0.000
65	90.389	19.05	23.3	24.6	3.375	0.000
66	90.389	19.05	23.3	24.6	3.750	0.000
67	90.389	19.05	23.3	24.6	3.188	0.000
68	90.389	19.05	23.3	24.6	4.500	0.000
69	90.389	19.05	23.3	24.6	3.000	0.000
70	90.389	19.05	23.3	24.6	0.750	0.000
71	90.389	19.05	23.3	24.6	1.875	0.000
72	90.389	19.05	23.3	24.6	1.500	0.000
73	90.389	19.05	23.3	24.6	1.688	0.267
74	90.389	19.05	23.3	24.6	2.063	0.181
75	90.389	19.05	23.3	24.6	1.125	0.140
78	90.389	19.05	23.3	24.6	1.500	0.261
79	90.389	19.05	23.3	24.6	1.500	0.390
80	90.389	19.05	23.3	24.6	3.000	0.155
82	90.389	19.05	23.3	24.6	1.875	0.000
83	90.389	19.05	23.3	24.6	0.750	0.000
84	90.389	19.05	23.3	24.6	1.125	0.000
85	90.389	19.05	23.3	24.6	1.500	0.000
86	90.389	19.05	23.3	24.6	1.875	0.000
87	90.389	19.05	23.3	24.6	1.875	0.000
91	90.389	19.05	23.3	24.6	1.500	0.000
92	90.389	19.05	23.3	24.6	3.000	0.000
93	90.389	19.05	23.3	24.6	1.125	0.000

Continued on next page

Table 11: Solids behavior for Texas Tech Experiments —
Continued

ID	ρ	D_{50}	D_{84}	D_{90}	$V_{solids-exit}$	$V_{solids-barrel}$
94	90.389	19.05	23.3	24.6		0.000
95	90.389	19.05	23.3	24.6	0.000	0.000
96	90.389	19.05	23.3	24.6	0.750	0.000
101	90.389	19.05	23.3	24.6	0.000	0.000
102	90.389	19.05	23.3	24.6	2.250	0.000
103	90.389	19.05	23.3	24.6	0.750	0.000
104	90.389	19.05	23.3	24.6	1.125	0.000
105	90.389	19.05	23.3	24.6		0.000
106	90.389	19.05	23.3	24.6	1.825	0.000
107	90.389	19.05	23.3	24.6	1.125	0.000
108	90.389	19.05	23.3	24.6	0.750	0.000
109	90.389	19.05	23.3	24.6	4.500	0.000
113	90.389	19.05	23.3	24.6	0.000	0.000
114	90.389	19.05	23.3	24.6	0.375	0.000
115	90.389	19.05	23.3	24.6	1.125	0.000
116	90.389	19.05	23.3	24.6		0.000
117	90.389	19.05	23.3	24.6	0.563	0.000
118	92.987	9.5	11.7	12.3	0.000	0.000
119	92.987	9.5	11.7	12.3		0.000
120	92.987	9.5	11.7	12.3	0.000	0.000
121	92.987	9.5	11.7	12.3	0.375	0.000
122	92.987	9.5	11.7	12.3	0.188	0.000
123	92.987	9.5	11.7	12.3		0.000
125	92.987	9.5	11.7	12.3	0.563	0.000
126	92.987	9.5	11.7	12.3	2.250	0.000
127	92.987	9.5	11.7	12.3	0.750	0.000
128	92.987	9.5	11.7	12.3	0.563	0.000
129	92.987	9.5	11.7	12.3	0.000	0.000
130	92.987	9.5	11.7	12.3	0.750	0.000
131	92.987	9.5	11.7	12.3	0.000	0.000
132	92.987	9.5	11.7	12.3	0.750	0.000
133	92.987	9.5	11.7	12.3	0.750	0.000
134	92.987	9.5	11.7	12.3	2.063	0.000
135	92.987	9.5	11.7	12.3	2.250	0.000
136	92.987	9.5	11.7	12.3	2.063	0.000
137	92.987	9.5	11.7	12.3	1.500	0.000
138	92.987	9.5	11.7	12.3	1.125	0.000
139	92.987	9.5	11.7	12.3	0.938	0.000
140	92.987	9.5	11.7	12.3	0.563	0.000

Continued on next page

Table 11: Solids behavior for Texas Tech Experiments —
Continued

ID	ρ	D_{50}	D_{84}	D_{90}	$V_{solids-exit}$	$V_{solids-barrel}$
141	92.987	9.5	11.7	12.3	4.125	0.000
142	92.987	9.5	11.7	12.3	5.250	0.000
143	92.987	9.5	11.7	12.3	5.438	0.000
144	92.987	9.5	11.7	12.3	5.813	0.000
145	92.987	9.5	11.7	12.3		0.000
146	92.987	9.5	11.7	12.3	4.500	0.000
147	92.987	9.5	11.7	12.3	3.563	0.000
148	92.987	9.5	11.7	12.3	4.500	0.000
149	92.987	9.5	11.7	12.3	4.125	0.000
150	92.987	9.5	11.7	12.3	3.750	0.000
151	92.987	9.5	11.7	12.3	4.500	0.000
152	92.987	9.5	11.7	12.3	4.875	0.000
153	92.987	9.5	11.7	12.3	4.875	0.000
154	92.987	9.5	11.7	12.3	5.063	0.000
155	92.987	9.5	11.7	12.3	4.688	0.000
156	92.987	9.5	11.7	12.3	5.250	0.000
157	92.987	9.5	11.7	12.3	3.938	0.000
158	92.987	9.5	11.7	12.3	3.000	0.000
159	92.987	9.5	11.7	12.3	3.938	0.000
160	92.987	9.5	11.7	12.3	1.313	0.000
161	92.987	9.5	11.7	12.3	2.250	0.000
162	92.987	9.5	11.7	12.3	2.250	0.000
163	92.987	9.5	11.7	12.3	3.563	0.000
164	92.987	9.5	11.7	12.3	3.188	0.000
165	92.987	9.5	11.7	12.3	3.563	0.000
166	92.987	9.5	11.7	12.3	3.188	0.080
167	92.987	9.5	11.7	12.3	2.625	0.065
168	92.987	9.5	11.7	12.3	2.813	0.084
169	92.987	9.5	11.7	12.3	1.688	0.000
170	92.987	9.5	11.7	12.3	1.125	0.000
171	92.987	9.5	11.7	12.3	1.125	0.000
172	92.987	9.5	11.7	12.3	4.500	0.000
173	92.987	9.5	11.7	12.3	3.000	0.109
174	92.987	9.5	11.7	12.3	3.000	0.000
175	92.987	9.5	11.7	12.3	3.750	0.078
176	92.987	9.5	11.7	12.3	2.625	0.157
177	92.987	9.5	11.7	12.3	3.375	0.091
178	92.987	9.5	11.7	12.3	1.875	0.000
179	92.987	9.5	11.7	12.3	1.313	0.000

Continued on next page

Table 11: Solids behavior for Texas Tech Experiments — Continued

ID	ρ	D_{50}	D_{84}	D_{90}	$V_{solids-exit}$	$V_{solids-barrel}$
180	92.987	9.5	11.7	12.3	2.250	0.000
181	92.987	9.5	11.7	12.3	3.188	0.067
182	92.987	9.5	11.7	12.3	2.813	0.000
183	92.987	9.5	11.7	12.3	2.625	0.000
184	92.987	9.5	11.7	12.3	2.813	0.337
185	92.987	9.5	11.7	12.3	2.250	0.371
186	92.987	9.5	11.7	12.3	2.250	0.369
187	92.987	9.5	11.7	12.3	2.625	0.000
188	92.987	9.5	11.7	12.3	2.625	0.000
189	92.987	9.5	11.7	12.3	2.813	0.000

TEXAS TECH UNIVERSITY
Multidisciplinary Research in Transportation

Disclaimer

The United States Government and the State of Texas do not endorse products or manufacturers. Trade or manufacturers' names appear herein solely because they are considered essential to the object of this report.